



AFRL-RX-TY-TR-2011-0025-01

FULL-SCALE EXPERIMENTAL EVALUATION OF PARTIALLY GROUTED, MINIMALLY REINFORCED CONCRETE MASONRY UNIT (CMU) WALLS AGAINST BLAST DEMANDS

James S. Davidson
Department of Civil Engineering
Auburn University
238 Harbert Engineering Center
Auburn, AL 36849

John M. Hoemann
U.S. Army Engineer Research & Development Center
3909 Halls Ferry Road
CEERD-GS-M
Vicksburg, MS 39180-6199

Jonathon S. Shull
Black & Veatch, Federal Services Division
1805 Meadow Moor Drive
Webb City, MO 64870

Hani A. Salim
Department of Civil and Environmental Engineering
University of Missouri
E2509 Lafferre Hall
Columbia, MO 65211-2200

Robert J. Dinan
Air Force Civil Engineering Support Agency
139 Barnes Drive, Suite 1
Tyndall AFB, FL 32403-5323

Michael I. Hammons and Bryan T. Bewick
Air Force Research Laboratory
Airbase Technologies Division
139 Barnes Drive, Suite 2
Tyndall Air Force Base, FL 32403-5323

Contract No. FA8903-08-D-8768-0002

November 2010

DISTRIBUTION STATEMENT A: Approved for public release; distribution is unlimited.
88ABW-2102-0416, 27 January 2012.

**AIR FORCE RESEARCH LABORATORY
MATERIALS AND MANUFACTURING DIRECTORATE**

■ Air Force Materiel Command ■ United States Air Force ■ Tyndall Air Force Base, FL 32403-5323

DISCLAIMER

Reference herein to any specific commercial product, process, or service by trade name, trademark, manufacturer, or otherwise does not constitute or imply its endorsement, recommendation, or approval by the United States Air Force. The views and opinions of authors expressed herein do not necessarily state or reflect those of the United States Air Force.

This report was prepared as an account of work sponsored by the United States Air Force. Neither the United States Air Force, nor any of its employees, makes any warranty, expressed or implied, or assumes any legal liability or responsibility for the accuracy, completeness, or usefulness of any information, apparatus, product, or process disclosed, or represents that its use would not infringe privately owned rights.

NOTICE AND SIGNATURE PAGE

Using Government drawings, specifications, or other data included in this document for any purpose other than Government procurement does not in any way obligate the U.S. Government. The fact that the Government formulated or supplied the drawings, specifications, or other data does not license the holder or any other person or corporation; or convey any rights or permission to manufacture, use, or sell any patented invention that may relate to them.

This report was cleared for public release by the 88th Air Base Wing Public Affairs Office at Wright Patterson Air Force Base, Ohio and is available to the general public, including foreign nationals. Copies may be obtained from the Defense Technical Information Center (DTIC) (<http://www.dtic.mil>).

AFRL-RX-TY-TR-2011-0025-01 HAS BEEN REVIEWED AND IS APPROVED FOR PUBLICATION IN ACCORDANCE WITH ASSIGNED DISTRIBUTION STATEMENT.

BEWICK.BRYAN.
T.1290370414

Digitally signed by BEWICK.BRYAN.T.1290370414
DN: cn=US, o=U.S. Government, ou=DoD, ou=PKI,
ou=USAF, cn=BEWICK.BRYAN.T.1290370414
Date: 2011.05.31 09:42:25 -0500

BRYAN T. BEWICK, PhD
Work Unit Manager

RICHLIN.DEBRA.L
.1034494149

Digitally signed by RICHLIN.DEBRA.L.1034494149
DN: cn=US, o=U.S. Government, ou=DoD, ou=PKI,
ou=USAF, cn=RICHLIN.DEBRA.L.1034494149
Date: 2011.05.30 13:30:14 -0500

DEBRA L. RICHLIN, DR-III
Acting Chief, Airbase Engineering
Development Branch

PILSON.DONNA.L
.1186939324

Digitally signed by PILSON.DONNA.L.1186939324
DN: cn=US, o=U.S. Government, ou=DoD, ou=PKI,
ou=USAF, cn=PILSON.DONNA.L.1186939324
Date: 2012.01.23 11:15:18 -0600

DONNA L. PILSON, LtCol, USAF
Deputy Chief, Airbase Technologies Division

This report is published in the interest of scientific and technical information exchange, and its publication does not constitute the Government's approval or disapproval of its ideas or findings.

REPORT DOCUMENTATION PAGE				Form Approved OMB No. 0704-0188	
<p>The public reporting burden for this collection of information is estimated to average 1 hour per response, including the time for reviewing instructions, searching existing data sources, gathering and maintaining the data needed, and completing and reviewing the collection of information. Send comments regarding this burden estimate or any other aspect of this collection of information, including suggestions for reducing the burden, to Department of Defense, Washington Headquarters Services, Directorate for Information Operations and Reports (0704-0188), 1215 Jefferson Davis Highway, Suite 1204, Arlington, VA 22202-4302. Respondents should be aware that notwithstanding any other provision of law, no person shall be subject to any penalty for failing to comply with a collection of information if it does not display a currently valid OMB control number.</p> <p>PLEASE DO NOT RETURN YOUR FORM TO THE ABOVE ADDRESS.</p>					
1. REPORT DATE (DD-MM-YYYY) 30-NOV-2010		2. REPORT TYPE Technical Report		3. DATES COVERED (From - To) 11-AUG-2008 -- 20-NOV-2010	
4. TITLE AND SUBTITLE Full-scale Experimental Evaluation of Partially Grouted, Minimally Reinforced Concrete Masonry Unit (CMU) Walls Against Blast Demands				5a. CONTRACT NUMBER FA8903-08-D-8768-0002	
				5b. GRANT NUMBER	
				5c. PROGRAM ELEMENT NUMBER 0909999F	
				5d. PROJECT NUMBER GOVT	
6. AUTHOR(S) # Davidson, James S.; ## Hoemann, John M.; ** Shull, Jonathon S.; #### Dinan, Robert J.; ### Salim, Hani A.; * Bewick, Bryan T.; * Hammons, Michael I.				5e. TASK NUMBER F0	
				5f. WORK UNIT NUMBER QF101000	
7. PERFORMING ORGANIZATION NAME(S) AND ADDRESS(ES) #Department of Civil Engineering, Auburn University, 238 Harbert Engineering Center, Auburn, AL 36849; ## U.S. Army Engineer Research & Development Center, 3909 Halls Ferry Road, CEERD-GS-M, Vicksburg, MS 39180-6199; ** Black & Veatch, Federal Services Division, 1805 Meadow Moor (Continued on next page)				8. PERFORMING ORGANIZATION REPORT NUMBER	
9. SPONSORING/MONITORING AGENCY NAME(S) AND ADDRESS(ES) *Air Force Research Laboratory Materials and Manufacturing Directorate Airbase Technologies Division 139 Barnes Drive, Suite 2 Tyndall Air Force Base, FL 32403-5323				10. SPONSOR/MONITOR'S ACRONYM(S) AFRL/RXQEM	
				11. SPONSOR/MONITOR'S REPORT NUMBER(S) AFRL-RX-TY-TR-2011-0025-01	
12. DISTRIBUTION/AVAILABILITY STATEMENT Distribution Statement A: Approved for public release; distribution unlimited.					
13. SUPPLEMENTARY NOTES Ref Public Affairs Case # 88ABW-2012-0416, 27 January 2012. Document contains color images.					
14. ABSTRACT This report presents the results of blast load resistance testing of masonry walls that minimally meet applicable Unified Facilities Criteria (UFC) reinforcement requirements. The testing and analyses presented in this report involved partially-grouted (1) 6-inch, (2) 8-inch, and (3) insulated clay brick veneer (cavity wall) concrete masonry test panels. Three blast load experiments were conducted; each experiment tested one each of the three test panel designs (nine test panels total). The impulse loading to the panels varied significantly between each of the three experiments. Failure mechanism observations were made using interior and exterior high-speed videos that captured the response of each panel. A post-test forensic investigation was also conducted after each experiment to further explore and document the ultimate response of each test article. Dynamic deflections were captured and the responses were compared to blast analysis codes used for masonry design.					
15. SUBJECT TERMS blast load resistance testing of masonry walls, Unified Facilities Criteria reinforcement requirements					
16. SECURITY CLASSIFICATION OF:			17. LIMITATION OF ABSTRACT UU	18. NUMBER OF PAGES 195	19a. NAME OF RESPONSIBLE PERSON Bryan Bewick
a. REPORT U	b. ABSTRACT U	c. THIS PAGE U			19b. TELEPHONE NUMBER (Include area code)

Reset

Standard Form 298, Block 7 (continued)

Drive, Webb City, MO 64870; ### Department of Civil and Environmental Engineering,
University of Missouri, E2509 Laferre Hall, Columbia, MO 65211-2200; #### Air Force Civil
Engineering Support Agency, 139 Barnes Drive, Suite 1, Tyndall Air Force Base, FL 32403-
5323

TABLE OF CONTENTS

LIST OF FIGURES	ii
LIST OF TABLES	iv
ACKNOWLEDGEMENTS	v
1. INTRODUCTION AND BACKGROUND	1
1.1. Introduction.....	1
1.2. Objectives	4
1.3. Scope and Methodology	5
2. TEST PROGRAM.....	6
2.1. Section Designs.....	6
2.2. Construction Materials.....	11
2.3. Materials Testing	12
2.4. Test Panel Construction	12
2.5. Full-scale Dynamic Test Methodology.....	18
2.6. Full-scale Dynamic Test Results	23
2.6.1. Experiment 1	23
2.6.2. Experiment 2.....	35
2.6.3. Experiment 3.....	49
3. ANALYSIS, EVALUATION, AND COMPARISON.....	65
3.1. Flexural Resistance of Reinforced Masonry.....	65
3.2. Analytical Input	68
3.2.1. SDOF Blast Effects Design Spreadsheets (SBEDS)	68
3.2.2. Wall Analysis Code (WAC)	70
3.2.3. Static Resistance Function Analyses	71
3.3. Analytical and Experimental Static Resistance Comparisons	72
3.4. Analytical and Experimental Dynamic Response Comparisons	73
4. CONCLUSIONS AND RECOMMENDATIONS.....	81
5. REFERENCES	83
Appendix A: Material Test Results.....	85
Appendix B: Construction Photos	91
Appendix C: Test Results Photos	127
LIST OF FIGURES	127
LIST OF SYMBOLS, ABBREVIATIONS AND ACRONYMS	191

LIST OF FIGURES

	Page
Figure 1. Typical Brick Veneer Cavity Wall Geometry (Insulation not Shown)	2
Figure 2. 6-inch CMU Panel Design.....	7
Figure 3. Front View Showing Rebar and Grouted Cell Locations for the 6-inch CMU Panel	8
Figure 4. 8-inch CMU Panel Design.....	9
Figure 5. Front View Showing Rebar and Grouted Cell Locations for the 8-inch CMU Panel and Cavity Wall	10
Figure 6. Cavity Wall Panel Design	11
Figure 7. Construction of Test Panels.....	14
Figure 8. Construction of Test Panels (continued)	15
Figure 9. Positioning for Testing	16
Figure 10. Top and Bottom Connections.....	17
Figure 11. Interior Embed.....	18
Figure 12. Panels in Reaction Structure Ready for Testing.....	20
Figure 13. Plan View of the Test Set-up and Instrumentation Layout	21
Figure 14. Summary of Average Pressures and Impulses	22
Figure 15. Front View of the Test Set-up Describing Instrumentation Position and Designation	22
Figure 16. Plan View of the Test Set-up Describing Videography Position and Designation	23
Figure 17. Experiment 1 Post-detonation Front View	24
Figure 18. Experiment 1 Post-detonation Side Views.....	25
Figure 19. Experiment 1 6-inch CMU Panel Deflections.....	26
Figure 20. Experiment 1 6-inch CMU Panel Interior Images.....	27
Figure 21. Experiment 1 Post-Detonation 6-inch CMU Panel Exterior View (left) and Interior View (right).....	28
Figure 22. Experiment 1 8-inch CMU Panel Deflections.....	29
Figure 23. Experiment 1 8-inch CMU Panel Interior Images.....	30
Figure 24. Experiment 1 Post-detonation 8-inch CMU Panel Exterior View (left) and Interior View (right).....	31
Figure 25. Experiment 1 Breaching Failure of the 8-inch CMU Panel	32
Figure 26. Experiment 1 Cavity Wall Deflections.....	33
Figure 27. Experiment 1 Cavity Wall Interior Images	34
Figure 28. Experiment 1 Post-detonation Cavity Wall Exterior View (left) and Interior View (right)	35
Figure 29. Experiment 2 Post-Detonation Front View	35
Figure 30. Experiment 2 Post-Detonation Side Views	36
Figure 31. Experiment 2 6-inch CMU Panel Deflections.....	37
Figure 32. Experiment 2 6-inch CMU Panel Interior Images.....	38
Figure 33. Experiment 2 Post-detonation 6-inch CMU Panel Exterior View (left) and Interior View (right).....	39
Figure 34. Experiment 2 Post-detonation 6-inch CMU Panel Closer Outside Views	40
Figure 35. Experiment 2 8-inch CMU Panel Deflections.....	41
Figure 36. Experiment 2 8-inch CMU Panel Interior Images.....	42
Figure 37. Experiment 2 Post-detonation 8-inch CMU Panel Exterior View (left) and Interior View (right).....	43

Figure 38. Experiment 2 Post-detonation 8-inch CMU Panel CMU Damage.....	44
Figure 39. Experiment 2 Post-detonation 8-inch CMU Panel CMU Damage.....	45
Figure 40. Experiment 2 Cavity Wall Deflections.....	46
Figure 41. Experiment 2 Cavity Wall Interior Images	47
Figure 42. Experiment 2 Post-detonation Cavity Wall Exterior View (left) and Interior View (right)	48
Figure 43. Experiment 2 Post-detonation Cavity Wall Foam Damage	49
Figure 44. Experiment 3 Post-detonation Front View	50
Figure 45. Experiment 3 Post-detonation Side Views.....	50
Figure 46. Experiment 3 6-inch CMU Panel Deflections.....	51
Figure 47. Experiment 3 6-inch CMU Panel Interior Images.....	52
Figure 48. Experiment 3 Post-detonation 6-inch CMU Panel Exterior View (left) and Interior View (right).....	53
Figure 49. Experiment 3 Post-detonation 6-inch CMU Panel Close-up Views	54
Figure 50. Experiment 3 8-inch CMU Panel Deflections.....	55
Figure 51. Experiment 3 8-inch CMU Panel Interior Images.....	56
Figure 52. Experiment 3 Post-detonation 8-inch CMU Panel Exterior View (left) and Interior View (right).....	57
Figure 53. Experiment 3 Post-detonation 8-inch CMU Panel Close-up Exterior Views	58
Figure 54. Experiment 3 Post-detonation 8-inch CMU Panel Close-up Interior Views	59
Figure 55. Experiment 3 Cavity Wall Deflections.....	60
Figure 56. Experiment 3 Cavity Wall Interior Video Capture.....	61
Figure 57. Experiment 3 Post-detonation Cavity Wall Exterior View (left) and Interior View (right)	62
Figure 58. Experiment 3 Post-detonation Cavity Wall Close-up Views	63
Figure 59. Experiment 3 Post-detonation Cavity Wall Close-up Views	64
Figure 60. Moment-curvature Relationship for Reinforced Masonry Beams	66
Figure 61. Resistance-displacement Idealization for Reinforced Masonry Beams	66
Figure 62. Experimental Static Resistance Results.....	72
Figure 63. 6-inch CMU Panel Analytical and Experimental Static Resistance Comparisons.....	73
Figure 64. 8-inch CMU Panel Analytical and Experimental Static Resistance Comparisons.....	73
Figure 65. Experiment 1 6-inch CMU Panel Analytical and Experimental Dynamic Response Comparisons	76
Figure 66. Experiment 1 8-inch CMU Panel Analytical and Experimental Dynamic Response Comparisons	76
Figure 67. Experiment 1 Cavity Wall CMU Panel Analytical and Experimental Dynamic Response Comparisons	77
Figure 68. Experiment 2 6-inch CMU Panel Analytical and Experimental Dynamic Response Comparisons	77
Figure 69. Experiment 2 8-inch CMU Panel Analytical and Experimental Dynamic Response Comparisons	78
Figure 70. Experiment 2 Cavity Wall CMU Panel Analytical and Experimental Dynamic Response Comparisons	78
Figure 71. Experiment 3 6-inch CMU Panel Analytical and Experimental Dynamic Response Comparisons	79

Figure 72. Experiment 3 8-inch CMU Panel Analytical and Experimental Dynamic Response Comparisons	79
Figure 73. Experiment 3 Cavity CMU Panel Analytical and Experimental Dynamic Response Comparisons	80

LIST OF TABLES

	Page
Table 1. Test Panel Summary	6
Table 2. Construction Material Specifications.....	12
Table 3. Material Tests Results.....	13
Table 4. Loading	19
Table 5. Analytical Definitions.....	67
Table 6. Analytical Input	68
Table 7. Analytical Output.....	68
Table 8. SBEDS Input, 6-inch CMU Panel	69
Table 9. SBEDS Input, 8-inch CMU Panel and Cavity Wall	70
Table 10. WAC Input, 6-inch CMU Panel	71
Table 11. WAC Input, 8-inch CMU Panel	71

ACKNOWLEDGEMENTS

The experimental components of this project were sponsored by the Airbase Technologies Division of the Air Force Research Laboratory (AFRL); testing was conducted at Tyndall Air Force Base Florida. The current technical points of contact for the AFRL Engineering Mechanics and Explosive Effects Research Group (EMEERG) are Dr. Michael Hammons and Dr. Bryan Bewick. The AFRL program manager during the experimental phase of this work was Dr. Robert Dinan. Experimental samples were provided through a Cooperative Research and Development Agreement (CRADA) with the Portland Cement Association (PCA) (CRADA # 05-119-ML-01). Mr. Dennis Graber from the National Concrete Masonry Association (NCMA) and Mr. Gregg Borchelt from the Brick Industry Association (BIA) assisted throughout the planning and execution of this program. Masonry material tests were conducted by NCMA. Employees of Black & Veatch and Applied Research Associates contributed to the execution of the experimental program. Under the guidance of Dr. James Davidson, Auburn University Department of Civil Engineering researchers Mary Schambeau and Michael Newberry provided pre-test support of the experimental program, as well as post-test analysis of the experimental data.

1. INTRODUCTION AND BACKGROUND

1.1. Introduction

Over the past decade, the US Government adopted construction requirements and incentives that promote energy efficiency and build green initiatives. The Energy Policy Act of 2005 [US Congress 2005] provided tax incentives and loan guarantees for energy solutions that could combat growing energy problems. It provides tax breaks for energy conservation improvements to energy systems in homes and commercial buildings. The Energy Independence Security Act of 2007 [US Congress 2007] was enacted “to move the United States toward greater energy independence and security, to increase the production of clean renewable fuels, to protect consumers, to increase the efficiency of products, buildings, and vehicles, to promote research on and deploy greenhouse gas capture and storage options, and to improve the energy performance of the Federal Government, and for other purposes.” It provided new initiatives for promoting conservation in buildings and industry, and new standards and grants for promoting efficiency in government and public institutions. Furthermore, military facilities construction requirements such as the Anti-Terrorism and Force Protection (ATFP), Unified Facilities Criteria (UFC), and the Military Construction (MILCON) Transformation initiatives also emphasize building economy and energy efficiency.

Masonry has been used in building construction for thousands of years. Worldwide, masonry units come in many different sizes and shapes and can be made with a variety of materials including concrete, clay, and glass. Masonry walls are site constructed using manufactured masonry units and site mixed mortar. The units are mortared together to various heights and can be oriented to create aesthetically attractive patterns on exterior walls. Masonry can form structural elements (bearing walls, columns, or pilasters) and/or finished cladding systems. Masonry walls also typically increase the fire resistance of the wall system or structural elements. Masonry walls can be single or multi-wythe, and the interior cells of the units comprising masonry walls may be empty or grouted. “Reinforced masonry” generally refers to placing steel reinforcing bars vertically within the interior cells, and then grouting only those cells (partially grouted) or all cells (fully grouted). Horizontal reinforcing can also be used in the form of rebar laid horizontally within grouted cells and/or as wire joint reinforcement.

Concrete masonry units (CMU) are made from a mixture of portland cement and aggregates under controlled conditions and must meet the requirements of ASTM C90. The units can be made to various dimensions, but typically have nominal face dimensions of 8 inches high by 16 inches wide. CMU mixes have a very low water content (generally referred to as dry mix) and are made in block machines where the material is vigorously vibrated under very high pressure to the desired shape and then cured in the manufacturing plant. The units are categorized based on weight (lightweight, medium weight, and normal weight).

One of the most commonly used modern construction geometries for exterior walls is “cavity wall” construction. This type of construction is generally comprised of an exterior clay or concrete masonry veneer, insulation board, air space, and an interior structural wythe comprised of concrete masonry (Fig. 1). The exterior veneer and interior wythe are connected by steel ties that come in many different geometries. Veneer walls are designed as “drainage walls”, where a drainage cavity is installed behind the masonry veneer to allow water that penetrates the masonry

to flow down to the base of the wall, and then the water is directed to the exterior through “weeps,” which are partially open header joints spaced at regular intervals along the lower course of the brick masonry exterior (See Fig. 1). This cavity must remain open to allow water to freely drain. The concrete masonry structural wythe may be unreinforced (grouted or not-grouted), reinforced but grouted in reinforced cells only (partially grouted), or reinforced and grouted in all cell voids (fully grouted). Furthermore, cavity wall systems may be “load bearing” or “non-load bearing,” depending upon whether the masonry is designed to resist gravity loads from above floors and frame, or simply used as interior or exterior in-fill partitions. They can serve as a simple exterior boundary or as part of a multi-wythe insulated wall. They may be designed and constructed with or without grouted and reinforced cells, which primarily depends upon out-of-plane loading demands.

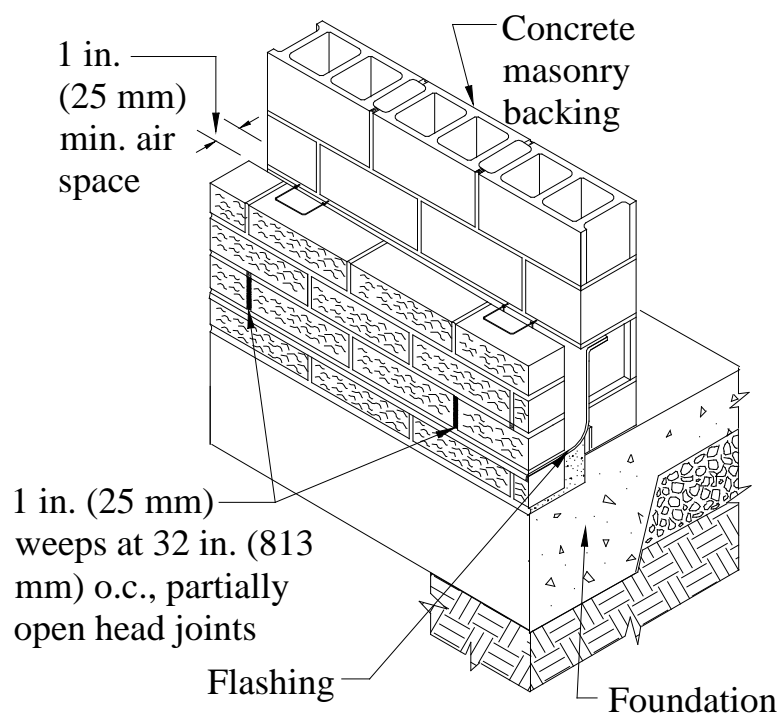


Figure 1. Typical Brick Veneer Cavity Wall Geometry (Insulation not Shown)

Exterior masonry walls must be designed to resist lateral loads from wind and earthquakes. In the US, loads are defined according to ASCE/SEI 7-05, “Minimum Design Loads for Buildings and Other Structures” [ASCE 2005]. MSJC 2008, “Building Code Requirements for Masonry Structures (TMS 402-08/ACI 530-08/ASCE 5-08)” [ACI 2008] is used for structural design of masonry. Design details can vary significantly between “West Coast” construction and “East Coast” construction, where the details of West Coast construction are typically governed by seismic design criteria, and East Coast construction is governed by wind forces design criteria. There are also subtle differences in construction approaches, such as in the common use of “A-block” in western states.

Government, military and diplomatic facilities are also commonly constructed with masonry exterior walls. In addition to standard wind and earthquake load resistance, these facilities must also be designed for security considerations and, pertinent to this effort, to withstand external explosions. For Department of Defense (DoD) buildings and facilities, the Unified Facilities Criteria (UFC) must be followed. Until recently, UFC 3-310-05A [DoD 2005] addressed the design of masonry structures for DoD construction. However, this was superseded by UFC 3-301-01 [DoD 2010], which provides general structural engineering guidance and refers the designer to other standard specifications such as ACI 530 and the International Building Code [IBC 2009].

Unfortunately, military and diplomatic facilities are targets of terrorist attacks. Populated public facilities such as residential buildings, office buildings, and restaurants are also targeted. The weapon most commonly used to target buildings and facilities is a vehicle that conceals several hundred to several thousand pounds of explosives, depending upon the size of the vehicle (commonly referred to as a vehicle borne improvised explosive device, VBIED). Most of the dynamic pressure resulting from external explosions interacts first with the exterior walls. Therefore, ensuring that the exterior walls of a structure are able to withstand blast loading without producing deadly fragments is a critical part of minimizing injuries to building occupants. At the same time, large deformation ability facilitates blast energy absorption, reduces the magnitude of connection forces, and reduces loads transferred to the host frame. When subjected to airblast overload, unreinforced CMU walls break into pieces that are propelled into the interior of the structure, causing severe injury or death to occupants. For these reasons, the DoD Antiterrorism/Force Protection Construction Standards [DoD 2007] prohibit the use of unreinforced CMU exterior walls for new military construction.

Although blast load resistance has become much more of a design concern over the past decade, engineering for explosion loading still tends to be a specialty field in which a smaller subset of architect/engineer (A/E) firms focus. This is particularly true for the design of government, diplomatic, military, and high-visibility facilities and infrastructure that are considered to be at a greater risk of an explosion incident. Design of exterior walls to resist impulse loads is one of the fundamental steps in the design for external explosions. This can be accomplished by using advanced analysis approaches, such as central difference finite element solvers, but more commonly is accomplished through simplified analyses approaches such as pressure-impulse (P-I) diagrams and single-degree-of-freedom (SDOF) models. A primary resource for such tools is the US Army Corp of Engineers Protective Design Center (PDC). For wall element design, two commonly used tools are SBEDS (SDOF Blast Effects Design Worksheet) [USACE-PDC 2005, 2006a, 2006b] and WAC (Wall Analysis Code) [Slawson 1995]. For the most part, these tools tend to mirror methodologies and requirements established by the Unified Facilities Criteria (UFC), and in particular for wall element design, UFC 4-010 “Minimum Antiterrorism Standards for Buildings” [DoD 2007] and UFC 3-340 “Structures to Resist the Effects of Accidental Explosions” [DoD 2008]. Overall, the resources provided by the PDC and methodologies outlined in relevant UFCs are serving the blast engineering community well within their current limitations. However, there is need to augment and improve the resistances used by these tools, specifically their representations of the blast energy absorbing capacities of modern multi-wythe insulated wall forms. There is also opportunity to use modern construction techniques to improve the energy efficiency of blast resistant construction.

In 2005, the Air Force Research Laboratory (AFRL) initiated research collaboration with US concrete industries professional associations interested in advancing the state-of-the-art knowledge and design of their products for protective structures applications. The stated objective of the research under this program was “to develop blast protection data for concrete building products (e.g. insulated form walls, precast/prestressed panels, tilt-up panels, masonry components, autoclaved concrete components, cast-in-place forming systems, etc.) typically used in construction and to develop improvements to these designs as needed to improve blast resistance.” Industry associations represented included: the Portland Cement Association (PCA), Precast/prestressed Concrete Institute (PCI), Tilt-Up Concrete Association (TCA), Insulating Concrete Form Association (ICFA), Concrete Foundations Association (CFA), National Concrete Masonry Association (NCMA), and the National Ready Mixed Concrete Association (NRMCA). Other government agencies involved in protective design R&D that were present at initial meetings included the Air Force Civil Engineering Support Agency (AFCEA) and the US Army Engineer Research and Development Center (USA-ERDC).

To meet these objectives, many tests, both static and dynamic, were conducted. Blast resistance of multi-wythe masonry construction is one of the topic areas of this program. The masonry component of this comprehensive investigation included (1) vacuum chamber (uniform pressure) static resistance testing, (2) full-scale dynamic testing (explosion-generated loads), (3) high-fidelity finite element modeling, and (4) the development of engineering-level analytical models. Specific emphasis was placed on determining the potential of foam insulation to attenuate impulse load energy and reduce the overall flexural response of the system. Single-wythe designs and double-wythe (cavity wall) designs with 2-inch extruded polystyrene board insulation were tested. The structural wythe was comprised of standard 6-inch or 8-inch concrete masonry units, and the veneer of the cavity configurations was typical clay brick. All cells of some test panels were fully grouted (Series I tests) and reinforced based on a 110 mph wind load design, while other panels were minimally reinforced with grout placed only in the cells containing vertical reinforcement (Series II tests). This report focuses on the full-scale blast testing of the partially grouted panels (Series II tests). Post-test forensic analyses were used to evaluate the extent of foam crushing and overall composite behavior during full-scale blast tests. In addition to overall methodology and findings, design and construction recommendations resulting from the investigation are presented.

1.2. Objectives

The overall objective of the work presented in this report was to evaluate the blast load performance of exterior infill masonry walls that minimally meet the requirements of the various applicable DoD design criteria. As such, the testing and analyses discussed in this report involved partially-grouted concrete masonry walls that meet current minimum UFC reinforcement requirements.

1.3. Scope and Methodology

The test program included both full-scale static flexural tests and full-scale blast tests. This report presents the results of the dynamic experiments; the static experiment results are presented in a separate report [Salim et al. 2010]. Three disparate designs were evaluated: (1) a 6-inch CMU wall reinforced with #3 bars, (2) an 8-inch CMU wall reinforced with #4 bars, and (3) an 8-inch CMU cavity wall with clay brick veneer. Three each of the three designs were constructed, and subsequently three dynamic experiments were conducted with each experiment testing one panel of each of the three designs (nine panels tested under three detonations). Pressure gages, deflection gages, and videography were used to record the response of each panel in each experiment. Failure mode observations were made from the high-speed videography and the residual condition of each panel after testing. The dynamic deflections were compared to existing blast load analysis software and methodology. This report summarizes construction of the test panels, material properties, testing methodologies, full-scale dynamic test response, analytical comparisons, and conclusions.

2. TEST PROGRAM

2.1. Section Designs

Three design sections were evaluated in a full-scale explosion arena test. Each test panel was 112 inches (7 blocks) wide by 136 inches (17 courses) high. The test panels were mounted in a reaction structure with bearing surfaces at the top and bottom of the wall (Fig. 2) so that the flexural response was one-way bending. At the top and bottom of the panels (where they bore on the reaction structure), the panels were installed in a continuous bed of fresh mortar to provide uniform bearing between the panel and the reaction structure. The test panels were partially grouted; grout was placed only in reinforced cells and bond beams. The edge cells of each panel were grouted and reinforced. Three each of the three panel designs were constructed (nine total). Table 1 summarizes the test panel designs; a brief description of each panel follows.

Table 1. Test Panel Summary

Description	Block	Reinforcement	Veneer
Panel 1	6-inch CMU	# 3 bars – 36 in. Avg., 40 in. max spacing	None
Panel 2	8-inch CMU	# 4 bars - 52 in. Avg., 56 in. max spacing	None
Panel 3	8-inch CMU	# 4 bars - 52 in. Avg., 56 in. max spacing	4-in. clay brick

Test Panel Design 1 was constructed of 6-inch standard block masonry reinforced with #3 rebar at 32 / 40 / 32-inch spacings (subsequently referred to as the “6-inch CMU panel”) (Fig. 2). The maximum spacing allowed is six times the block thickness (36 inches for 6-inch CMU walls) [UFC 3-310-05a, ACI 530 2008]. However, since cell centers are at 8 inch intervals, the largest practical rebar spacing interval that can be facilitated in 6-inch walls is 32 inches. Since the edge cells of the test panel must be grouted and reinforced, the reinforcement ratio used approximates the 36 inch maximum spacing. An elevation view that describes the spacing between vertical rebar is provided in Figure 3. The panel was constructed of 25% corner/sash nominal dimensions 6x8x16 inch CMU blocks. Bond beams to facilitate transfer of the reaction forces comprised of grouted 6x8x16 inch bond beam blocks and #3 reinforcement bars laid laterally were used at the bottom courses and at the course corresponding to the elevation of the reaction structure ceiling. Standard 4 inch width ladder joint reinforcement was used every-other course. Four 28 inch dowels were welded to the bottom of the frame to provide reaction continuity between the frame and the test panels. The lifting hooks were formed of standard #3 rebar with 16 inch legs. All dowels, hooks, vertical and horizontal reinforcement were #3, ASTM A706, Grade 60 reinforcement bars.

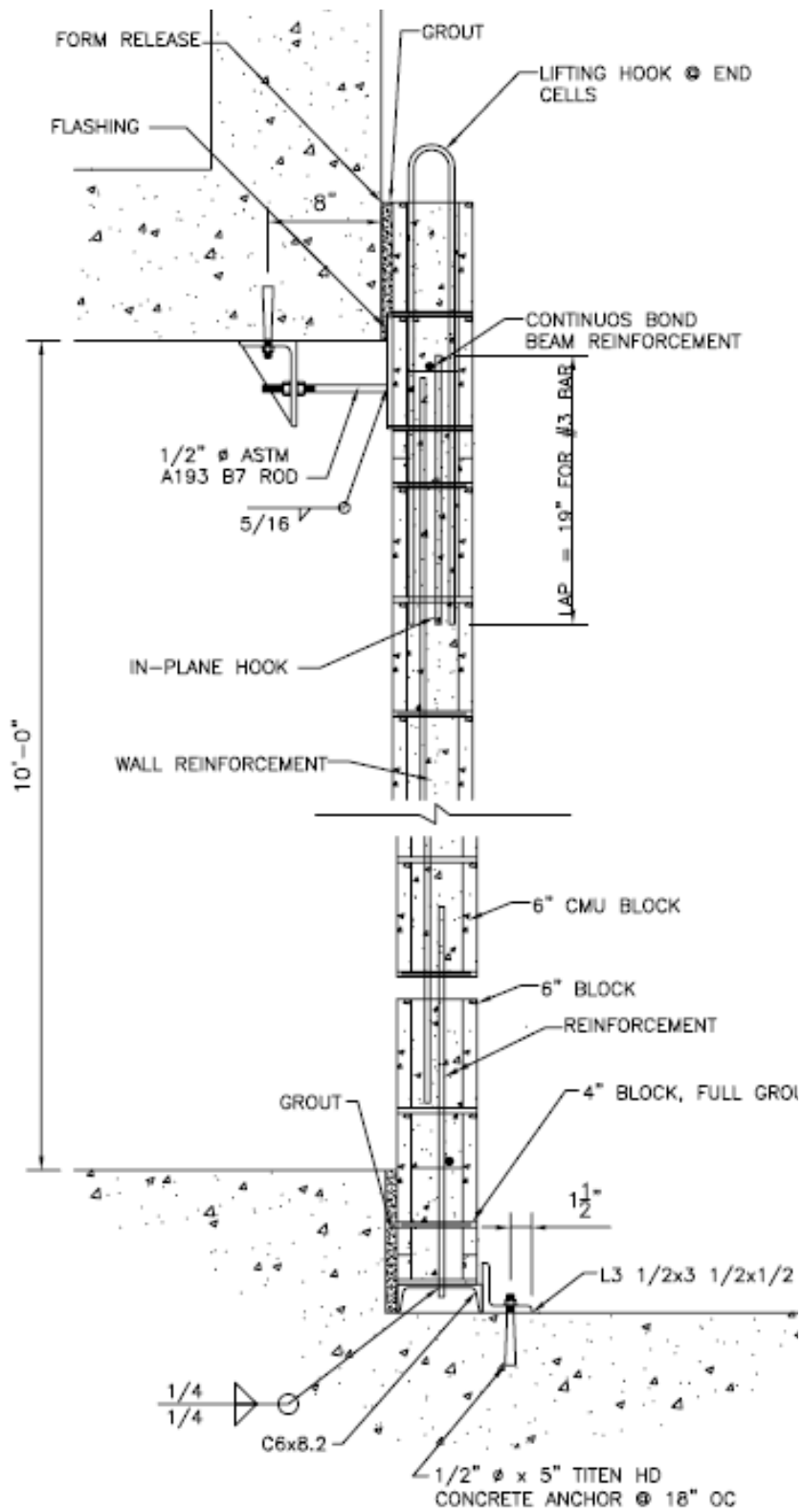


Figure 2. 6-inch CMU Panel Design

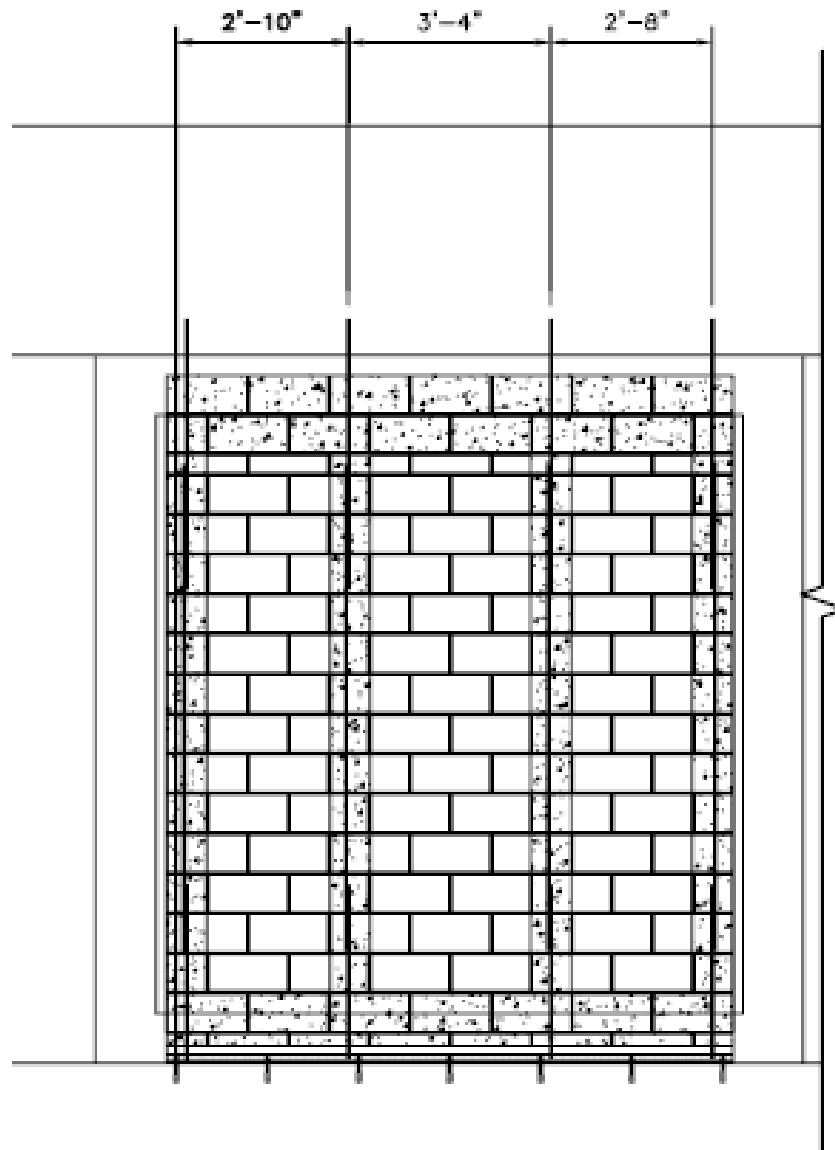


Figure 3. Front View Showing Rebar and Grouted Cell Locations for the 6-inch CMU Panel

Test Panel Design 2 was constructed of 8-inch standard block masonry reinforced with #4 rebar at 48 and 56 inch spacings (subsequently referred to as the “8-inch CMU panel”) (Fig. 4). An elevation view that describes the spacing between vertical rebar is provided in Figure 5. The panel was constructed of nominal dimensions 8x8x16 inch double corner CMU blocks. Bond beams comprised of grouted 8x8x16 inch bond beam blocks and #4 reinforcement bars were used at the top and bottom courses. Standard 8-inch width ladder joint reinforcement was used every-other course. Three 34-inch dowels were welded to the bottom of the frame. The hooks were formed of standard #4 rebar with 22-inch legs. All dowels, hooks, vertical and horizontal reinforcement were #4, ASTM A706, Grade 60 reinforcement bars.

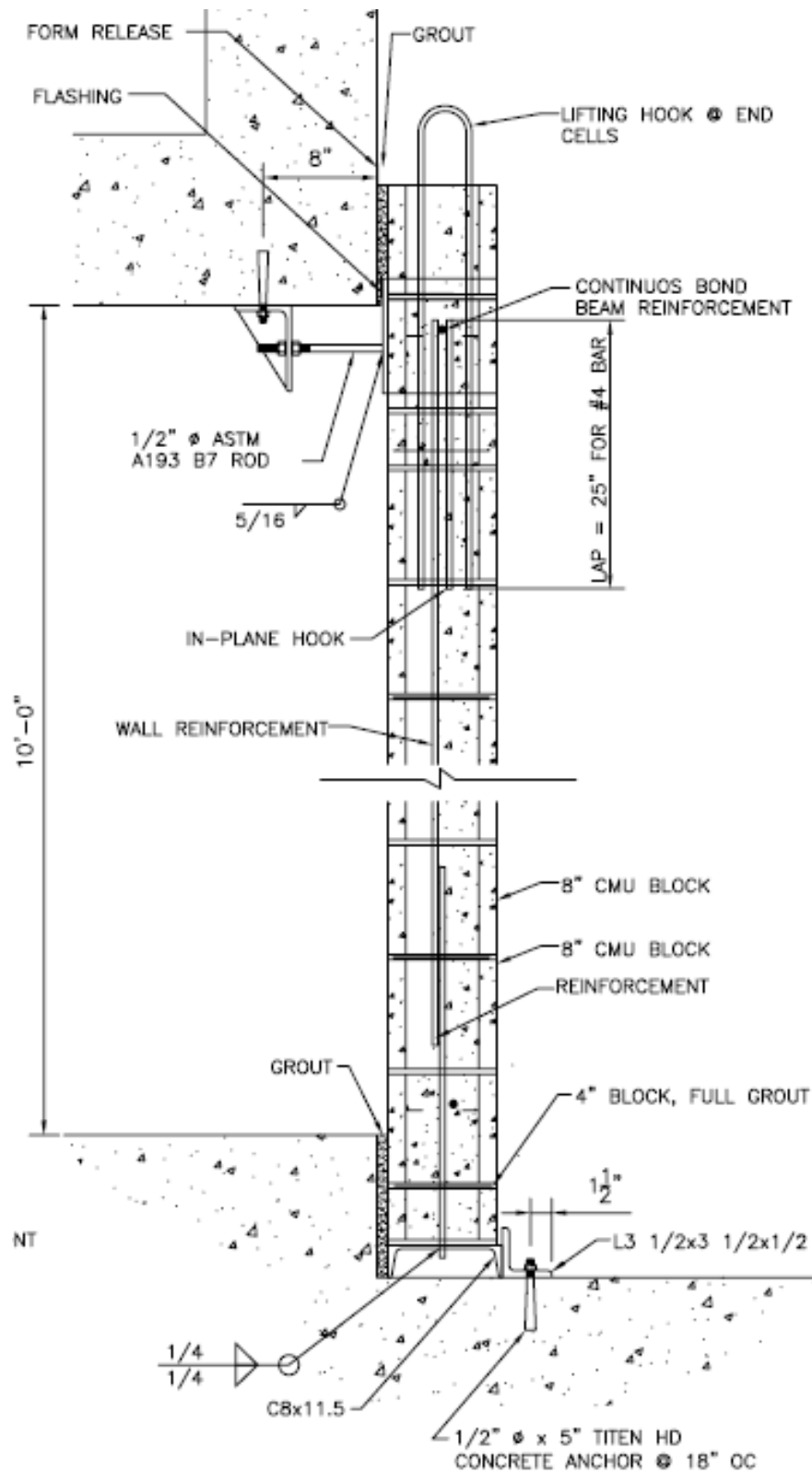


Figure 4. 8-inch CMU Panel Design

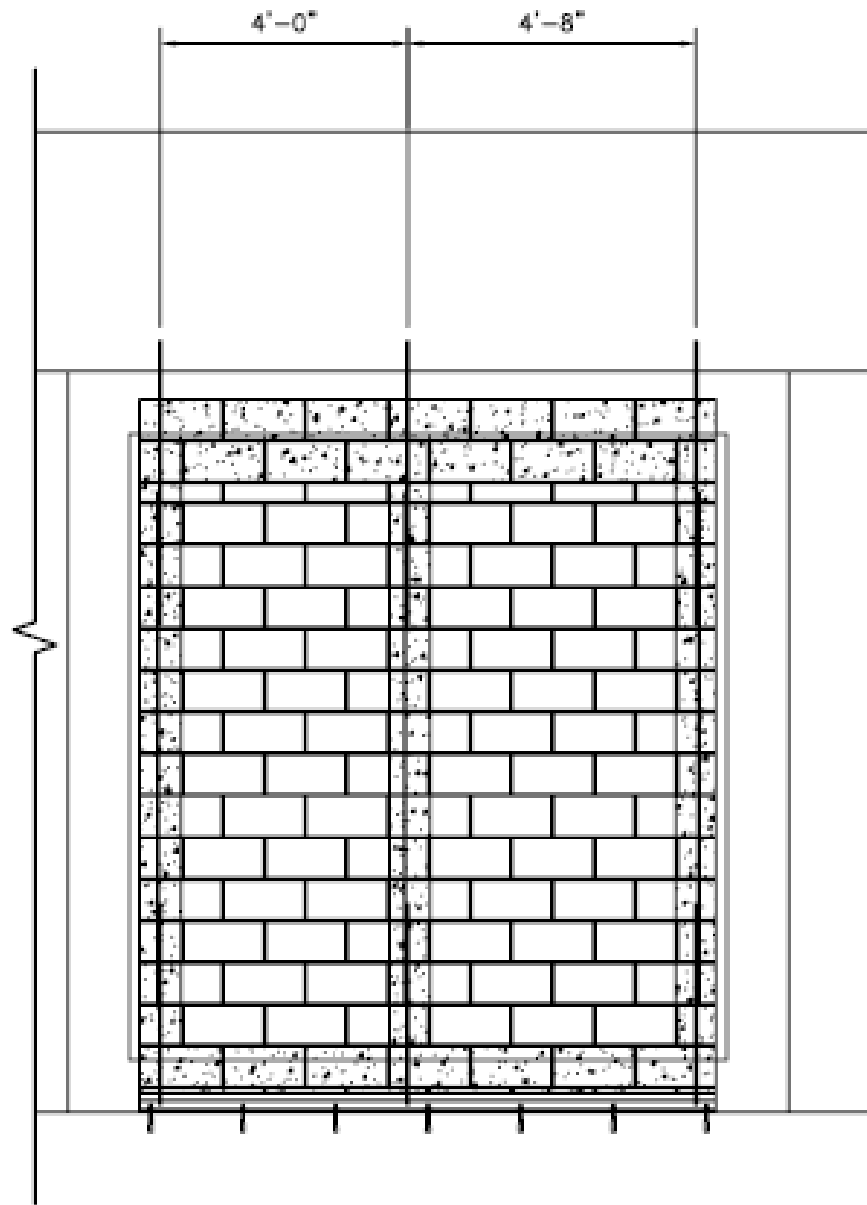


Figure 5. Front View Showing Rebar and Grouted Cell Locations for the 8-inch CMU Panel and Cavity Wall

Test Panel Design 3 was the same as the 8-inch CMU panel, plus a 4-inch clay facing brick veneer with 2 inch thick extruded polystyrene rigid board insulation and a 1-inch air gap between the structural wythe and the veneer (subsequently referred to as the “cavity wall”) (Fig. 6). Ladder joint reinforcement with eye and pintle adjustable tie anchors were used to connect the clay brick veneer to the CMU wythe. The insulation seams were located at the elevation of the joint reinforcement. Mortar netting was placed in the bottom of this space to catch excess mortar.

Table 2. Construction Material Specifications

CMU block	ASTM C90, normal weight, 6 and 8 inch, standard square end units
mortar	ASTM C270, type S PCL premix mortar, 3/8-inch joints, cross webs mortared to confine grout
grout	ASTM C476
rebar	ASTM 615, grade 60 and ASTM A 706, grade 60
joint reinforcement	ASTM A951, W1.7 (9 gage, 8 inch) ladder, located vertically every other course
masonry ties	ASTM A82 (galvanized), W2.8 double eye & pintle, 2-2/3 sq ft of wall per tie, 16 inch max horizontal and vertical distance
insulation	2 inch extruded polystyrene
brick	ASTM C216, grade SW, type FBS
welding	AWS D1.1.

2.3. Materials Testing

The material testing and averaged results are summarized in Table 3. Details of the material test results are provided in Appendix A.

2.4. Test Panel Construction

Three each of the three test panel designs (nine total) were constructed by professional masons at a staging site approximately ¼ mile from the test arena. The wall panels were constructed on channels with rebar dowels welded in place. Vibrator size was limited to ¾ inch. Lap splice lengths were stipulated as 19 inch for # 3 bars and 25 inch for #4 bars. Bar positioners were used to align vertical reinforcement in the CMU walls and grout stop mesh was used for top bond beam construction. Figures 7 and 8 illustrate the construction of the test panels; additional construction photos are provided in Appendix B.

The test panels cured for approximately 12 weeks before the first three panels were moved into position for the first explosion testing experiment. There was approximately two weeks time span between each experiment. Prior to each dynamic test, the test panels were carefully stabilized and transported to the test arena. Each panel was positioned against the reaction structure, and grout placed in the space between each panel and the reaction structure top and bottom. The span height opening behind each panel was 10 ft. There was approximately 1.5 inch of space between the reaction structure and each vertical edge of each panel to ensure one-way flexure (wall panels were only laterally restrained top and bottom). The gaps between the panel edges and reaction structure were blocked with aluminum sheeting to prevent significant pressure, dust and debris from entering the interior space during the experiment. There was approximately 8 inch overlap between each test panel and reaction structure base at the bottom of the panels. The test panels were set such that the reaction structure floor elevation was

approximately mid-height of the bottom bond beam, and therefore dynamic lateral shear force was reacted by the robust grouted/reinforced bond beam. The top 12 inches of the panel overlapped with the reaction structure so that the reaction structure ceiling was at the same elevation as the mid-height of the top bond beam. To prevent outward collapse, the panels were connected to the ceiling of the reaction structure using embed plates welded to the ceiling of the reaction structure. Figures 9-11 describe the positioning of the panels and the connections between the test panels and the reaction frame. Additional images of the test panel positioning are provided in Appendix B.

Table 3. Material Tests Results

Masonry Compressive Strength (Prism Test)	ASTM C1314, “Standard Test Method for Compressive Strength of Masonry Prisms”; 4 sets of three prism test specimens (three 8-inch grouted, three 8-inch ungrouted, three 6-inch grouted, three 6-inch ungrouted)	Grouted 6-inch CMU = 4872 psi; Grouted 8-inch CMU = 4266 psi Hollow 6-inch CMU = 2080 psi; Hollow 8-inch CMU = 1292 psi Clay Brick = 4460 psi
Masonry Block	ASTM C140, “Standard Test Method for Sampling and Testing Concrete Masonry Units and Related Units”	Density: 6-inch CMU = 112.2 lb/ft ³ 8-inch CMU = 100.8 lb/ft ³ Clay brick = 138.3 lb/ft ³
Mortar	ASTM C780, “Method for Preconstruction and Construction Evaluation of Mortars for Masonry” twenty-five samples	Total average = 3190 psi
Grout	ASTM C1019, “Standard Test Method for Sampling and Testing Grout”; nine total samples	Total average = 7524 psi
Rebar Tensile Strength	ASTM A370, “Standard Test Methods and Definitions for Mechanical Testing of Steel Products”; three samples each for the #3 and #4 bars	#3 bars: $f_y = 73865$ ksi, $f_u = 112802$ ksi, $\epsilon_{max} = 0.141$ #4 bars: $f_y = 66804$ ksi $f_u = 106066$ ksi $\epsilon_{max} = 0.143$



Figure 7. Construction of Test Panels



Figure 8. Construction of Test Panels (continued)



Figure 9. Positioning for Testing



Figure 10. Top and Bottom Connections



Figure 11. Interior Embed

2.5. Full-scale Dynamic Test Methodology

One each of the three panel designs were tested in three separate experiments (three detonations, each detonation tested three panels; one of each of the three panel designs were tested in each experiment). Figure 12 shows three panels ready for testing. An explosive charge was positioned perpendicular to the middle of the center panel with its center of gravity at an elevation of approximately 30 inches (Fig. 13). The loading is summarized in Table 4 in terms of scaled

distance and in Figure 14 with values normalized to the Experiment 1 average reflected pressures and impulses.

Table 4. Loading

Experiment	Scaled Distance (ft/lb^{1/3})
1	8.0
2	6.5
3	5.2

Data collected included (1) dynamic deflections, (2) pressures, and (3) videography. The overall layout of instrumentation is illustrated in Figures 13 and 15; videography type, location and target are described in Figure 16. After each test completion, the residual condition of each test panel was carefully recorded with still photography.

(1) Dynamic deflection measurements: Three displacement gauges recorded time-histories of the displacements at quarter points through the height of each of the panels (nine total for each experiment, D1 through D9) (Fig. 15).

(2) Pressure measurements: Both free field and reflected pressure measurements were taken for each experiment. Four reflected pressure gauges were mounted on the reaction structure at an elevation corresponding to mid-span of the panel near the edge of each panel (Fig. 15). One free field pressure gage was placed within the interior of each reaction structure bay, and two free field pressure gages were placed outside of the reaction structure (Figs. 13 and 15).

(3) Videography: The exterior of the experiment was recorded with two high-speed cameras, positioned at approximately 20 degrees to the left and right of the reaction structure in order to capture the wall panel responses from the outside, and one exterior real-time camera that captures an overall view of the experiment. A high-speed camera was also placed in each reaction structure bay to capture the failure modes from an inward deflection response viewpoint. (Figs. 13 and 16)



Figure 12. Panels in Reaction Structure Ready for Testing

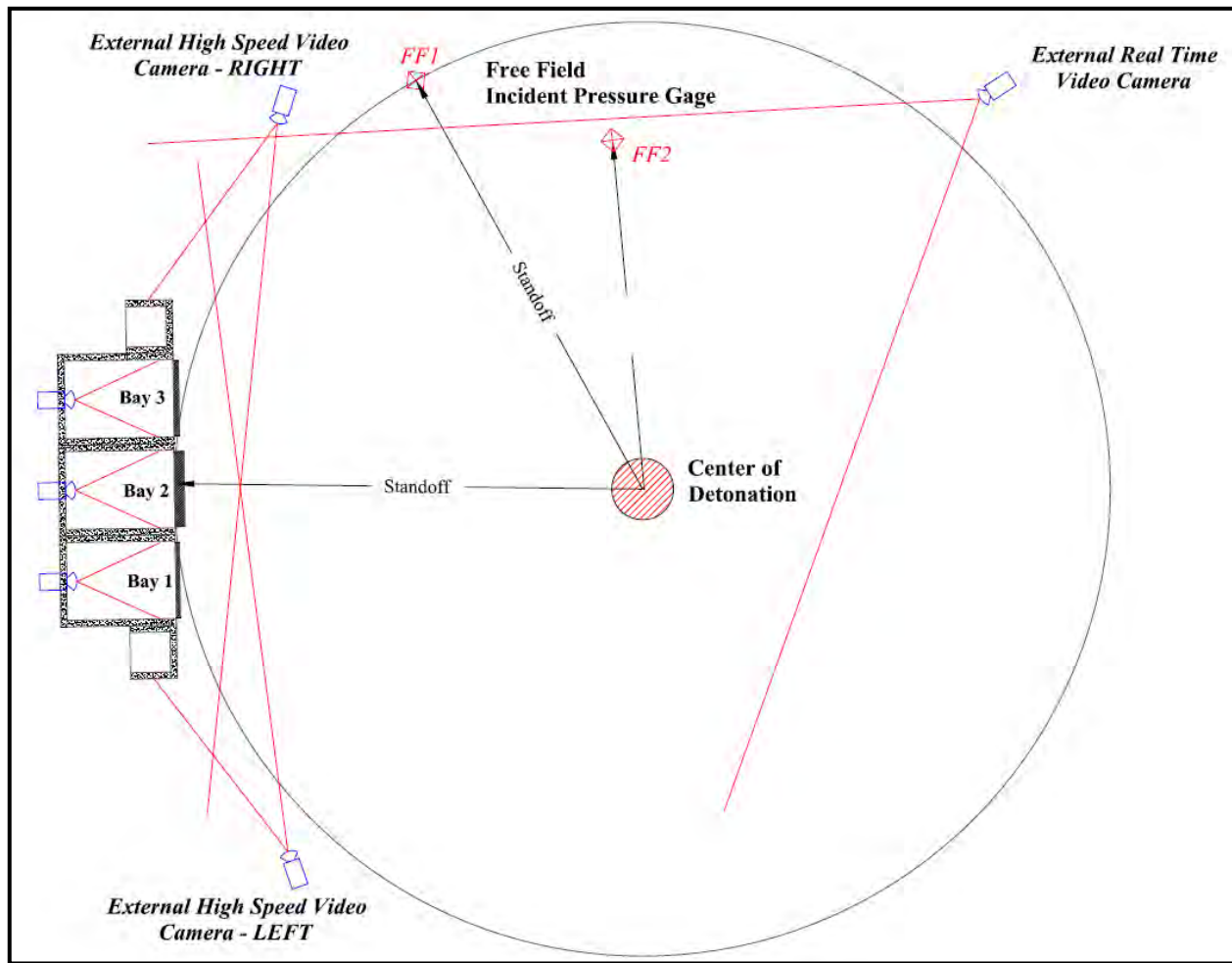


Figure 13. Plan View of the Test Set-up and Instrumentation Layout

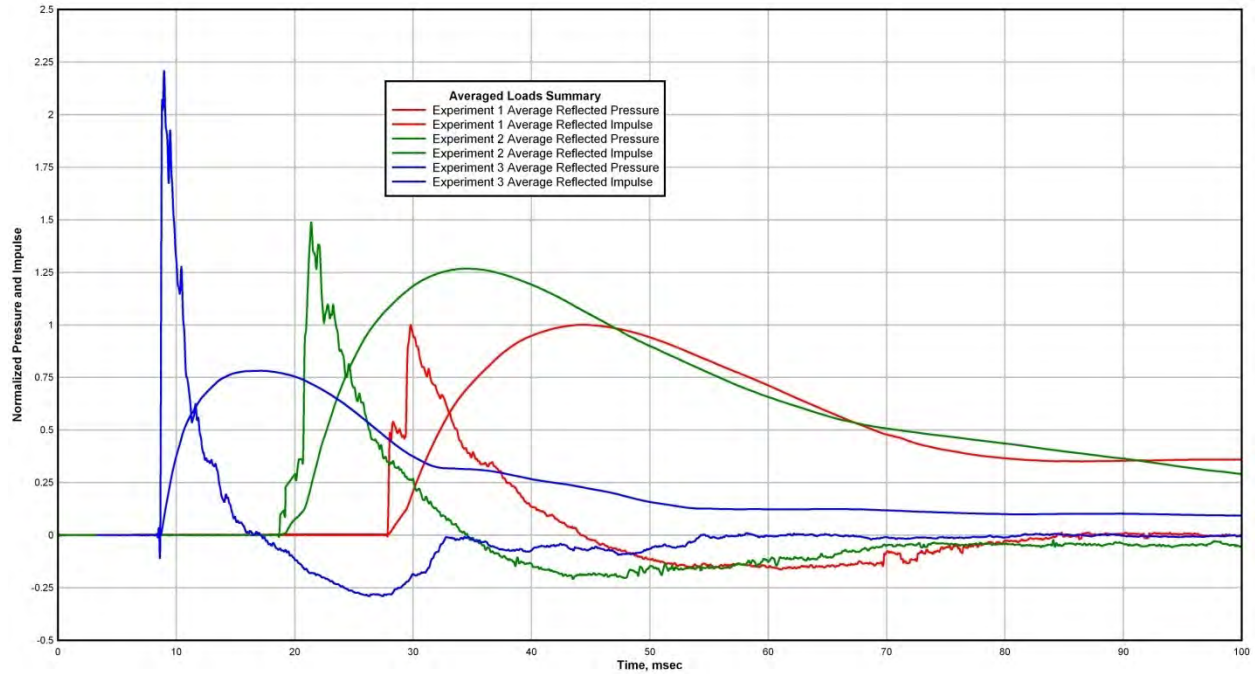


Figure 14. Summary of Average Pressures and Impulses

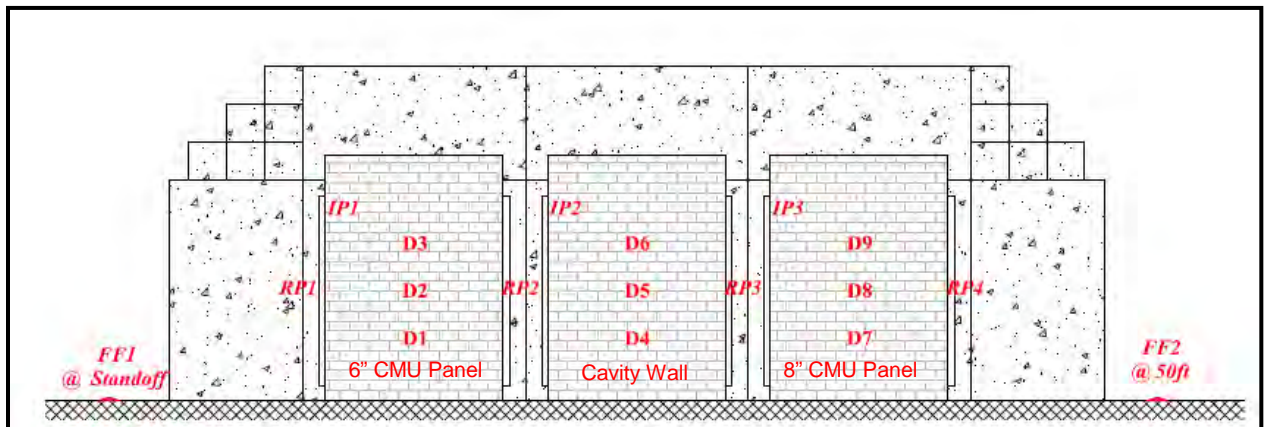


Figure 15. Front View of the Test Set-up Describing Instrumentation Position and Designation

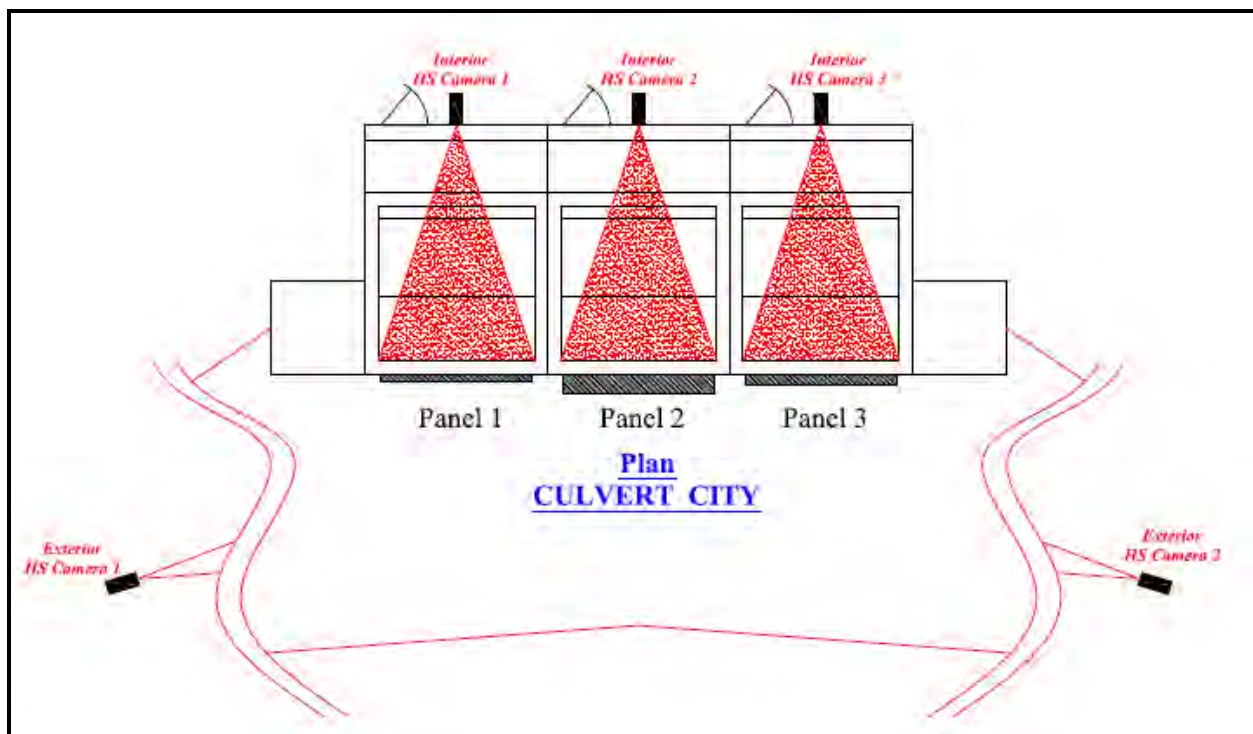


Figure 16. Plan View of the Test Set-up Describing Videography Position and Designation

2.6. Full-scale Dynamic Test Results

2.6.1. Experiment 1

Exterior views of the residual condition of all three test panels are depicted in Figures 17 and 18.



Figure 17. Experiment 1 Post-detonation Front View



Figure 18. Experiment 1 Post-detonation Side Views

6-inch CMU Panel

The deflection gauge measurements are shown in Figure 19, where the maximum dynamic deflection at mid-span of the panel of 10.5 inches can be noted. Selected still images captured from high-speed video illustrating the progression of failure are provided in Figure 20. Interior and exterior views of the residual condition of the 6-inch CMU panel are provided in Figure 21. The response is characterized by a relatively ductile flexural response with a rotation of approximately 10 degrees. Flexural tension cracking occurred along the center one-third mortar joints. Only one small (approximately 4 in²) piece of CMU spalled from the inside surface of the panel. A residual plastic deflection of approximately 9 inches was retained. There was no significant fracture of the front surface of the panel.

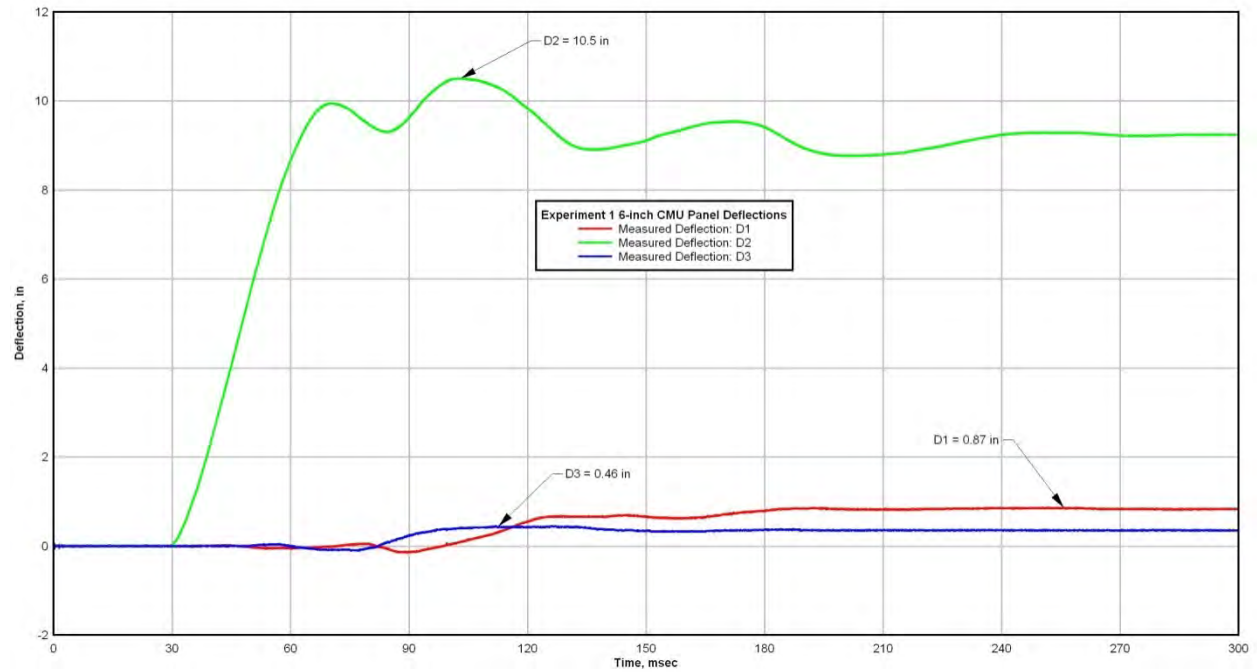


Figure 19. Experiment 1 6-inch CMU Panel Deflections

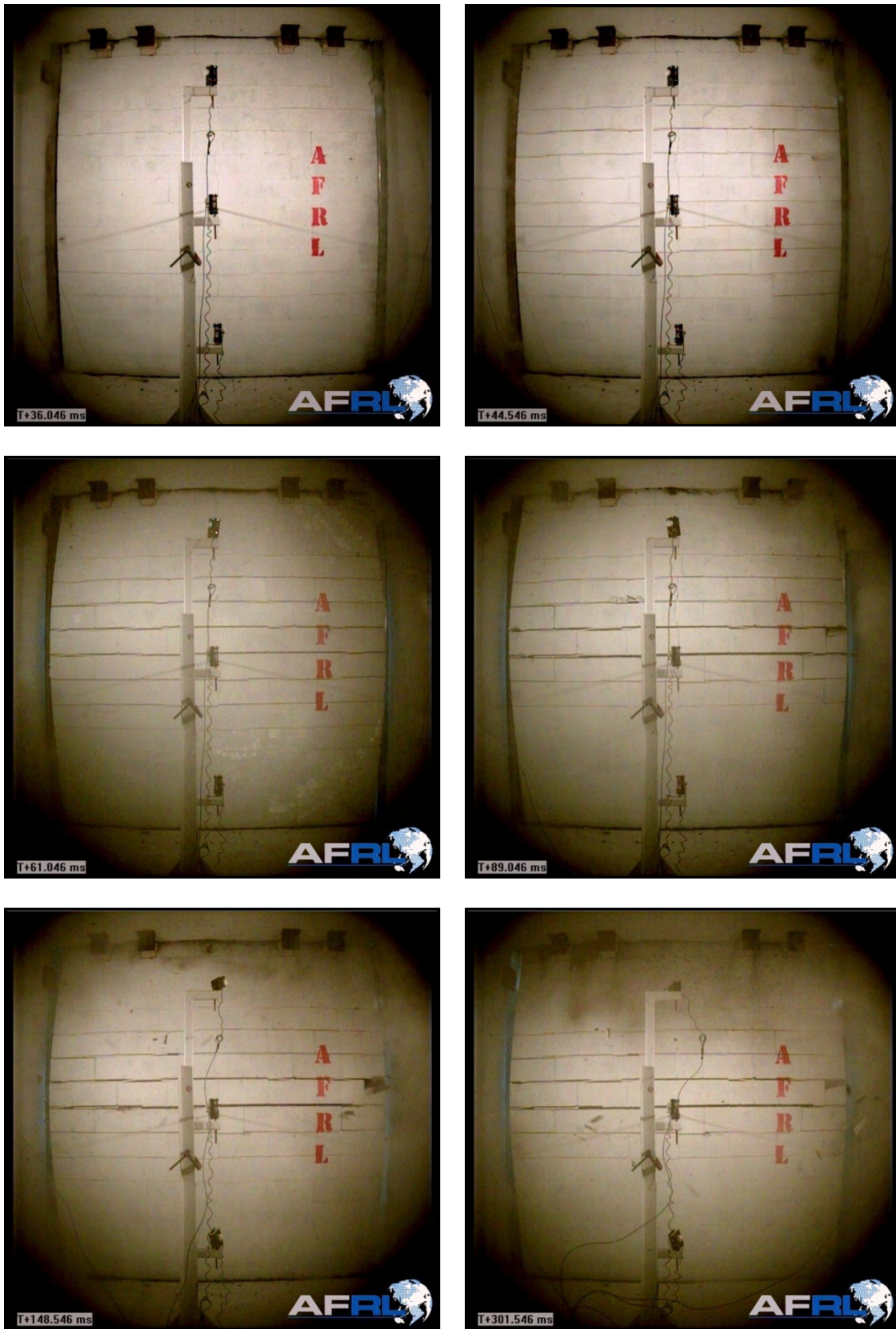


Figure 20. Experiment 1 6-inch CMU Panel Interior Images

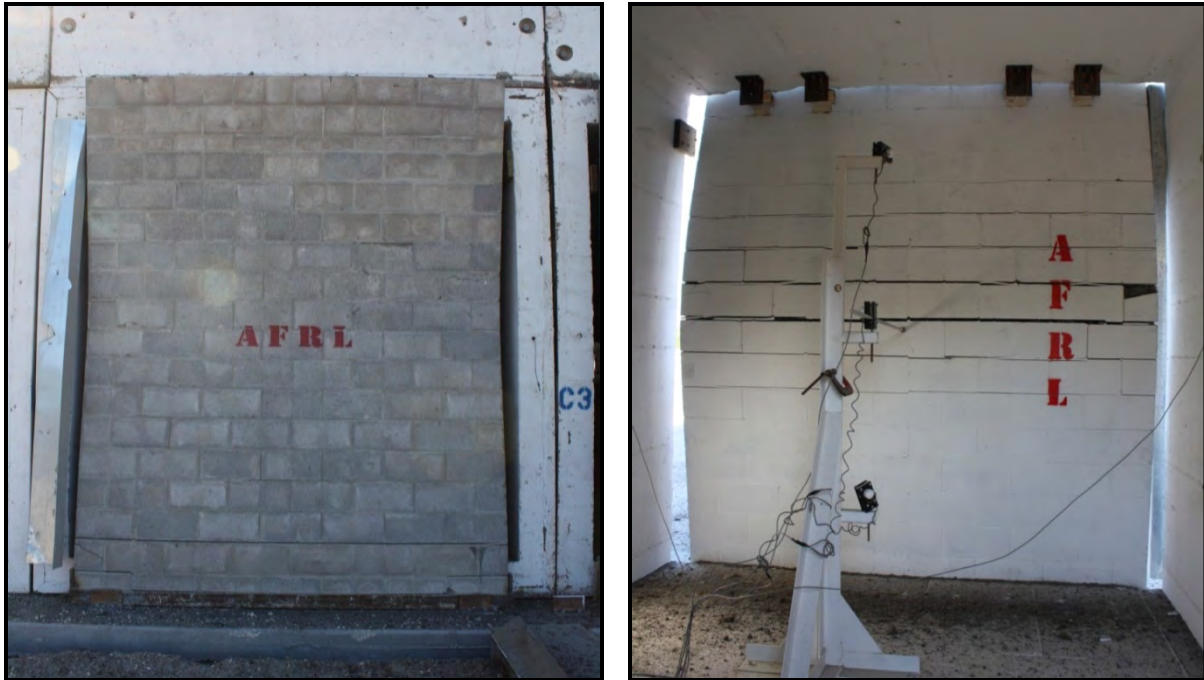


Figure 21. Experiment 1 Post-Detonation 6-inch CMU Panel Exterior View (left) and Interior View (right)

8-inch CMU Panel

The deflection gauge measurements are shown in Figure 22. The maximum dynamic deflection at mid-span of the panel was 8.1 inches. Selected still images captured from high-speed video illustrating the progression of failure are provided in Figure 23. Interior and exterior views of the residual condition of the 8-inch CMU panel are provided in Figure 24. The response is characterized by flexural cracks initiating across the fifth-from-bottom and fourth-from-top mortar joints, then progressing to a spalling failure of the inside face shell of six CMUs in the ungrouted/unreinforced region near the center of the panel (Figs. 25-27). The maximum rotation was approximately 7.7 degrees. A residual plastic deflection of approximately 7 inches was retained. Complete breaching of an approximately 10 in² area occurred.

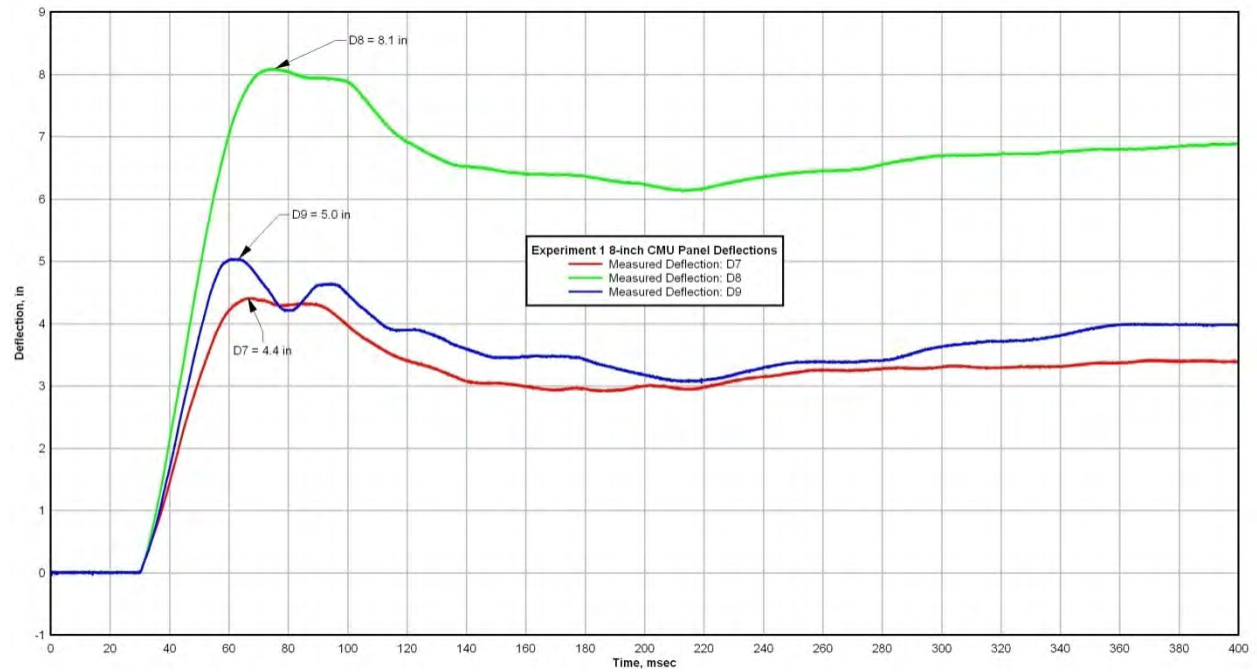


Figure 22. Experiment 1 8-inch CMU Panel Deflections

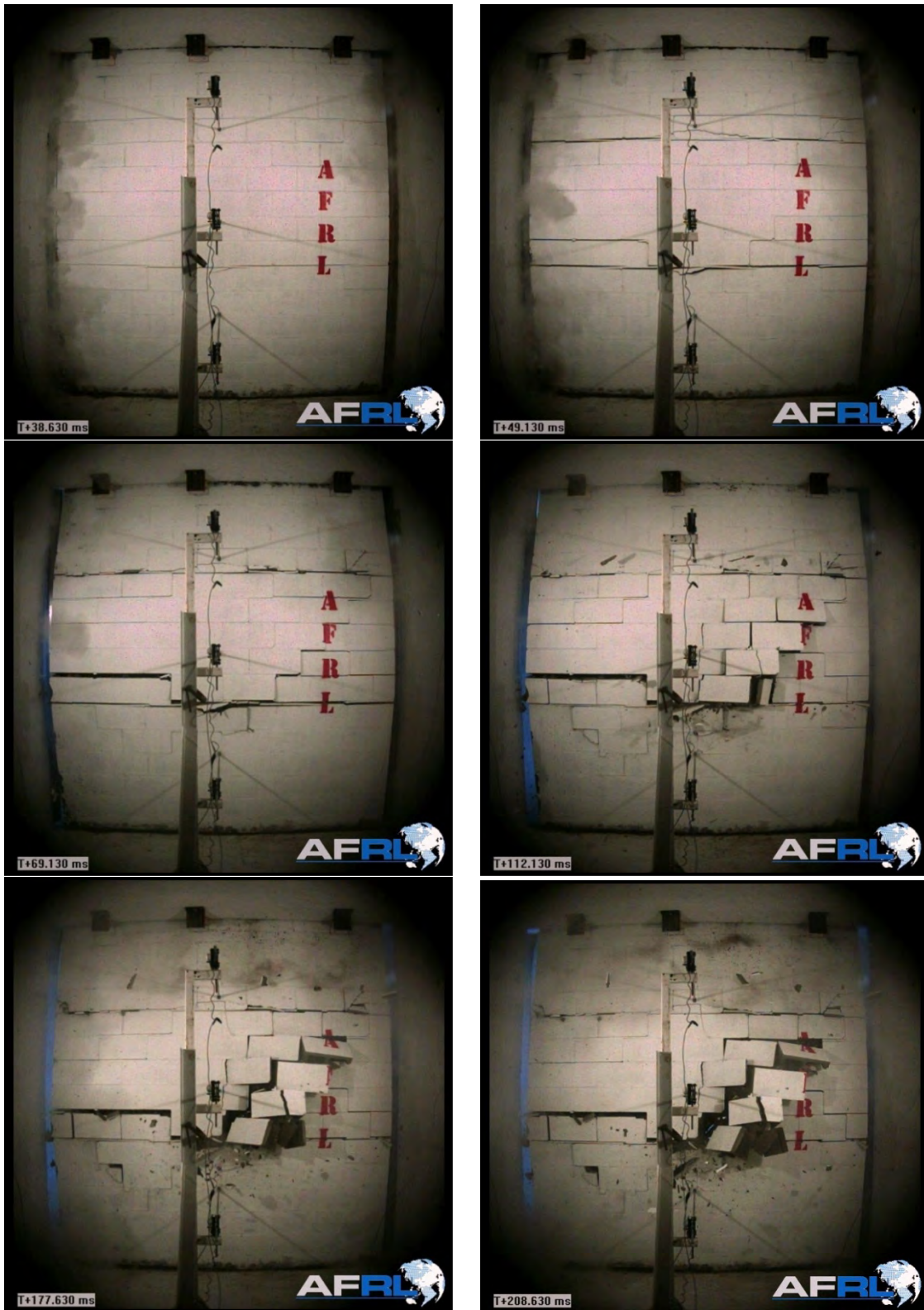


Figure 23. Experiment 1 8-inch CMU Panel Interior Images



Figure 24. Experiment 1 Post-detonation 8-inch CMU Panel Exterior View (left) and Interior View (right)

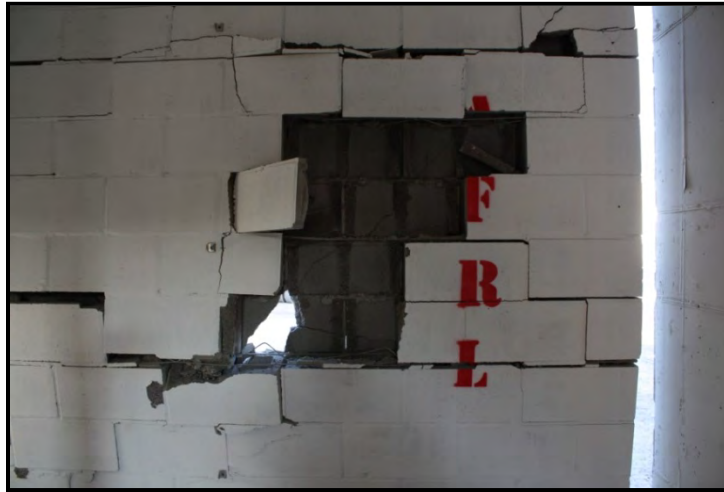


Figure 25. Experiment 1 Breaching Failure of the 8-inch CMU Panel

Cavity Wall Panel

The deflection gauge measurements are shown in Figure 26, where the maximum dynamic deflection at mid-span of the panel of 5.7 inches was observed. Selected still images captured from high-speed video illustrating the progression of failure are provided in Figure 27. Interior and exterior views of the residual condition of the cavity wall panel are provided in Figure 28. The response is characterized by flexural tension cracking along the center one-third mortar joints, with a prominent step pattern in early timing. The maximum rotation was approximately 5.4 degrees. A residual plastic deflection of approximately 3 inches was retained. There was no significant fracturing of the CMUs, such as occurred in the comparable wall without veneer (8-inch CMU Panel). The upper five courses of brick veneer collapsed in front of the panel, but much of the veneer remained attached and stable.

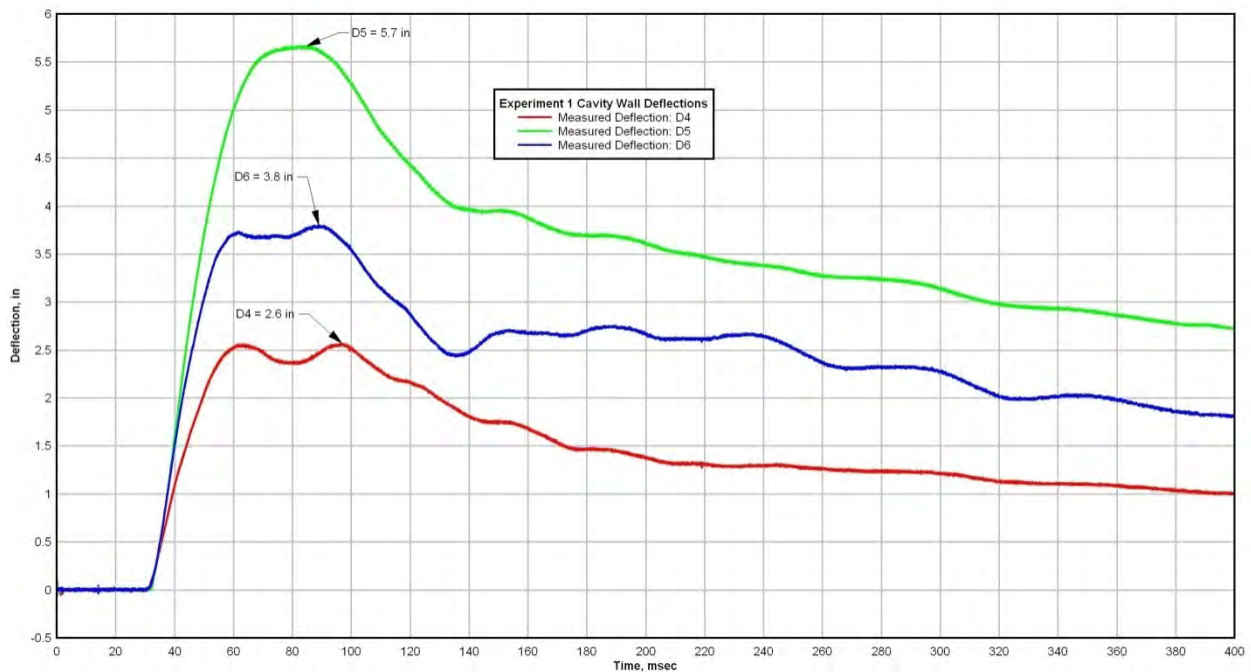


Figure 26. Experiment 1 Cavity Wall Deflections

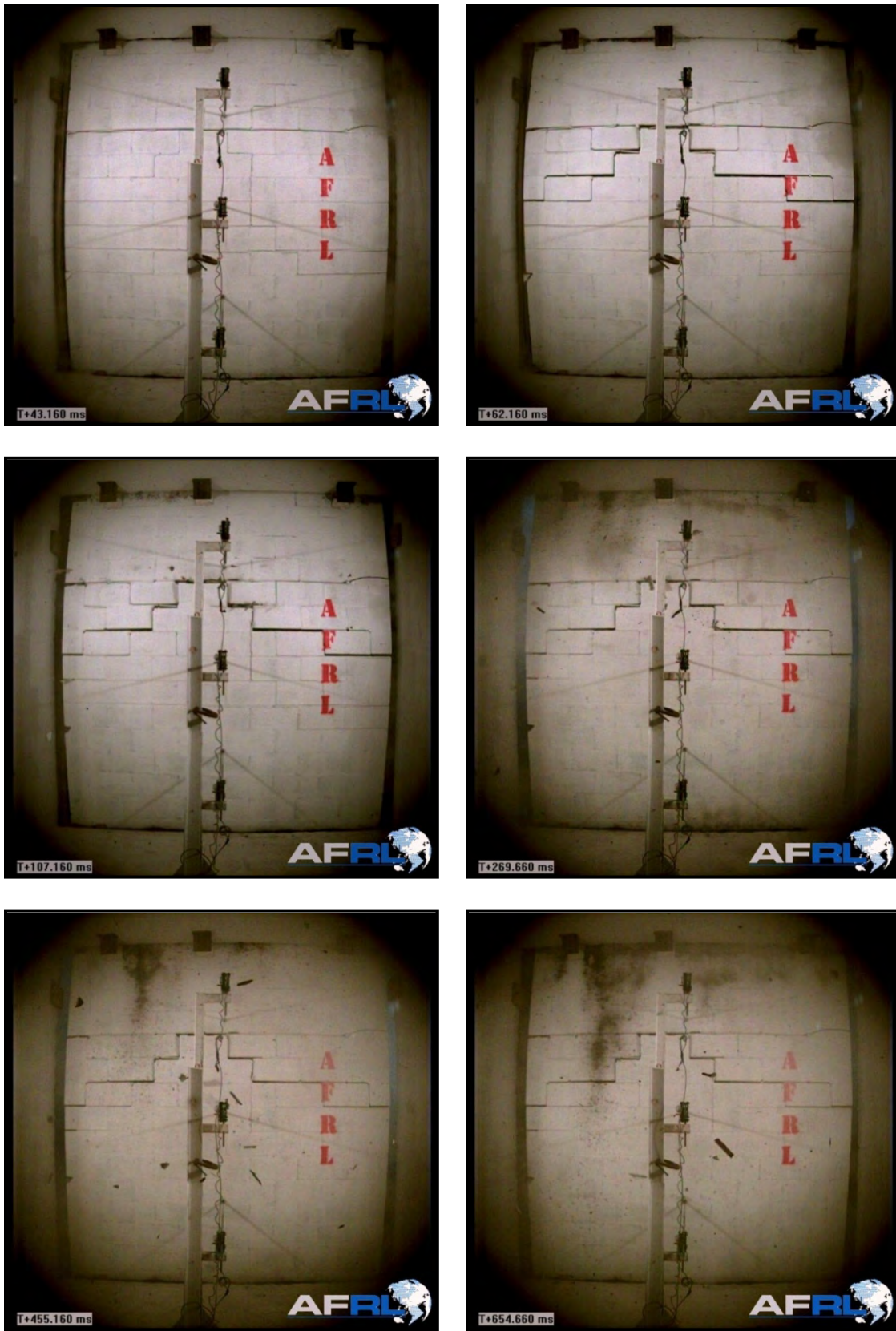


Figure 27. Experiment 1 Cavity Wall Interior Images



Figure 28. Experiment 1 Post-detonation Cavity Wall Exterior View (left) and Interior View (right)

2.6.2. Experiment 2

Exterior views of the residual condition of all three test panels are depicted in Figures 29 and 30.



Figure 29. Experiment 2 Post-Detonation Front View



Figure 30. Experiment 2 Post-Detonation Side Views

6-inch CMU Panel

The deflection gauge measurements are shown in Figure 31, where the maximum dynamic deflection at mid-span of the panel of 20.1 inches was measured. Selected still images captured from high-speed video illustrating the progression of failure are provided in Figure 32. Interior and exterior views of the residual condition of the 6-inch CMU panel are described in Figures 33 and 34. The response is characterized by flexural cracks uniformly initiating across the center 50% of the mortar joints, then progressing to a large joint opening at mid-span of the panel. Spalling of one half-CMU face shell and complete breaching of another half-CMU occurred. There was no significant fracturing of the exterior surface of the panel. The panel remained stable after a maximum rotation of approximately 19 degrees. A residual plastic deflection of approximately 18 inches was retained.

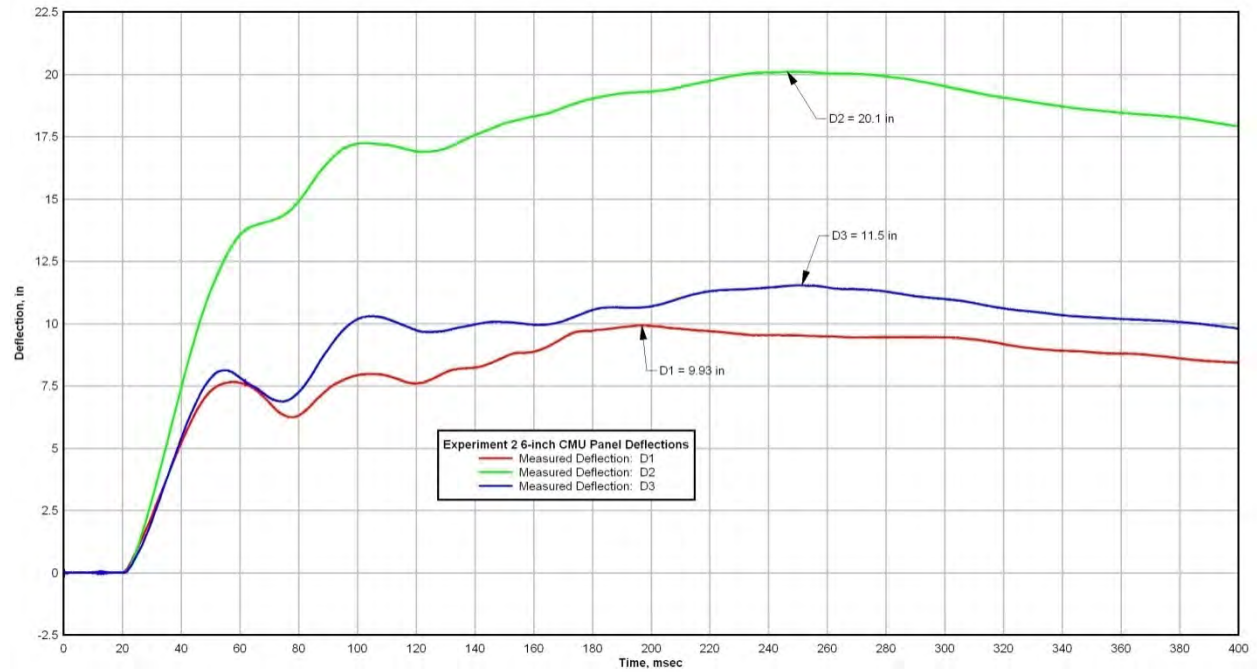


Figure 31. Experiment 2 6-inch CMU Panel Deflections

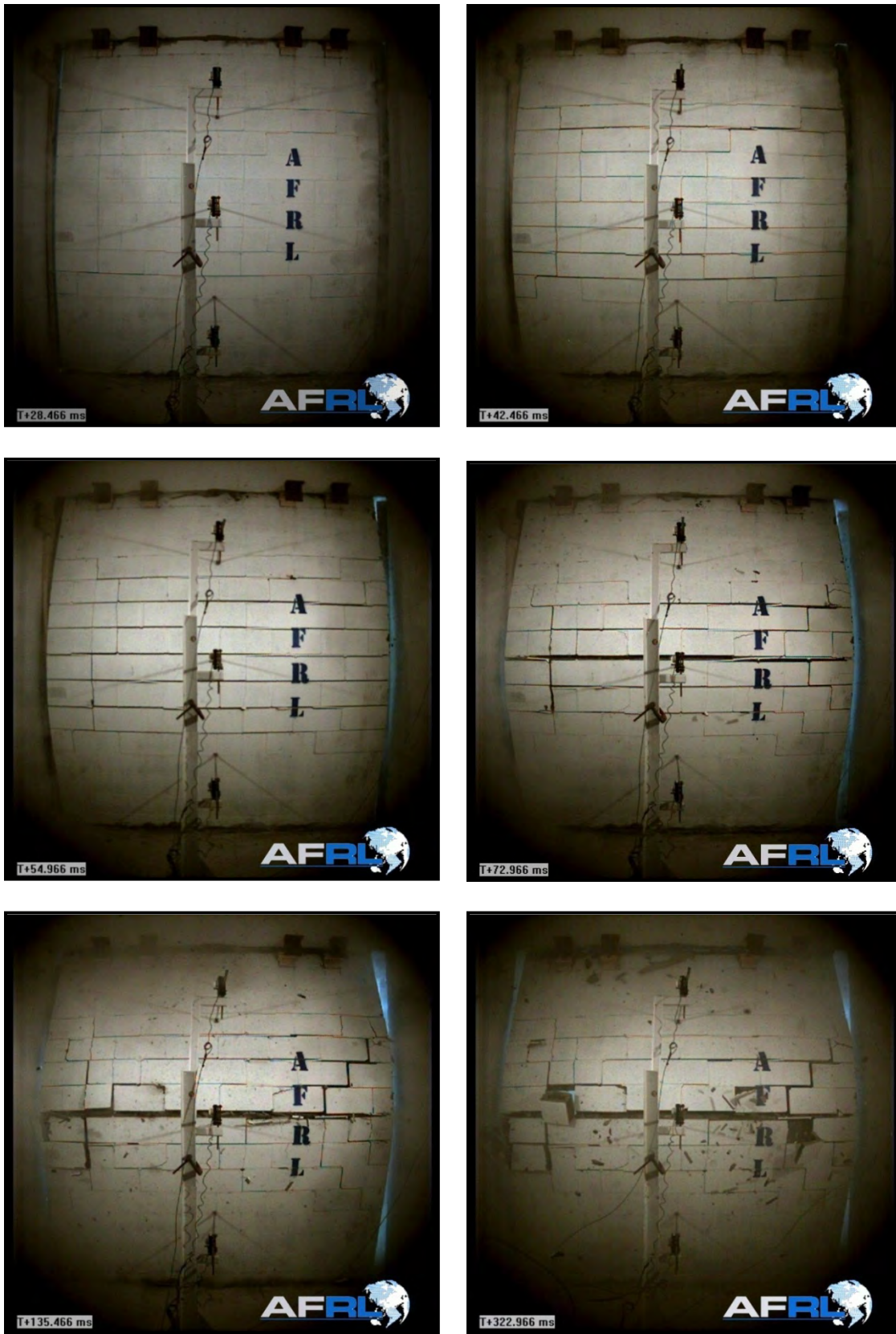


Figure 32. Experiment 2 6-inch CMU Panel Interior Images



Figure 33. Experiment 2 Post-detonation 6-inch CMU Panel Exterior View (left) and Interior View (right)

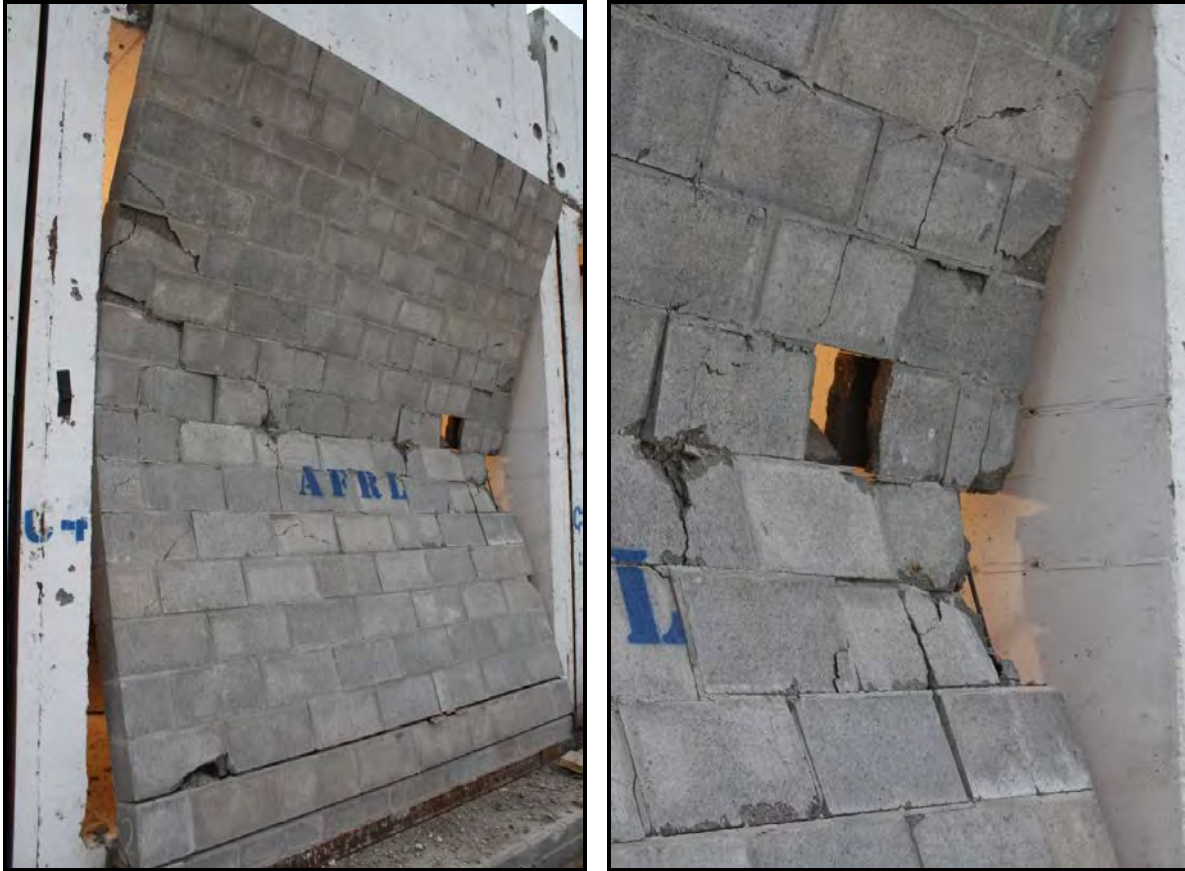


Figure 34. Experiment 2 Post-detonation 6-inch CMU Panel Closer Outside Views

8-inch CMU Panel

The deflection gauge measurements are shown in Figure 35, where the maximum dynamic deflection at mid-span of the panel was 10.9 inches. Selected still images captured from high-speed video illustrating the progression of failure are provided in Figure 36. Interior and exterior views of the residual condition of the 8-inch CMU panel are described in Figure 37. The response is characterized by a very dramatic breaching of the center 50% of the panel; CMUs between the grouted and reinforced cells fractured into many pieces (Fig.38). Practically all of the CMU breach fragments ended up inside the reaction structure bay. Mortar joint separation at one grouted/reinforced cell location also occurred.

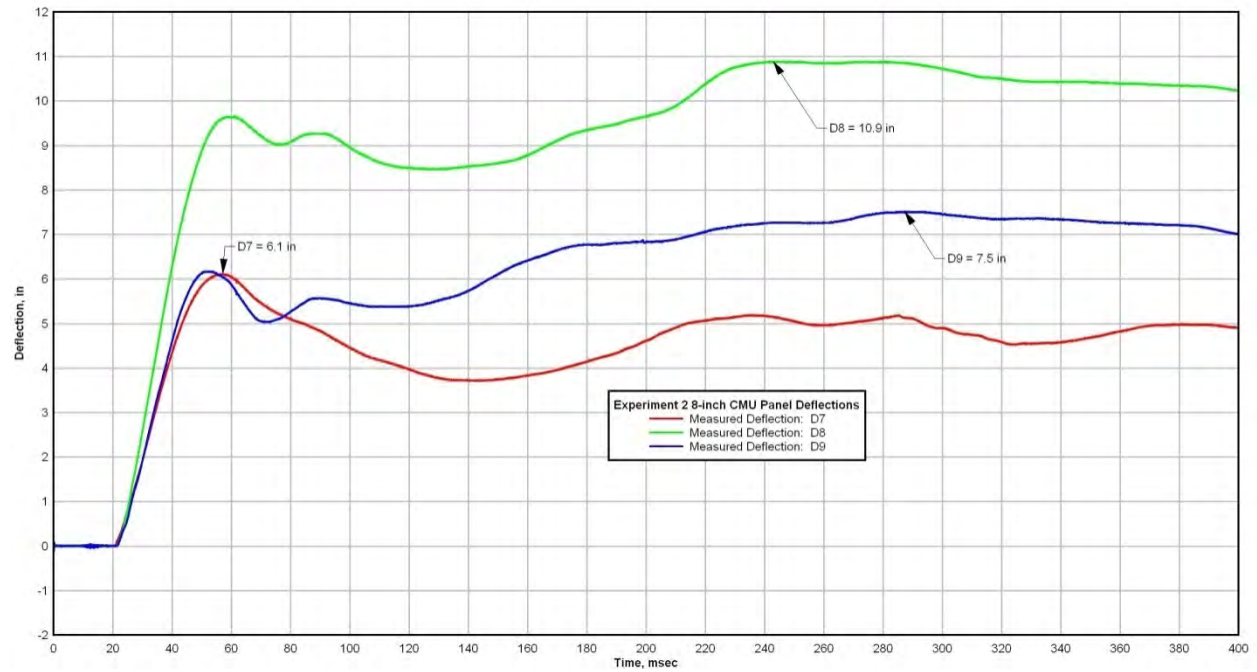


Figure 35. Experiment 2 8-inch CMU Panel Deflections

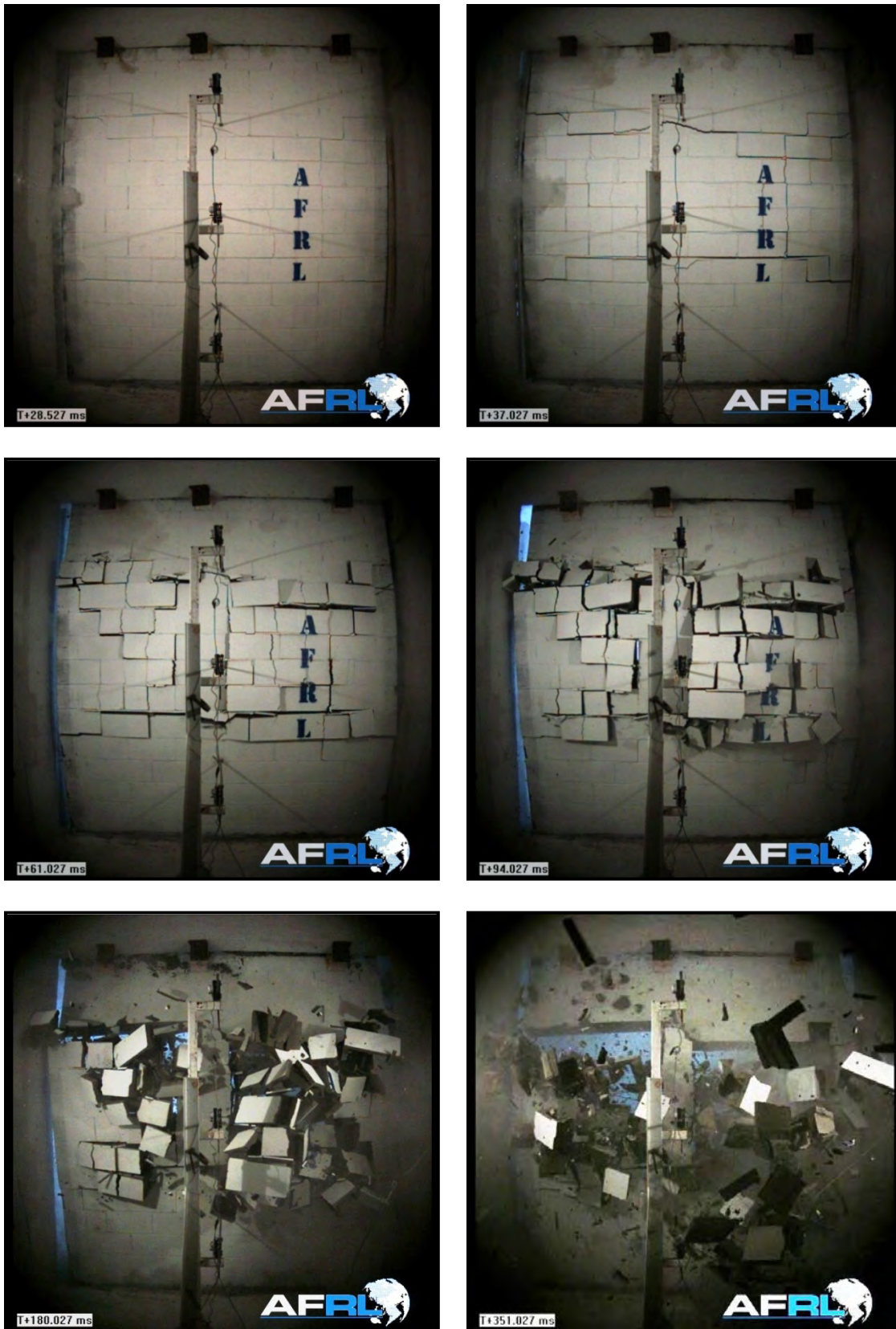


Figure 36. Experiment 2 8-inch CMU Panel Interior Images



Figure 37. Experiment 2 Post-detonation 8-inch CMU Panel Exterior View (left) and Interior View (right)



Figure 38. Experiment 2 Post-detonation 8-inch CMU Panel CMU Damage



Figure 39. Experiment 2 Post-detonation 8-inch CMU Panel CMU Damage

Cavity Wall Panel

The deflection gauge measurements are shown in Figure 40, where the maximum dynamic deflection at mid-span of the panel of 10.4 inches was observed. Selected still images captured from high-speed video illustrating the progression of failure are provided in Figure 41. Interior and exterior views of the residual condition of the cavity wall panel are described in Figure 42. The response is characterized by significant spalling of the interior face shells at the center of the panel and complete breaching of the bottom three courses. The brick veneer completely collapsed in front of the reaction structure. The foam insulation of the top half of the panel remained attached to the 8-inch CMU wythe. Local indentation of the foam occurred; however, significant crushing was not apparent.

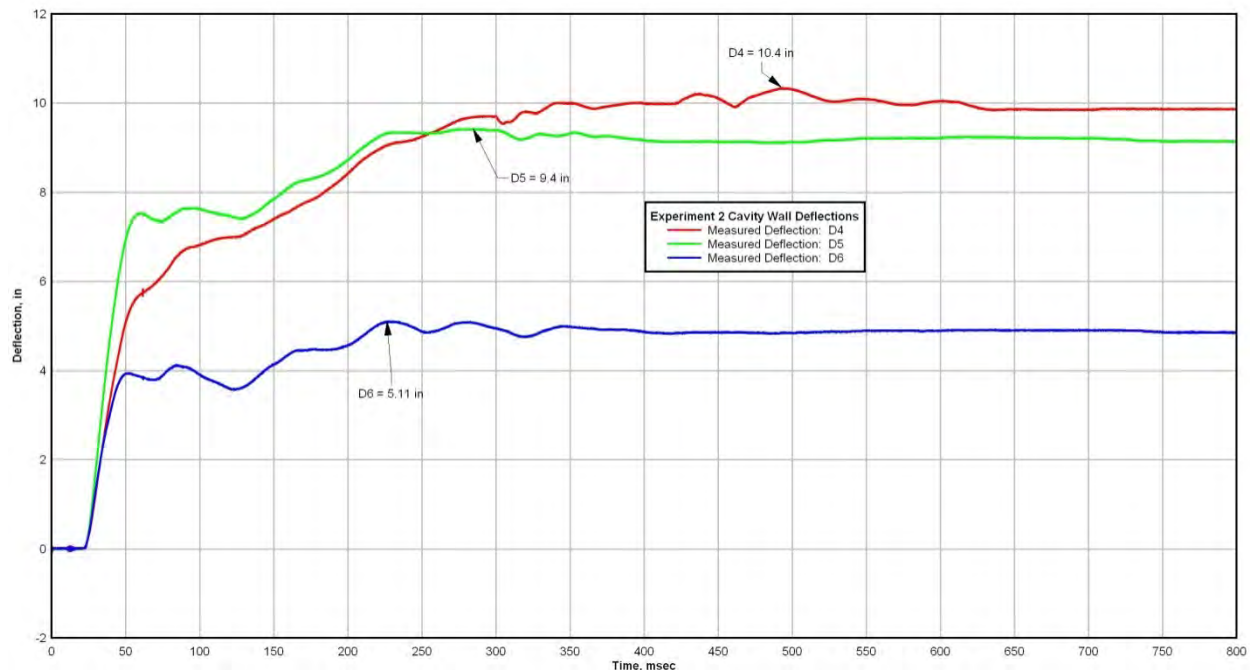


Figure 40. Experiment 2 Cavity Wall Deflections

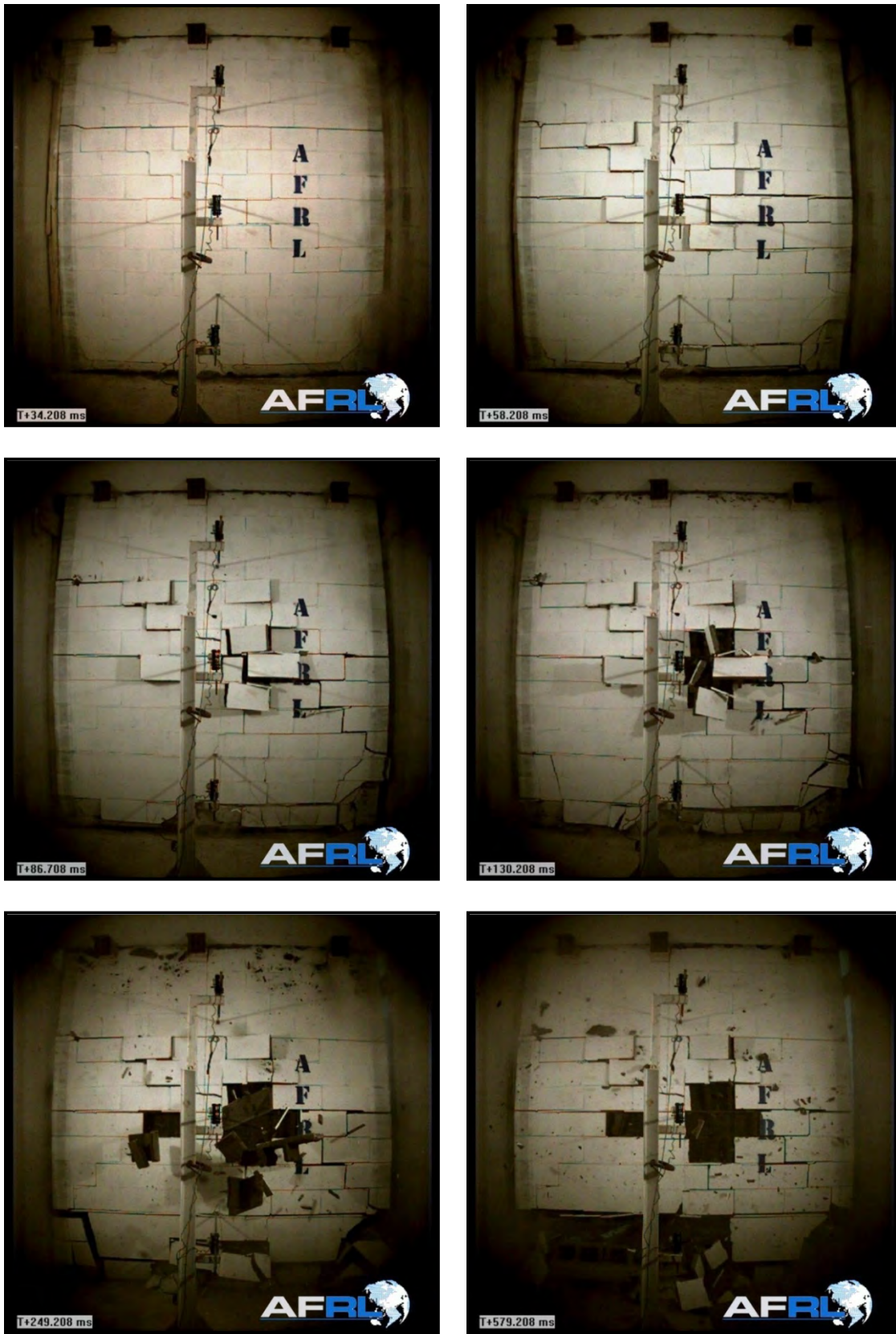


Figure 41. Experiment 2 Cavity Wall Interior Images



Figure 42. Experiment 2 Post-detonation Cavity Wall Exterior View (left) and Interior View (right)



Figure 43. Experiment 2 Post-detonation Cavity Wall Foam Damage

2.6.3. Experiment 3

Exterior views of the residual condition of all three test panels are depicted in Figures 44 and 45.



Figure 44. Experiment 3 Post-detonation Front View



Figure 45. Experiment 3 Post-detonation Side Views

6-inch CMU Panel

The deflection gauge measurements are shown in Figure 46, where the maximum dynamic deflection at mid-span of the panel was 12.8 inches. Selected still images captured from high-speed video illustrating the progression of failure are provided in Figure 47. Interior and exterior views of the residual condition of the 6-inch CMU panel are described in Figures 48 and 49. The response is characterized by flexural cracks uniformly initiating across the center 60% of the mortar joints then progressing to a breaching of approximately 9 CMUs at the lower side of the panel. This breaching was exacerbated by grout voids in the column nearest to the breach. There was no other significant spalling on the interior. Face shell fracture occurred along the bottom two courses on the front of the panel.

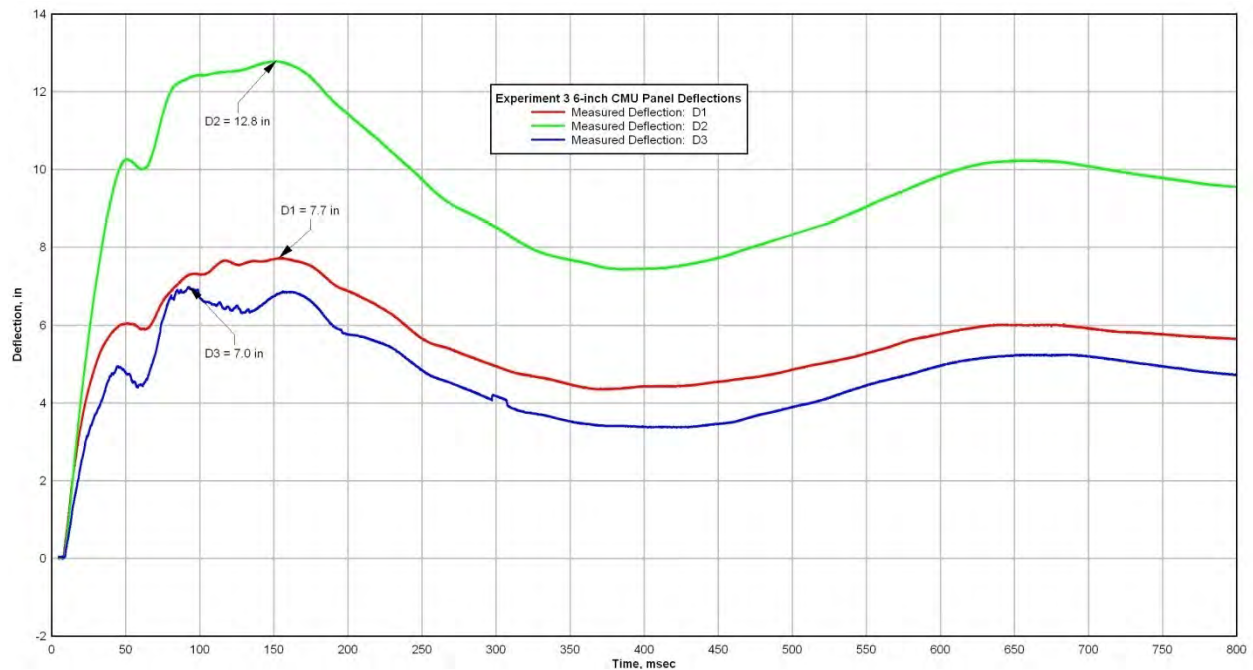


Figure 46. Experiment 3 6-inch CMU Panel Deflections

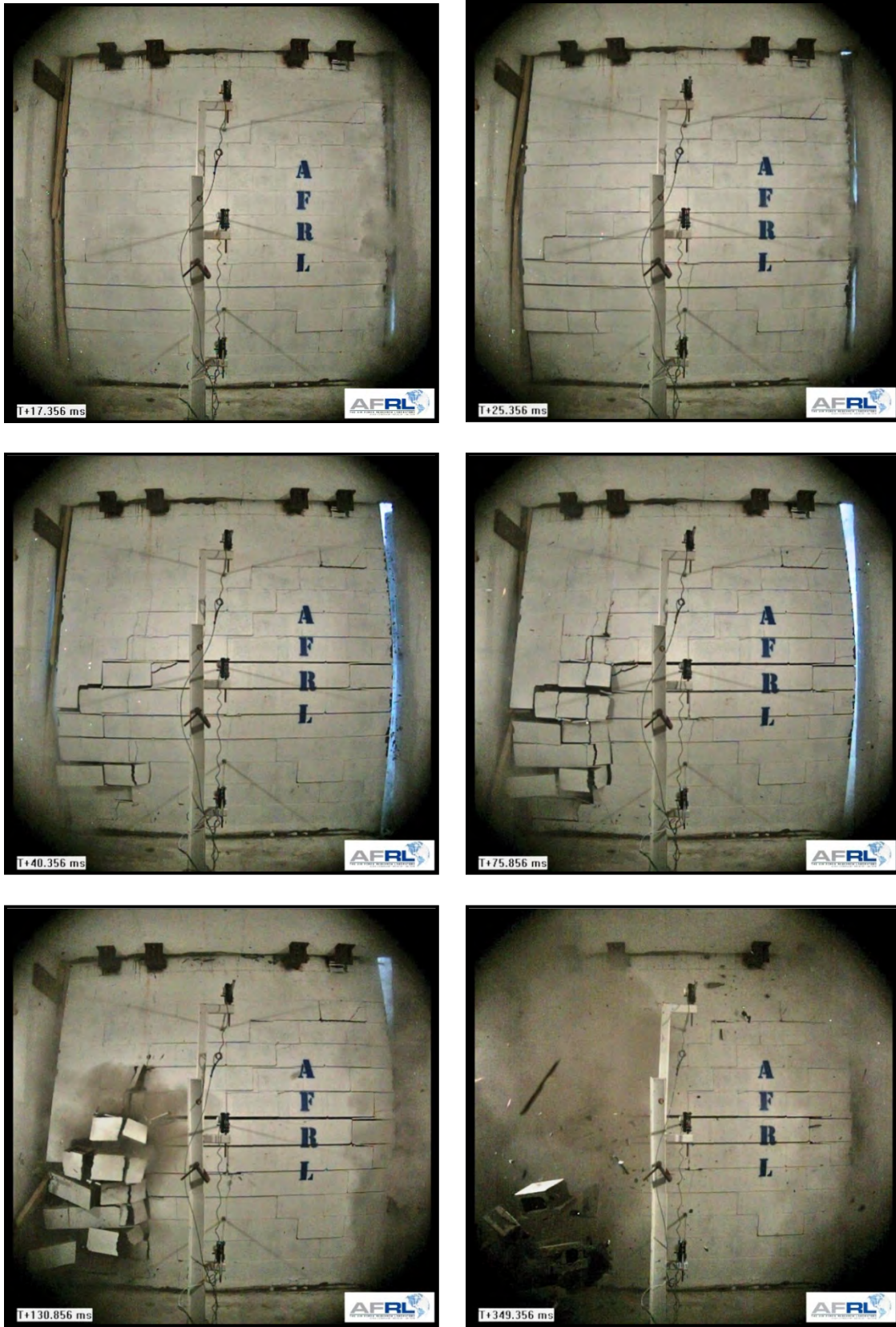


Figure 47. Experiment 3 6-inch CMU Panel Interior Images



Figure 48. Experiment 3 Post-detonation 6-inch CMU Panel Exterior View (left) and Interior View (right)

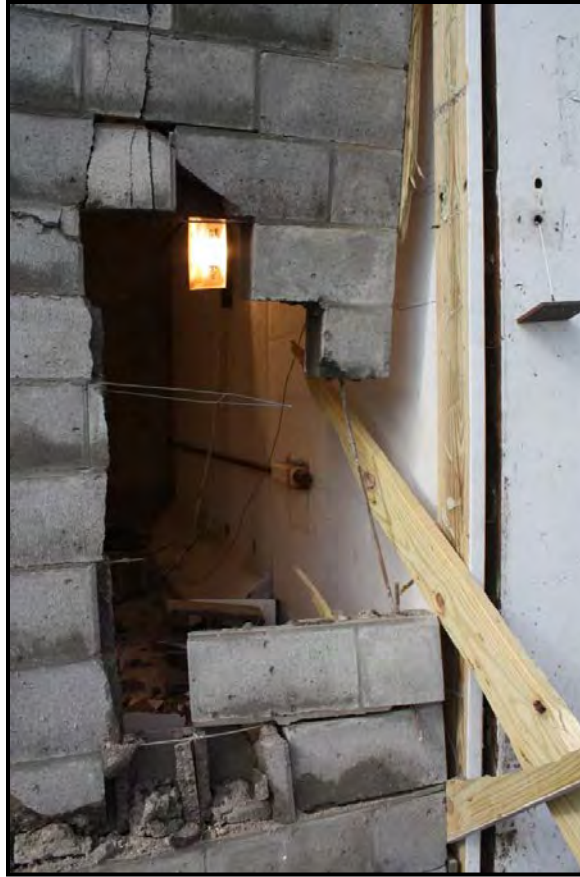


Figure 49. Experiment 3 Post-detonation 6-inch CMU Panel Close-up Views

8-inch CMU Panel

The deflection gauge measurements are shown in Figure 50, where the maximum dynamic deflection at mid-span of the panel was 9.9 inches. Selected still images captured from high-speed video illustrating the progression of failure are provided in Figure 51. Interior and exterior views of the residual condition of the 8-inch CMU panel are described in Figures 52-54. The response is characterized by breaching of approximately 40% of the CMUs between the two most distant grouted cells. This breaching was exacerbated by grout voids in the edge grouted cells nearest to the breach. Face shell fracture occurred along the bottom three courses on the front of the panel (Figs. 52-54).

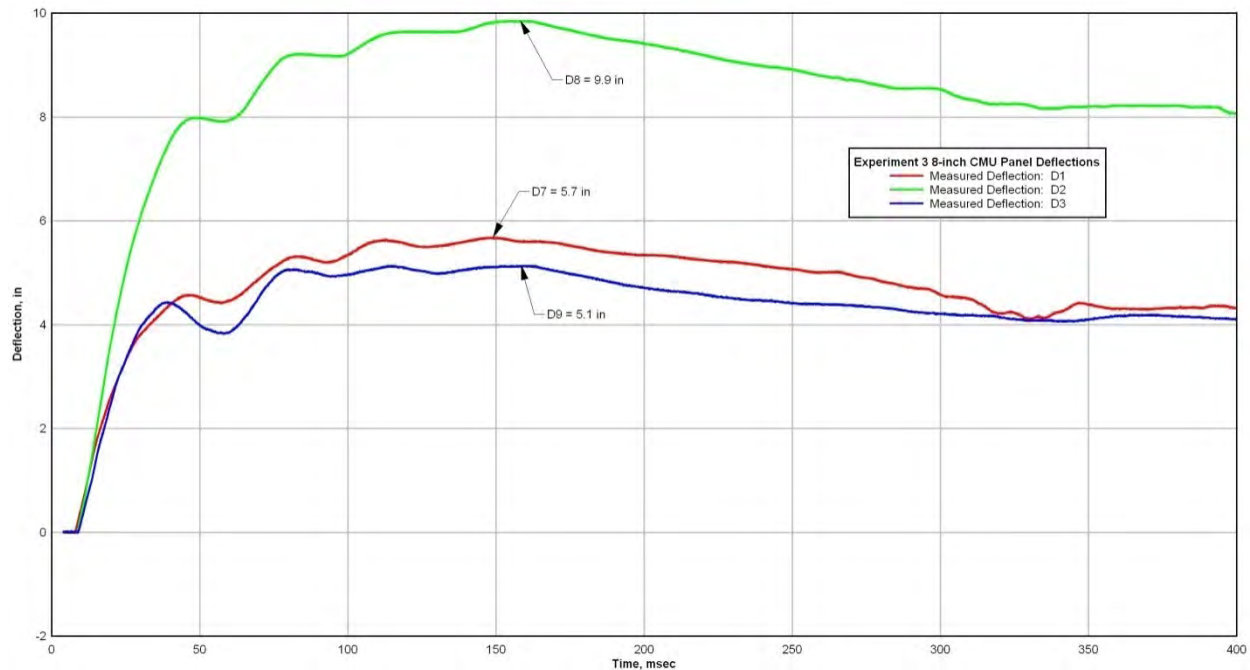


Figure 50. Experiment 3 8-inch CMU Panel Deflections

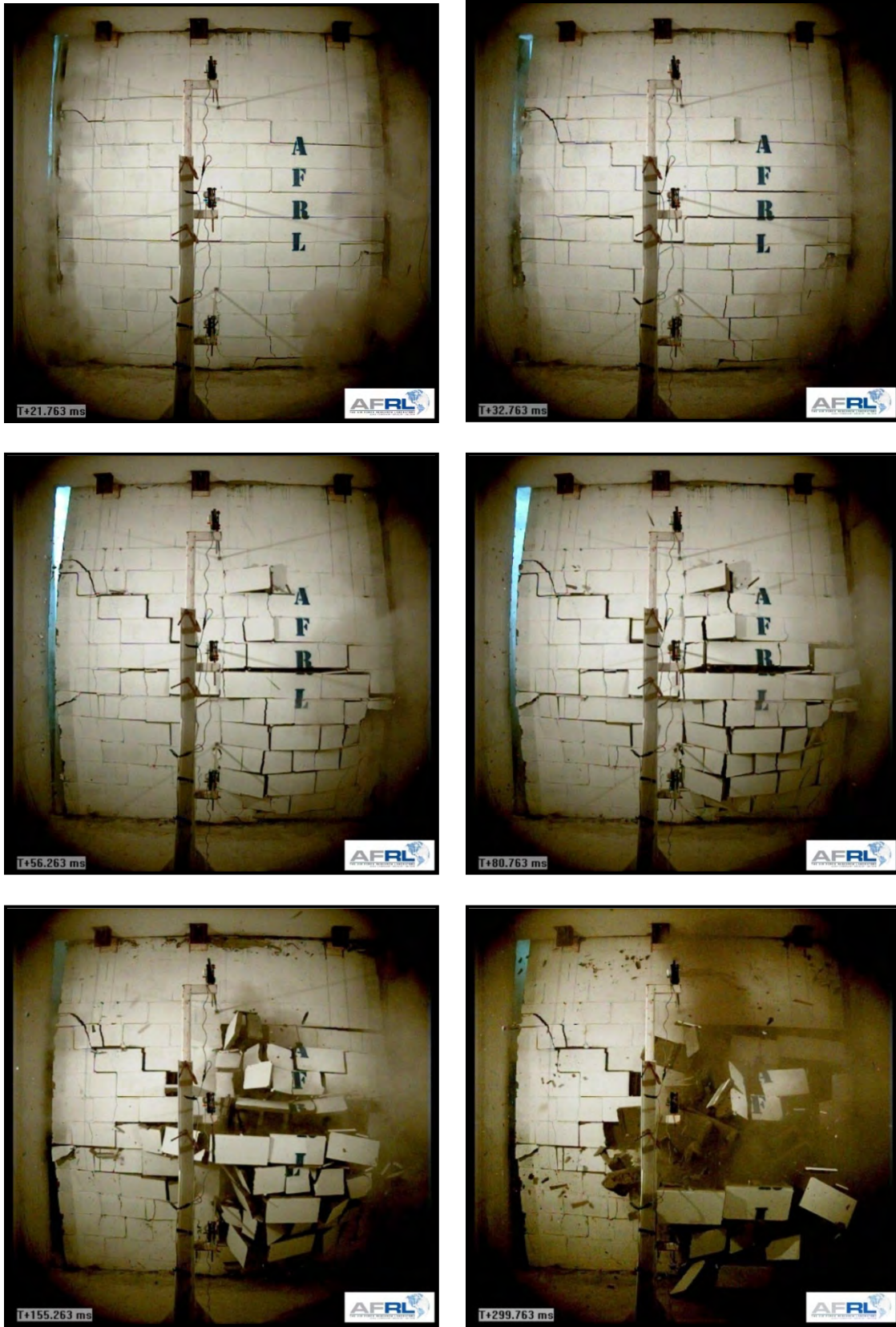


Figure 51. Experiment 3 8-inch CMU Panel Interior Images



Figure 52. Experiment 3 Post-detonation 8-inch CMU Panel Exterior View (left) and Interior View (right)



Figure 53. Experiment 3 Post-detonation 8-inch CMU Panel Close-up Exterior Views



Figure 54. Experiment 3 Post-detonation 8-inch CMU Panel Close-up Interior Views

Cavity Wall Panel

The deflection gauge measurements are shown in Figure 55, where the maximum dynamic deflection at mid-span of the panel of 6.6 inches was observed. Selected still images captured from high-speed video illustrating the progression of failure are provided in Figure 56. Interior and exterior views of the residual condition of the cavity wall panel are described in Figures 57-59. The response is characterized by breaching of approximately 30% of the CMUs between the grouted/reinforced cells, along with spalling of another 30% of the interior face shells. 80% of the brick veneer collapsed in front of the reaction structure. The foam insulation was extensively fragmented, but the insulation of the top 70% of the panel remained attached to the 8-inch CMU wythe.

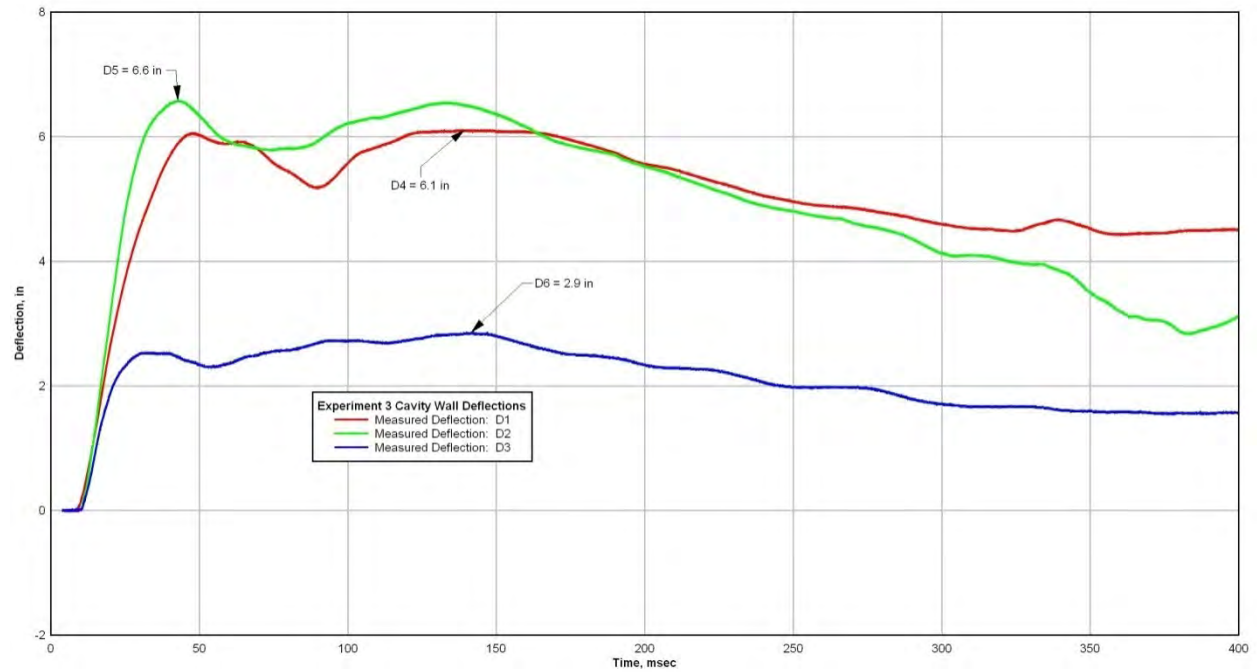


Figure 55. Experiment 3 Cavity Wall Deflections

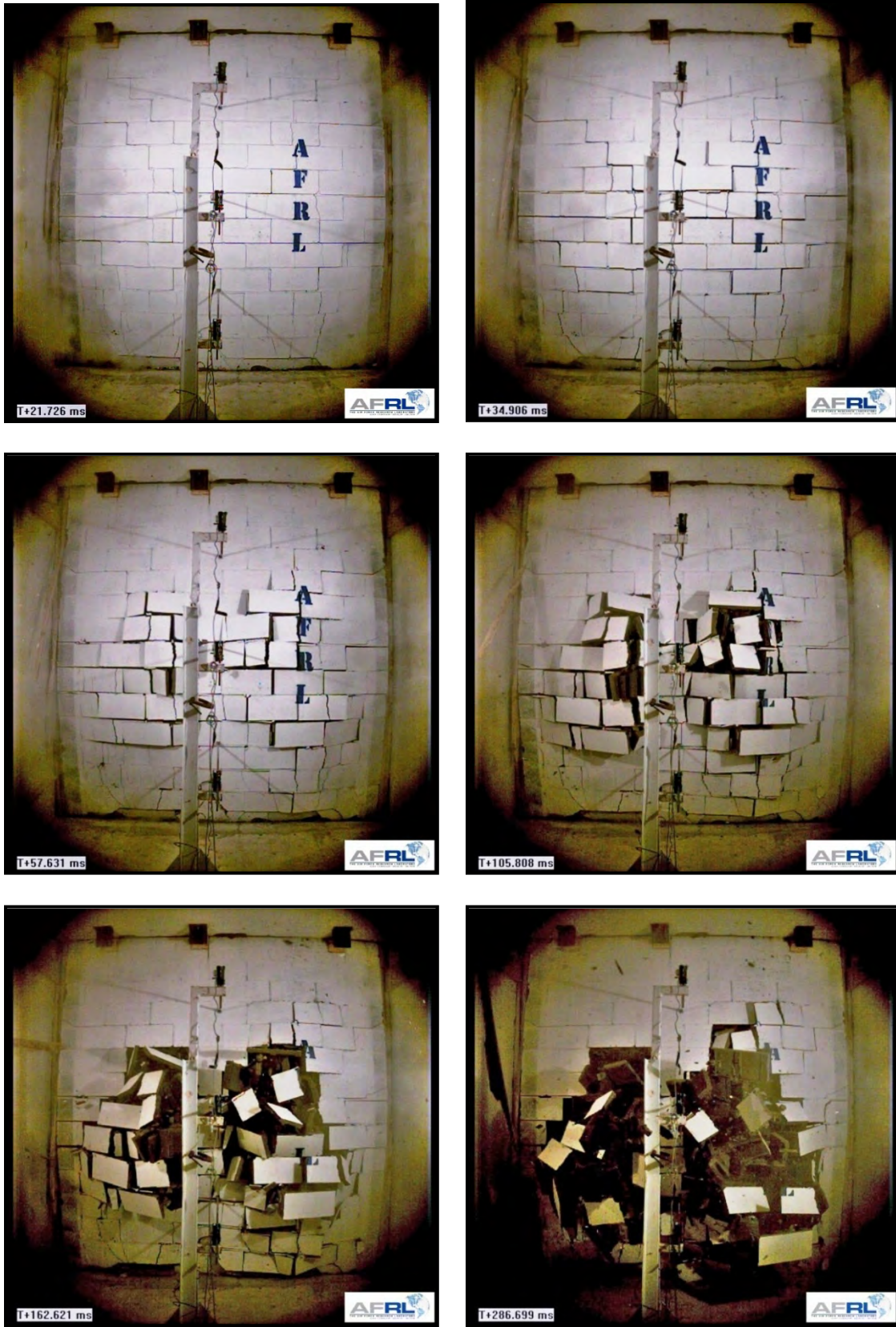


Figure 56. Experiment 3 Cavity Wall Interior Video Capture



Figure 57. Experiment 3 Post-detonation Cavity Wall Exterior View (left) and Interior View (right)



Figure 58. Experiment 3 Post-detonation Cavity Wall Close-up Views



Figure 59. Experiment 3 Post-detonation Cavity Wall Close-up Views

3. ANALYSIS, EVALUATION, AND COMPARISON

3.1. Flexural Resistance of Reinforced Masonry

In general, the out-of-plane resistance of reinforced masonry is defined using the same principles and methodology as used for reinforced concrete design. For general commercial and residential construction in the US, the masonry design resistances are defined using ACI 530 and ACI 530.1 (MSJCC, Masonry Standards Joint Committee Code, Building Code Requirements for Masonry Structures). Reinforced masonry tends to be lightly reinforced, resulting in the ability to provide a ductile response. The three test panel configurations considered in these experiments were designed and constructed at the minimum standards for reinforcement, and therefore, would be considered lightly reinforced.

A generic moment-curvature representation for an under-reinforced masonry section is provided in Figure 60. Prior to cracking, the resistance is defined by net section properties of the uncracked section; the minimal contribution of the steel reinforcement can be ignored. Furthermore, for minimally reinforced sections, it is typical that one line of vertical reinforcing bars be placed at the thru-thickness center of the wall, and therefore would not significantly contribute to the gross uncracked moment of inertia. After cracking has occurred but while elastic behavior continues, the properties of the transformed section are used to define the stiffness. The resulting compression zone is either rectangular or a T-section, depending on the location of the neutral axis and whether the section is solid, hollow, partially grouted, or fully grouted. For lightly reinforced sections, the neutral axis is typically within the face shell of partially grouted hollow masonry; therefore, a rectangular section is used in the analysis. Calculations for the effective moment of inertia similar to those used for reinforced concrete can be used for deflection calculations; however, the deflection calculations become increasingly inaccurate with increasing displacement. After yielding of the reinforcement, increases in the externally applied moment result in a shift in the neutral axis toward the compression face. The increased moment is resisted by the increased moment arm due to movement of the compression force resultant. The decreased depth of the compression zone requires an increase in the maximum compressive stress to maintain equilibrium. Finally, as large deformations and crack openings occurs, the crushing strain of the masonry is reached at the extreme compression fiber of the masonry, and spalling of the masonry units or crushing of the grout, or both, occurs. The design-based resistance-displacement relationship is described in Figure 61.

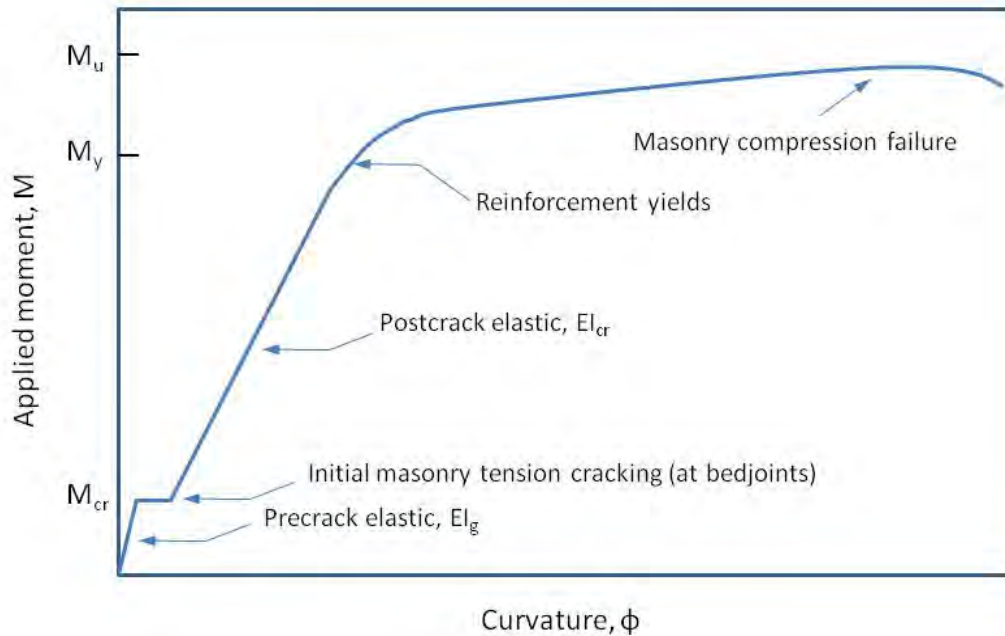


Figure 60. Moment-curvature Relationship for Reinforced Masonry Beams

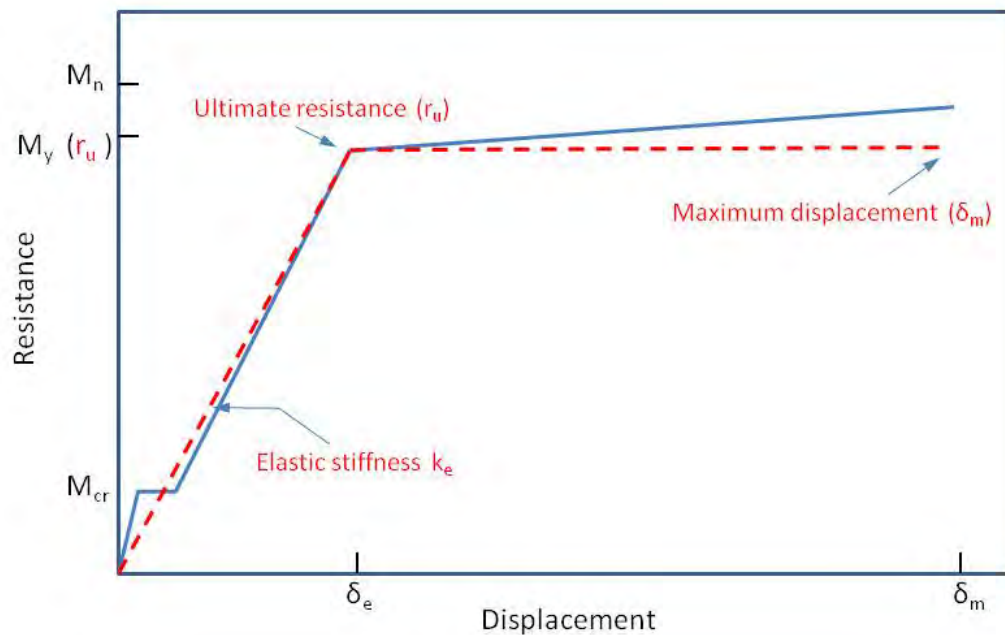


Figure 61. Resistance-displacement Idealization for Reinforced Masonry Beams

The equations used to define design resistance are summarized in Tables 5-7. The equations describe the input and output for the test panel static resistance analyses. Assumptions and engineering judgment are necessary for the use of these calculations; inaccuracies involved in the necessary assumptions are exacerbated by the non-uniform spacing between vertical

reinforcement in the test panels and the fact that the cells at each edge of all the test panels were grouted and reinforced. In other words, judgment of an accurate contributing width is not straight forward. The wall was analyzed as a simple beam supported at each end. This analysis assumes one-way flexural behavior. The analysis can be conducted using the full width of the test specimen with bars in each grouted cell taken as a collective area of steel, or using an average contributing width. A transformed section analysis is used to convert steel area into concrete area by the ratio of moduli, n , which is typical of reinforced concrete design. Moment of inertia and moment capacity are then calculated. The analytical maximum moment is then used to back-calculate wall pressure. For the cracking moment, all concrete and steel contributed to moment capacity since the section is not considered cracked. The yield moment is achieved when the reinforcement first reaches the yield stress, f_y . The nominal moment capacity is calculated from moment equilibrium between the steel reinforcement and the compression block. The ultimate usable strain of the masonry is assumed as 0.0025 in/in, along with a masonry stress of $0.80f'_m$ uniformly distributed over a stress block with a depth, a , of $0.80c$, where c is the neutral axis depth, as stipulated in MSJCC 3.3.2. Rotation is then estimated from the curvature and an approximation is made for the hinge length. Because the wall is assumed to act as a simple beam, the deflection can be approximated using simple trigonometry.

Table 5. Analytical Definitions

Eq. #	Output Type	Symbol	Equation
1	Cracking moment	M_{cr}	$M_{cr} = \frac{I_g f_r}{(t/2)}$
2	Masonry modulus	E_m	$E_m = 900 f'_m$
3	Displacement at M_{cr}	δ_{cr}	$\delta_{cr} = \frac{5 M_{cr} h^2}{48 E_m I_g}$
4	Modular ratio	n	$n = \frac{E_s}{E_c}$
5	Steel ratio	ρ	$\rho = \frac{A_s}{bd}$
6	Yield moment	M_y	$M_y = A_s f_y jd$ $jd = d - \frac{kd}{3}$ $k = \sqrt{2n\rho + (n\rho)^2} - n\rho$
7	Cracked moment of inertia	I_{cr}	$I_{cr} = \frac{b(kd)^3}{3} + nA_s (d - kd)^2$
8	Displacement at M_y	δ_y	$\delta_y = \frac{5 M_{cr} h^2}{48 E_m I_g} + \frac{5 (M_y - M_{cr}) h^2}{48 E_m I_{cr}}$
9	Nominal moment	M_n	$M_n = A_s f_y \left(d - \frac{a}{2} \right)$ $a = \frac{A_s f_y}{0.80 f'_m b}$
10	Curvature at nominal	ϕ_n	$\phi_n = \frac{\epsilon_{mu}}{c}$
11	Displacement at nominal	δ_n	$\theta_n = \phi_n d$ $\delta_n = \theta \left(\frac{L}{2} \right)$

Table 6. Analytical Input

Input Type	Symbol	6-inch	8-inch	Units
Block type / dimensions		6-inch standard CMU	8-inch standard CMU	inches
Effective beam width	b	32	48	inches
Modulus of rupture ungrouted	f_{ru}	63	63	psi
Modulus of rupture grouted	f_{rg}	163	163	psi
Percent grouted voids		30	21	%
Masonry prism compressive strength	f'_m	4,870	4,266	psi
Span	h	120	120	inches
Reinforcing steel modulus of elasticity	E_s	29×10^7	29×10^7	psi
Reinforcing steel yield	F_y	73,865	66,800	psi
Rebar ultimate strain	ϵ_{mu}	0.0025	0.0025	in/in
Depth of steel	d	2.8125	3.8125	inches
Area of steel per effective width	A_s	0.11	0.20	in ²

Table 7. Analytical Output

Output Type	Symbol	Eq. #	6-inch	8-inch	Units
Gross elastic moment of inertia	I_g		183	1,393	in ⁴
Modulus of rupture (interpolated)	f_r		93	84	psi
Cracking moment	M_{cr}	1	12,958	30,694	in-lb
Pressure resistance at M_{cr}	r_{cr}		0.225	0.3553	psi
Masonry modulus	E_m	2	4.38×10^6	3.84×10^6	psi
Displacement at M_{cr}	δ_{cr}	3	0.011316	0.008608	inch
Modular ratio	n	4	6.62	7.55	
Steel ratio	ρ	5	0.00122	0.00109	
Yield moment	M_y	6	2.19×10^4	4.98×10^4	in-lb
Pressure resistance at M_y	r_y		0.381	0.566	psi
Cracked moment of inertia	I_{cr}	7	4.87	18.5	in ⁴
Displacement at M_y	δ_y	8	0.1263	0.0767	inch
Nominal moment	M_n	9	22,587	50,390	in-lb
Curvature at nominal	ϕ_n	10	0.0302	0.0241	
Displacement at nominal	δ_n	11	5.10	5.52	inch

3.2. Analytical Input

3.2.1. SDOF Blast Effects Design Spreadsheets (SBEDS)

In standard analysis of reinforced concrete structures for blast loading, the cracking moment is ignored, and the resistance is simplified into a bilinear elastic-perfectly-plastic resistance (for single-hinge structures; also illustrated in Fig. 61). SBEDS [PDC 2005] was used to compare the

experimental resistances and impulse load responses to analytical results. The input used for SBEDS analyses of the three panel designs is provided in Tables 8 and 9. The panels were modeled as one-way flexural systems, with three different end conditions: simple-simple, simple-fixed, fixed-fixed. Some input limitations prevent a precise reflection of the test panels (for example CMU block density is fixed at lightweight, medium weight or normal weight), but overall, the mechanical characteristics of the tested systems were input. The average of the measured reflected pressures from each respective test were used as load input. Since the analyses were being compared to other SDOF analyses, the typical dynamic increase factors were set to “0” in the SBEDS input. For the cavity wall, the mass of the veneer was simply added as non-structural “supported weight.”

Table 8. SBEDS Input, 6-inch CMU Panel

Span Length	10 ft
Boundary Conditions	One-Way: Simple-Simple, Uniformly Loaded
Response Type	Flexural Only
Cross Section Type	Type I Cross Section
Total Wall Thickness	5.625 in
Bar Spacing	32 in
Reinforcing Steel	0.11 in ²
Distance to Center of Bars	2.8125 in
Masonry Type	Medium Weight CMU
Percent of Void Space Grouted	30%
Supported Weight	0
Masonry Compressive Strength	4871 psi
Masonry Dynamic Compressive Increase Factor	1.0 (default = 1.19)
Reinforcement Yield Strength	73865 psi
Reinforcement Ultimate Strength	112802 psi
Reinforcement Elastic Modulus	29000000 psi
Reinforcement Dynamic Increase Factor	1.0 (default = 1.17)
Blast Load Input Type	Pressure time history (from test data)

Table 9. SBEDS Input, 8-inch CMU Panel and Cavity Wall

Span Length	10 ft
Boundary Conditions	One-Way: Simple-Simple, Uniformly Loaded
Response Type	Flexural Only
Cross Section Type	Type I Cross Section
Total Wall Thickness	7.625 in
Bar Spacing	48 in
Reinforcing Steel	0.20 in ²
Distance to Center of Bars	3.81 in
Masonry Type	Medium Weight CMU
Percent of Void Space Grouted	21%
Supported Weight	0
Masonry Compressive Strength	4266 psi
Masonry Dynamic Compressive Increase Factor	1.0 (default = 1.19)
Reinforcement Yield Strength	66,804 psi
Reinforcement Ultimate Strength	106,066 psi
Reinforcement Elastic Modulus	29,000,000 psi
Reinforcement Dynamic Increase Factor	1.0 (default = 1.17)
Blast Load Input Type	Pressure time history (from test data)

3.2.2. Wall Analysis Code (WAC)

WAC [Slawson 1995] is another software tool developed to analyze exterior walls for blast loads, and therefore was also used to compare the experimental resistances and impulse load responses to analytical results. Overall, the same input methodology described above for SBEDS was used for the WAC models. The input used for WAC analyses of the three panel designs is provided in Tables 10 and 11.

Table 10. WAC Input, 6-inch CMU Panel

Wall Clear Height	10 ft
Wall Width	9.33 ft
Total Wall Thickness	5.625 inch
Unit Weight of Wall	110 pcf
Wall Type	Reinforced wall
Material Type	Masonry
Static Masonry Compressive Strength	4,870 psi
Reinforcement Yield Strength	73,865 psi
Masonry Rupture Strength	153 psi
Thickness of masonry block face shell	1 inch
Horizontal Spacing of vertical reinforcement	32 inch
Horizontal void length between vertical bars	26 inch
Support condition	One-way action; simple supports at each end
Vertical wall load	0 lb/ft
Reinforcement layout	Midheight vertical reinforcement
Inside [steel] area per foot length	0.0471 sq in
Distance from outside to center of inside	2.8125 inch

Table 11. WAC Input, 8-inch CMU Panel

Wall Clear Height	10 ft
Wall Width	9.33 ft
Total Wall Thickness	7.625 inch
Unit Weight of Wall	110 pcf; 200 pcf for cavity wall
Wall Type	Reinforced wall
Material Type	Masonry
Static Masonry Compressive Strength	4,266 psi
Reinforcement Yield Strength	66,800 psi
Masonry Rupture Strength	153 psi
Thickness of masonry block face shell	1 inch
Horizontal Spacing of vertical reinforcement	40 inch
Horizontal void length between vertical bars	26 inch
Support condition	One-way action; simple supports at each end
Vertical wall load	0 lb/ft
Reinforcement layout	Midheight vertical reinforcement
Inside [steel] area per foot length	0.0643 sq in
Distance from outside to center of inside	3.8125 inch

3.2.3. Static Resistance Function Analyses

The third SDOF approach used for the comparative dynamic analyses was a direct implementation of the resistances acquired through static testing [Salim et al. 2010] and the measured reflected pressures into central difference SDOF methodology [Biggs 1964].

3.3. Analytical and Experimental Static Resistance Comparisons

Figure 62 provides the resistance functions determined experimentally using comparable panel designs and dimensions [Salim et al. 2010]. Figures 63 and 64 compare the experimental and analytical static resistance functions for the 6-inch CMU panel and 8-inch panel designs considered in this test series. As can be noted, the SBEDS and WAC resistances for both the 6-inch and 8-inch CMU panels are closely aligned, but significantly lower than the test resistance. There is a slight difference between WAC and SBEDS resistances, which are due to input differences, rather than resistance definition differences. The design-code based resistances are further below the SBEDS and WAC generated resistances. From a design resistance standpoint, the veneer does not increase the resistance and the cavity wall resistance is therefore not shown in the comparison. However, a significant stability effect or vertical load resistance effect provided by the veneer can be interpreted from Figure 62.

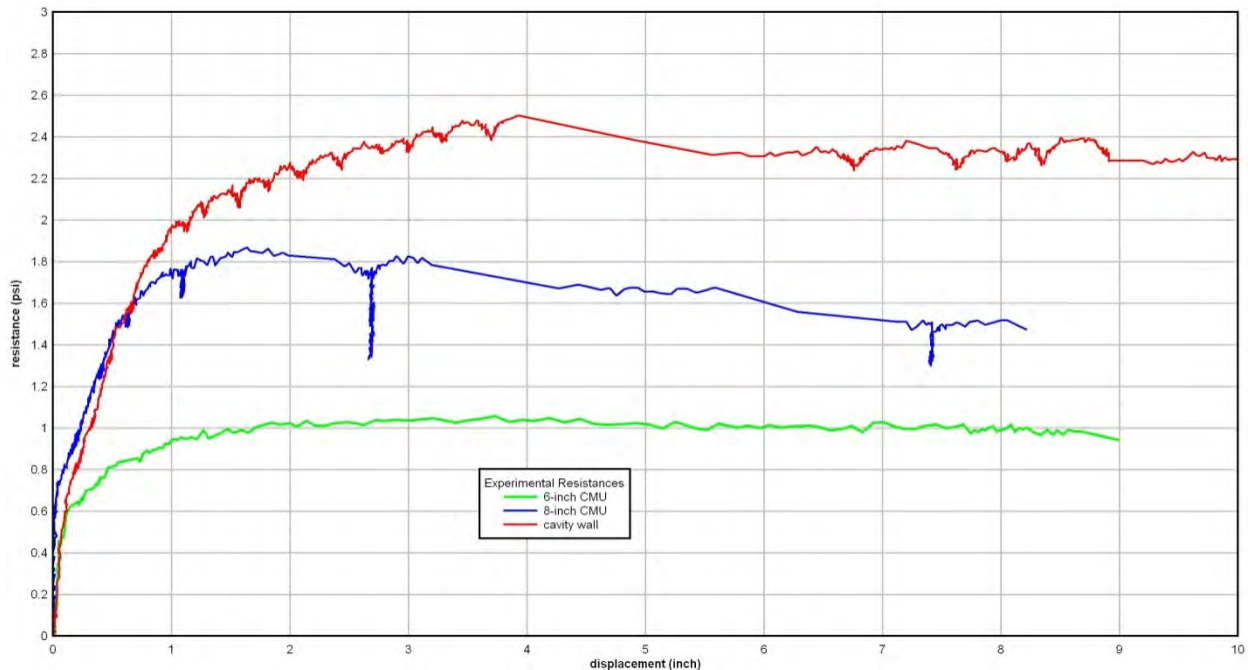


Figure 62. Experimental Static Resistance Results

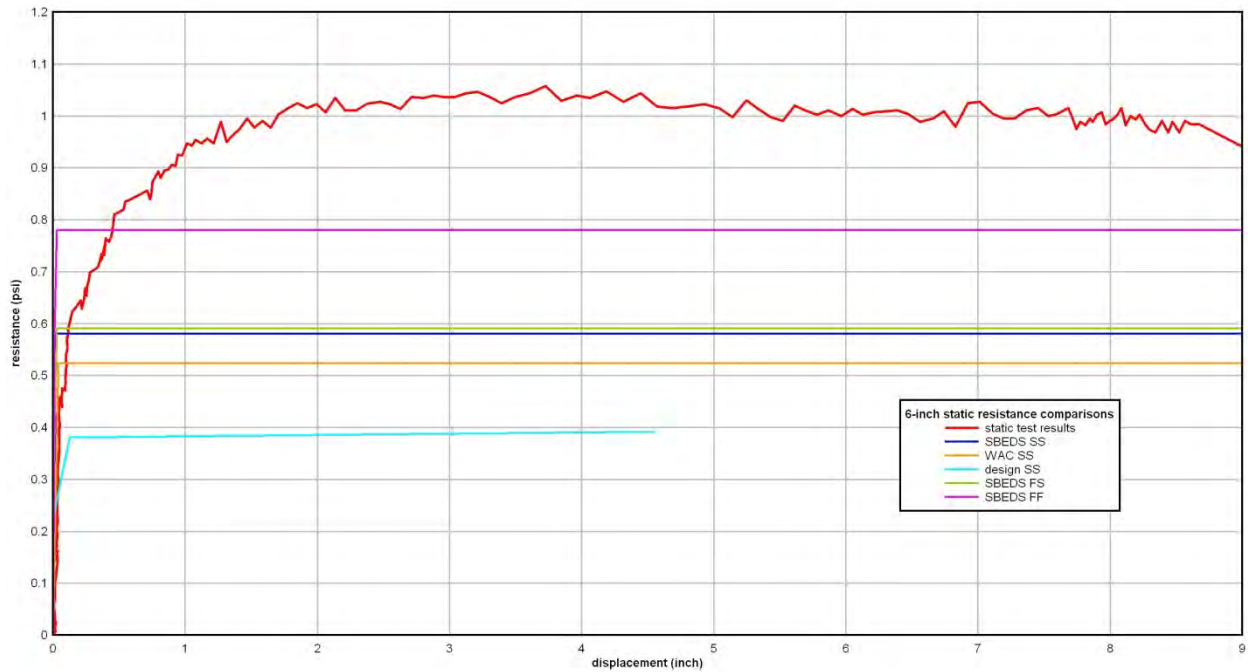


Figure 63. 6-inch CMU Panel Analytical and Experimental Static Resistance Comparisons

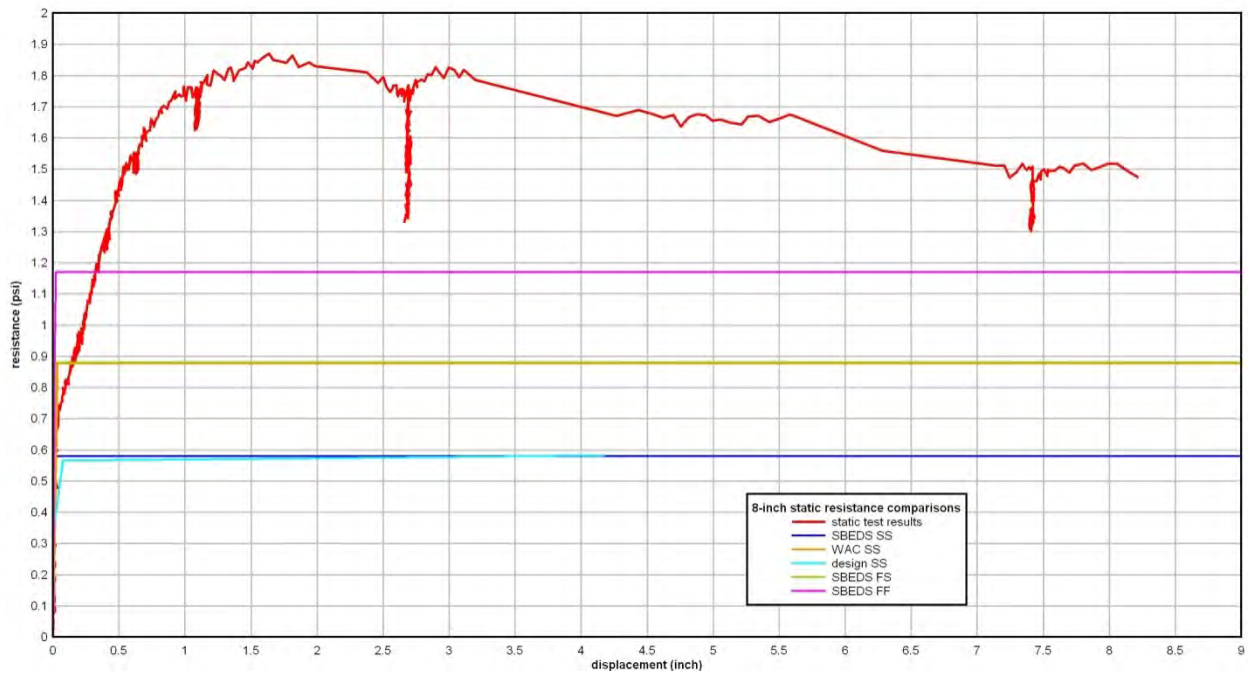


Figure 64. 8-inch CMU Panel Analytical and Experimental Static Resistance Comparisons

3.4. Analytical and Experimental Dynamic Response Comparisons

Figures 65-73 compare the experimental and analytical responses for the 6-inch CMU panel and 8-inch panel designs considered in this test series. Each plot includes (1) the measured mid-span

inward dynamic deflection, (2) an SDOF analyses using the measured static resistance function, (3) SBEDS results with simple support top and bottom edge conditions, (4) SBEDS results with fixed support top and bottom edge conditions, and (5) WAC results with simple support top and bottom edge conditions. It should be noted that no dynamic increase factors were included in the neither the SBEDS analyses nor the SDOF analyses using measured static resistances, whereas WAC includes dynamic strength effects without a user option to turn it off (19% increase in material strength for concrete and 17% for steel). Since the dynamic experiments inherently include any such increases in material strength due to strain rate effects, strain rate effects would contribute to lower test displacement responses compared to the analytical responses.

Experiment 1 6-inch CMU: The measured deflection is significantly lower, as expected, since the resistances used were lower than the actual resistances. The calculation using the measured static resistance function also resulted in higher overall displacement response, which is likely caused by assumptions regarding contributing mass and geometric and material strength differences between the static test article and the dynamic test article. There could also be differences between end restraints provided during the static tests versus the dynamic tests. There is a difference between the SBEDS simple support results and the WAC results; because the static resistance functions were similar, these differences are caused by input limitations and assumptions used for calculating contributing mass. Furthermore, it is not clear whether the static resistances extracted from WAC include strain rate increases. Based upon the analytical results herein, the analyses indicate that end restraints approximating fixed supports result in a prediction more closely aligned with the test results.

Experiment 1 8-inch CMU: The trends noted for the Experiment 1 6-inch CMU Panel also apply to the 8-inch comparisons.

Experiment 1 Cavity Wall: The trends noted for the 6-inch also apply to the Cavity Wall Panel comparisons, except that the analyses using the experiment resistance is significantly lower, which reflects the higher static resistance. This may indicate that the additional stability mechanisms provided by the veneer in the static experiments may not be present in the impulse load environment. Additionally, the difference could be related to inaccuracies associated with the way the mass of the veneer was included in the cavity wall analyses.

Experiment 2 6-inch CMU: Experiment 2 involved a significantly higher peak pressure and impulse than Experiment 1 loading. The recorded test deflection does not peak until after 200 msec. Overall, the analytical results are all rationally aligned except the simple support SBEDS results, which is higher (as in the other cases).

Experiment 2 8-inch CMU: There was significant breaching of the 8-inch CMU panel during Experiment 2. The measured deflection is significantly lower, because the resistances used were lower than the measured resistances. Also, fracturing and breaching perhaps provided some load relief. The calculation using the measured static resistance function also resulted in higher overall displacement response, likely be due to assumptions regarding contributing mass and geometric and material strength differences between the static test article and the dynamic test article. There is a notable difference between the SBEDS simple support results and the WAC results; because the static resistance functions were similar, these differences are caused by input

limitations and assumptions used for calculating contributing mass. In the context of the analytical results herein, the analyses indicate that end restraints approximating fixed supports would result in a prediction more closely aligned with the test results.

Experiment 2 Cavity Wall: Significant breaching of the Cavity Wall panel also occurred during Experiment 2. As with the Experiment 1 Cavity Wall comparison, the results using the experiment resistance is significantly lower reflecting the higher static resistance. This may indicate that the additional stability mechanisms provided by the veneer in the static experiments may not be present in the impulse load environment. Additionally, the difference could be related to inaccuracies associated with the way the mass of the veneer was included in the cavity wall analyses.

Experiment 3 6-inch CMU: Experiment 3 loading resulted in significant fracturing and breaching of the 6-inch test panel, which was exacerbated by grout voids cells at the panel edge. Therefore, the test deflection continues to increase up to approximately 150 msec. Both the simple support and fixed support SBEDS results are higher than the other analytical cases and the test response. The results using WAC and the experimental static resistance were markedly lower, which is a concern but cannot be explained without additional investigation.

Experiment 3 8-inch CMU: Experiment 3 loading also resulted in very extensive fracturing and breaching of the 8-inch test panel, which was exacerbated by grout voids in cells at the edge of the panel. The overall analytical results trends are the same as described for the 6-inch CMU panel in the previous paragraph.

Experiment 3 Cavity Wall: Experiment 3 loading also resulted in very extensive fracturing and breaching of the 8-inch test panel. For this case, all of the analytical results correlated relatively well at a peak of approximately 2.5 inches of deflection, but the measured peak deflection exceeded 6.5 inches of deflection for the mid-span deflection. This disparity is caused by the extreme breaching around the attachment point of the deflection gauge. It can be noted from Figure 55 that the maximum deflection of the top gauge was only approximately 3 inches.

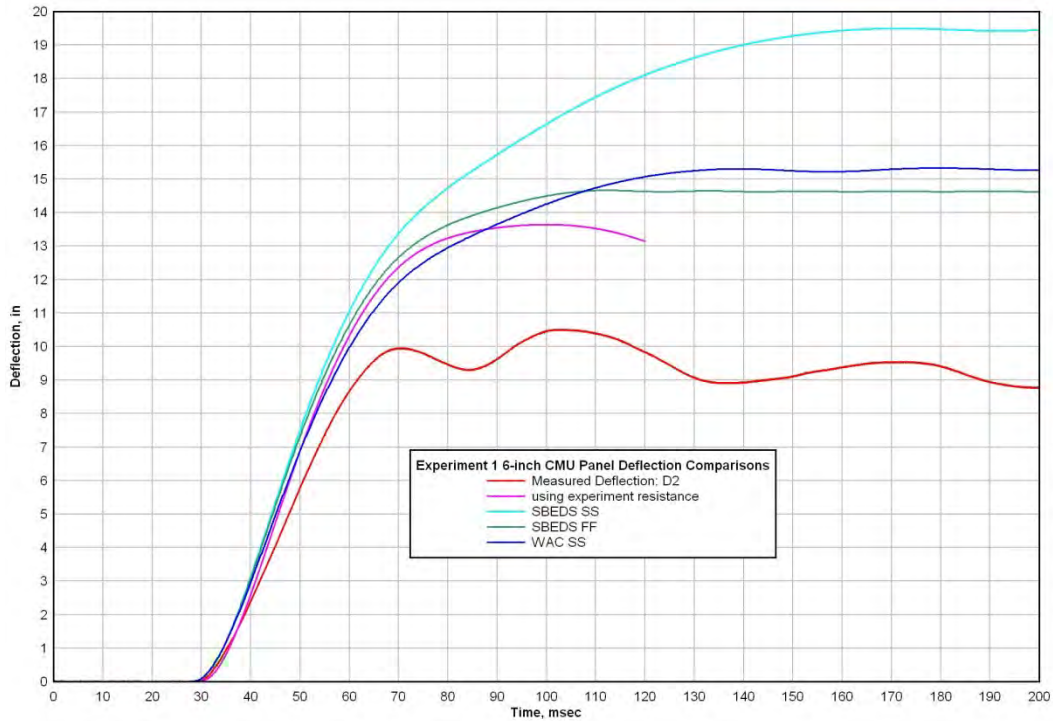


Figure 65. Experiment 1 6-inch CMU Panel Analytical and Experimental Dynamic Response Comparisons

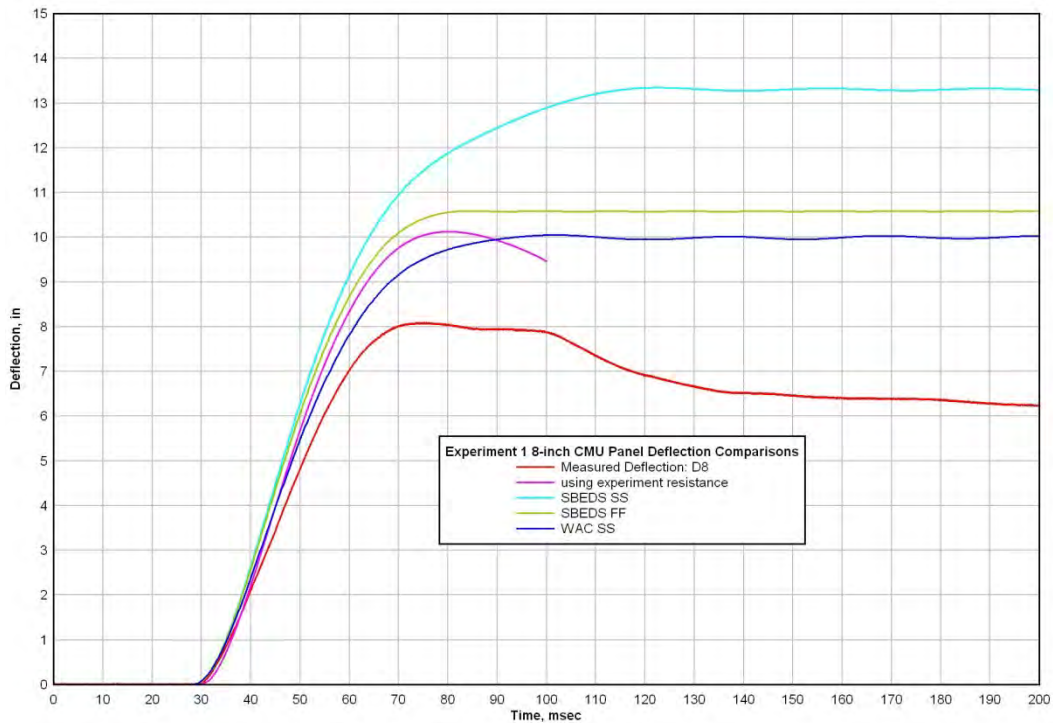


Figure 66. Experiment 1 8-inch CMU Panel Analytical and Experimental Dynamic Response Comparisons

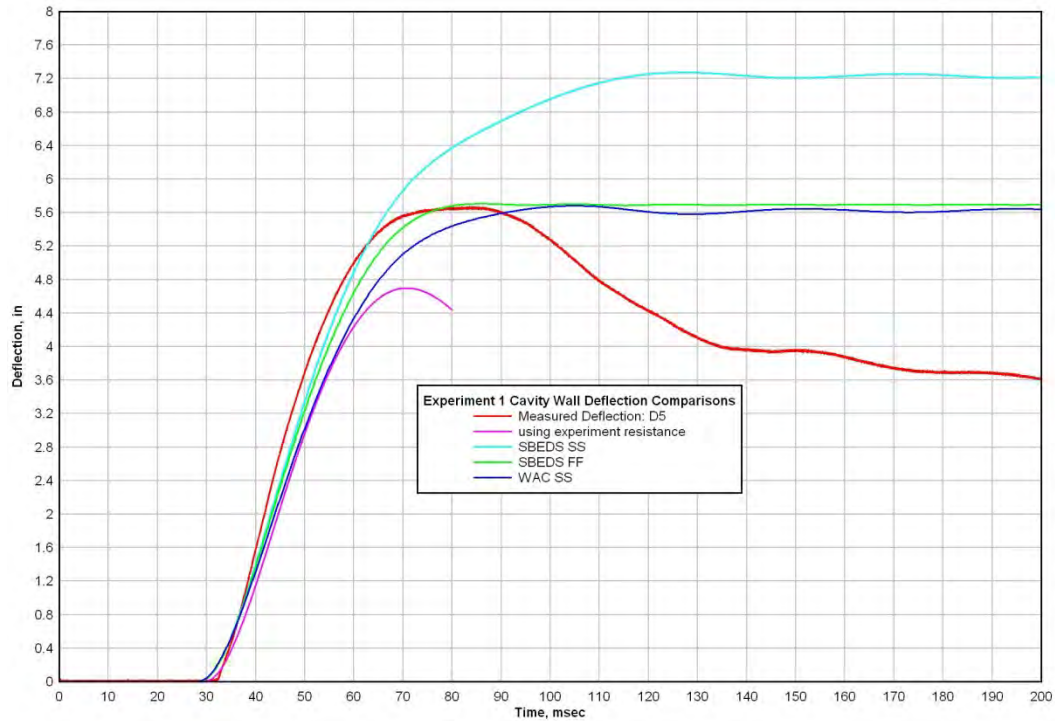


Figure 67. Experiment 1 Cavity Wall CMU Panel Analytical and Experimental Dynamic Response Comparisons

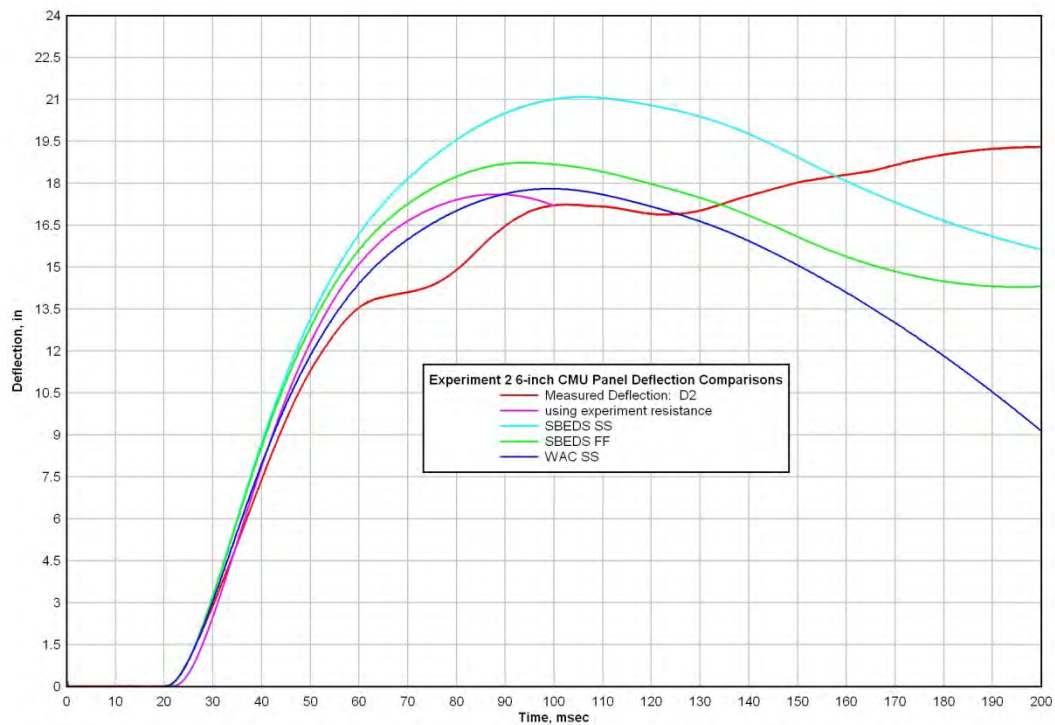


Figure 68. Experiment 2 6-inch CMU Panel Analytical and Experimental Dynamic Response Comparisons

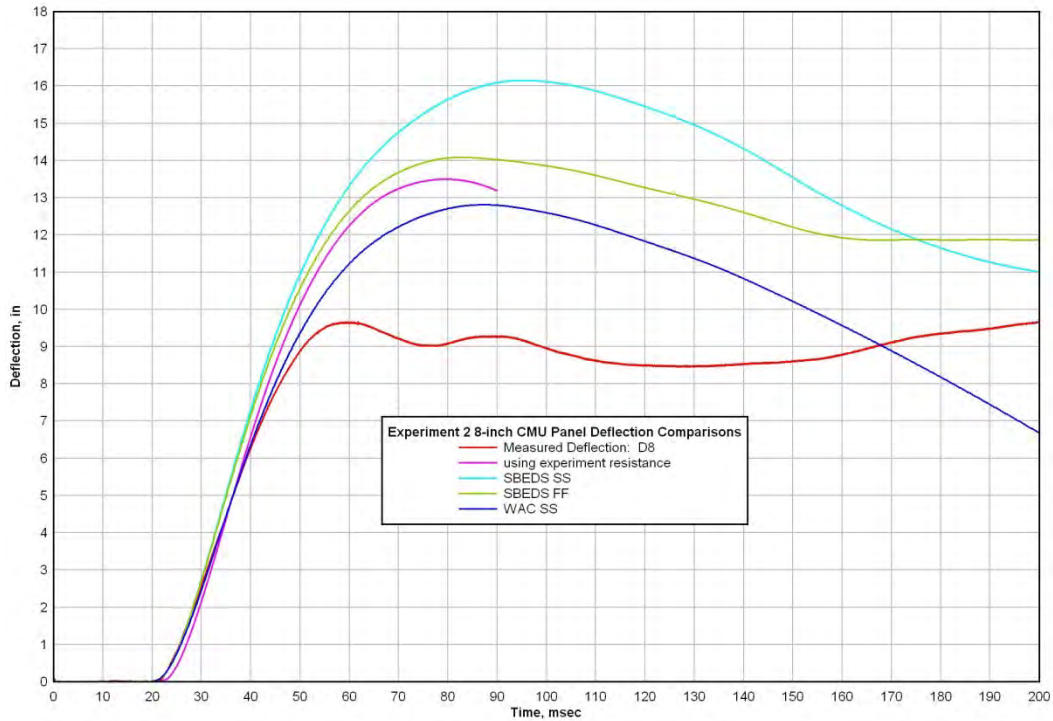


Figure 69. Experiment 2 8-inch CMU Panel Analytical and Experimental Dynamic Response Comparisons

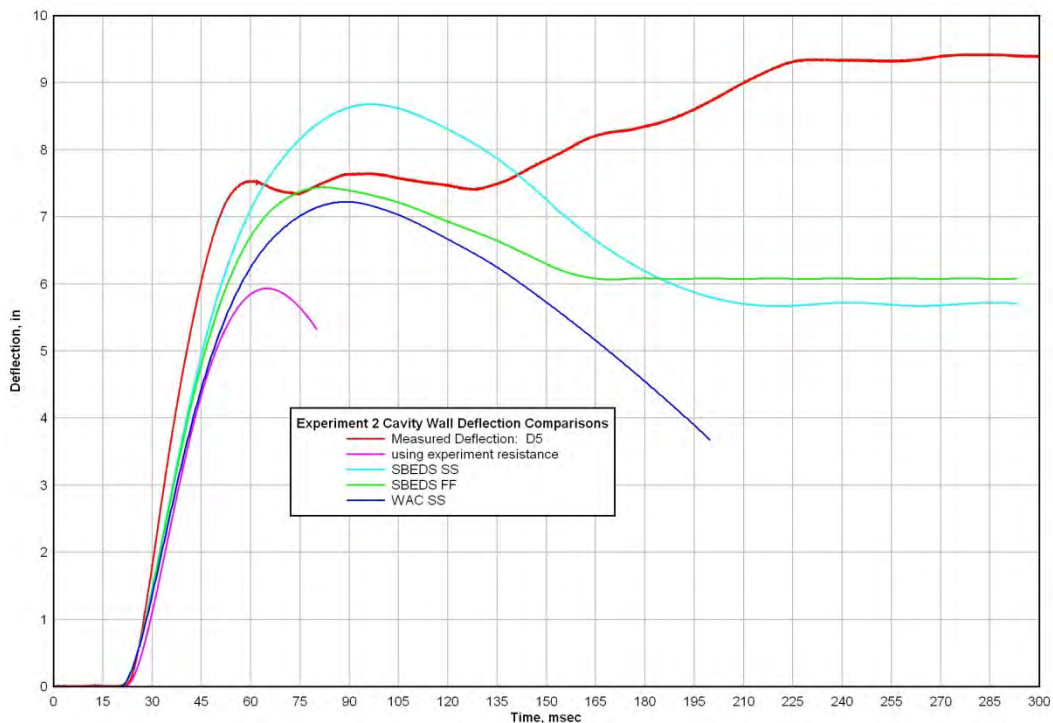


Figure 70. Experiment 2 Cavity Wall CMU Panel Analytical and Experimental Dynamic Response Comparisons

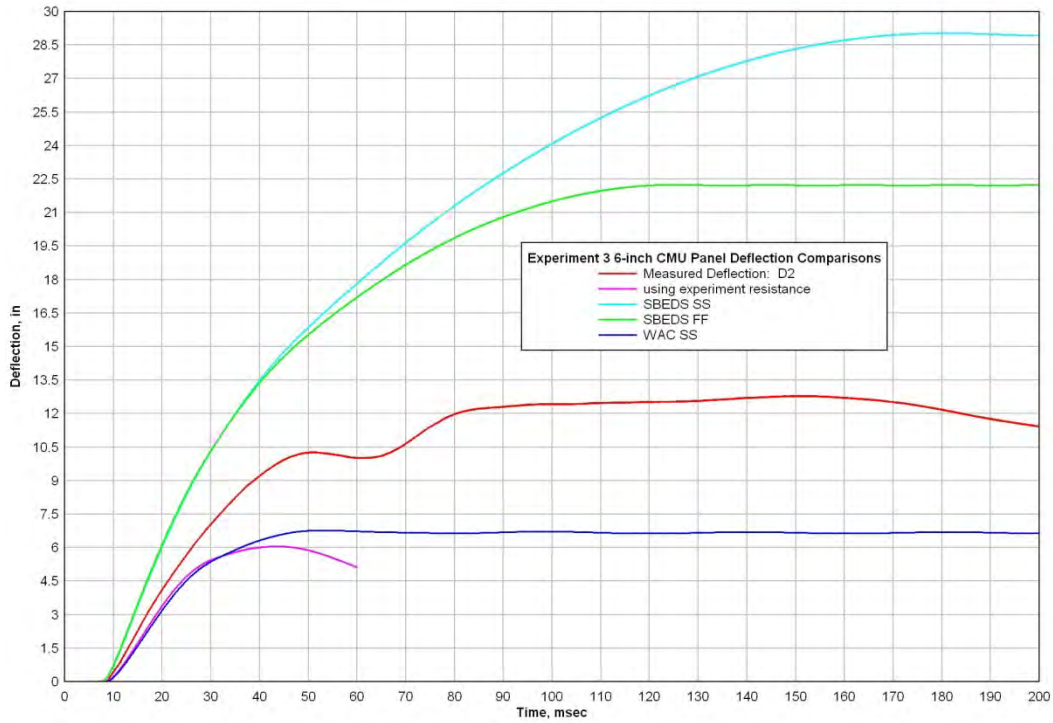


Figure 71. Experiment 3 6-inch CMU Panel Analytical and Experimental Dynamic Response Comparisons

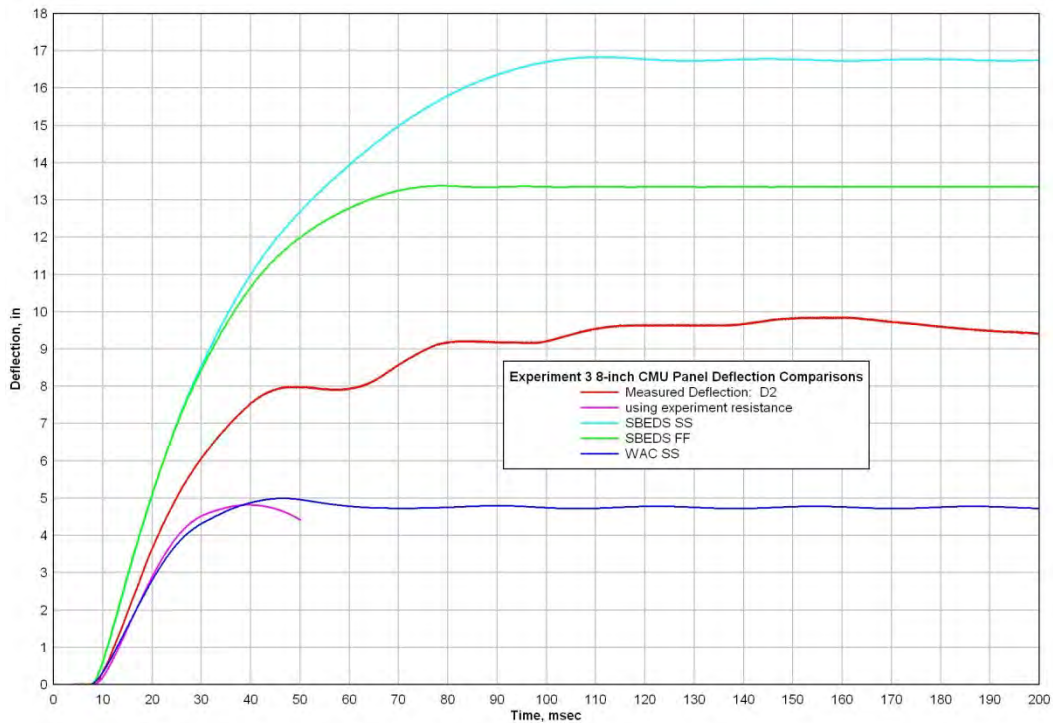


Figure 72. Experiment 3 8-inch CMU Panel Analytical and Experimental Dynamic Response Comparisons

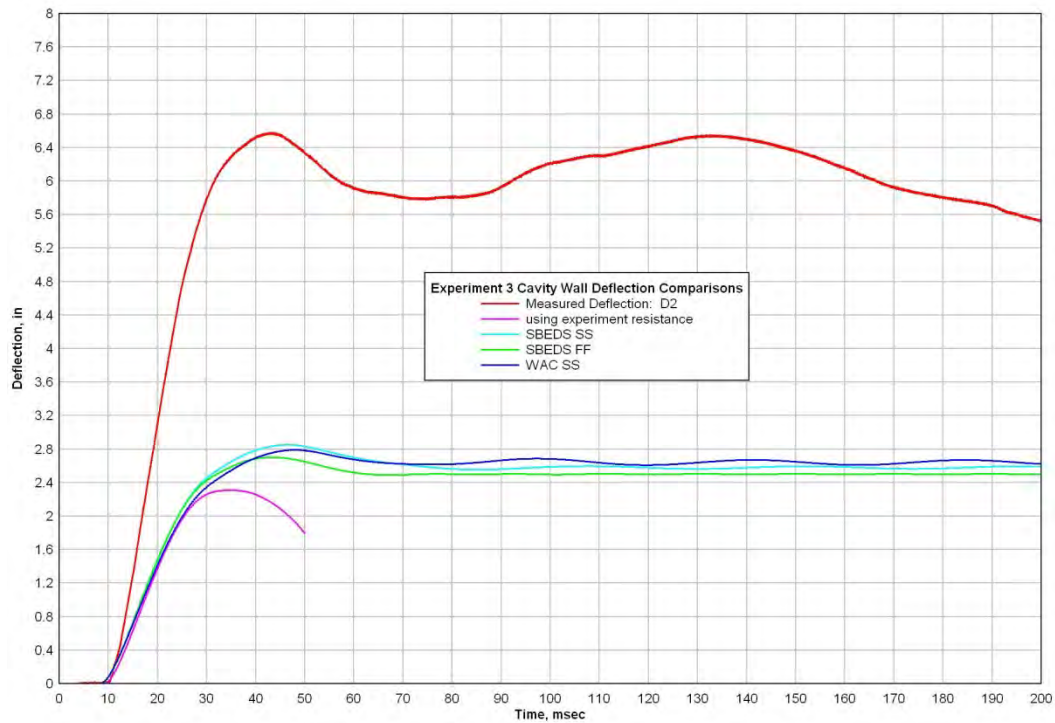


Figure 73. Experiment 3 Cavity CMU Panel Analytical and Experimental Dynamic Response Comparisons

4. CONCLUSIONS AND RECOMMENDATIONS

This report summarizes the results of three blast load experiments on three minimally reinforced concrete masonry designs (nine test panels total). The test articles included a partially grouted and reinforced 6-inch CMU panel, a partially grouted and reinforced 8-inch CMU panel, and a partially grouted and reinforced 8-inch CMU panel with clay brick veneer (typical of cavity wall construction). The impulse loading applied to the panels varied significantly for each of the three experiments. Failure mechanism observations were made using high-speed videos that captured the response of each panel. A detailed post-test forensic investigation was also conducted after each experiment to further explore and document the mechanisms of resistance and residual condition of each test article. Deflection time histories were captured so that the responses could be compared to existing blast analysis codes used for masonry design. The following general observations were made:

- In general a ductile flexural response was observed for the grouted and reinforced cells, with rotations up to approximately 20 degrees.
- In two cases (Experiment 3 6-inch and 8-inch panels), grout voids occurred during construction in cells at the side of the panel; these regions were breached under blast loading emphasizing the need for careful quality control during construction.
- Significant breaching of the unreinforced masonry between grouted/reinforced cells occurred in Experiments 2 and 3; the presence of the brick did not appear to significantly mitigate the breaching on the cavity wall panels.
- Overall, the design resistance used in blast analysis SDOF methodology appears to be conservative. However, there were some cases where the measured test dynamic deflections exceeded the analytical deflections. Significant breaching occurred in the region around the displacement gauge attachments for these cases, which may have affected the displacement records.
- The brick veneer tended to fracture extensively and fall to the outside of the structure.
- The foam insulation of the cavity wall panels was fractured extensively during Experiments 2 and 3, but did not appear to have been significantly crushed. Its effectiveness in absorbing energy and thereby reducing the maximum dynamic displacement and tendency for catastrophic failure mechanisms was not discernable. As discussed extensively in the Series I masonry tests [Browning et al. 2008], the veneer ties have robust axial load capacity, and likely transfer most of the force from the veneer to the structural wythe, thereby precluding significant energy absorption by the foam insulation.

The following conclusions and recommendations were drawn:

- Additional testing and analysis of the between-grouted-cells breaching phenomena is needed so that specific recommendations for the use of partially-grouted masonry construction can be developed and an analysis approach for shear breaching can be developed and verified. Given the failure mechanisms observed, a requirement that only fully-grouted masonry be used for new DoD and GSA construction may be warranted. This test program was designed to examine the flexural resistance of partially grouted masonry; the dimensions of the existing reaction structure resulted in irregular spacing of grouted/reinforced cells. Future full-scale shear breach tests may require a wider test panel opening so that panels with regular column spacing can be tested.

- The voids that occurred during the construction of several of the test panels emphasize the need for careful quality control and verification.
- Although it is conservative to assume that the veneer adds only mass to the dynamic resistance of the system, static resistance tests have demonstrated that the veneer provides additional large displacement stability to the system facilitating deflections significantly greater than the comparable system without veneer. However, except for considering the additional mass, an increase in capacity of the cavity wall over the comparable 8-inch CMU wall was not evident in the blast tests conducted in this test program. Additional investigation as to whether the large displacement stability effect provided by the veneer should be considered in analyses may be warranted.
- Additional analytical research could help to better understand the load transfer mechanisms between the veneer and structural wythe, and the energy absorbed, if any, by the foam insulation. Furthermore, the potential hazards posed by the veneer fracture and collapse may warrant additional consideration.
- This investigation considered only the most common brick veneer system and US standard concrete masonry infill wall systems. Worldwide, many other masonry configurations and materials are used for similar purposes, and additional testing of other common systems may be warranted.
- Load bearing systems and walls with window and door openings should be considered in future programs.

5. REFERENCES

American Society of Civil Engineers, ASCE/SEI 7 (2005), Minimum Design Loads for Buildings and Other Structures, ASCE/SEI 7-05, / 01-Jan-2006 / 424 pages, ISBN: 0784408092.

ACI Committee 530, 2008, "Building Code Requirements and Specification for Masonry Structures (ACI 530/530.1-08)," American Concrete Institute, Farmington Hills, MI.

Biggs, J. M., (1964). Introduction to Structural Dynamics, McGraw-Hill Book Company, New York.

Browning R.S., Davidson J.S., and Dinan R.J., 2008. "Resistance of Multi-Wythe Insulated Masonry Walls Subjected to Impulse Loads – Volume 1," Air Force Research Laboratory Report, AFRL-RX-TY-TR-2008-4603.

Department of Defense, 2005, "Masonry Structural Design for Buildings," UFC 3-310-05A.

Department of Defense, 2010, "Structural Engineering," UFC 3-301-01.

Department of Defense, 2007, "DoD Minimum Antiterrorism Standards for Buildings," UFC 4-010-01.

Department of Defense, 2008, "Structures to Resist the Effects of Accidental Explosions," UFC 3-340-02.

International Code Council, 2009, "International Building Code 2009," Country Club Hills, IL.

Salim H., Saucier A., Bell B, Hoemann J., Bewick B, Davidson J., Shull J., 2010, Experimental Evaluation of Full-Scale NCMA Walls Under Uniform Pressure Using Vacuum, draft report submitted to the Air Force Research Laboratory.

Slawson, T.R., (1995). "Wall Response to Airblast Loads: The Wall Analysis Code (WAC)," prepared for the U.S. Army ERDC, Vicksburg, MS, Contract DACA39-95-C-0009, ARA-TR-95-5208, November, 1995.

U.S. Army Corps of Engineers Protective Design Center, 2005, "Single-Degree-of-Freedom Blast Effects Design Spreadsheets (SBEDS)," PDC-TR 05-01.

U.S. Army Corps of Engineers Protective Design Center, 2006a, "Methodology Manual for the Single-Degree-of-Freedom Blast Effects Design Spreadsheets (SBEDS)," PDC-TR 06-01.

U.S. Army Corps of Engineers Protective Design Center, 2006b, "User's Guide for the Single-Degree-of-Freedom Blast Effects Design Spreadsheets (SBEDS)," PDC-TR 06-02.

United States Congress (2005) Energy Policy Act of 2005 Sec. 388 U.S. LibraryofCongress. 2005-08-08. [http://thomas.loc.gov/cgi-bin/query/F?c109:6:./temp/~c109fE8GRZ:e496969:.](http://thomas.loc.gov/cgi-bin/query/F?c109:6:./temp/~c109fE8GRZ:e496969:) Retrieved 2008-07-11.

United States Congress (2007) Energy Independence Security Act of 2007, <http://thomas.loc.gov/cgi-bin/bdquery/z?d110:H.R.6>.

Appendix A: Material Test Results

Table A-1. Summary of ASTM A 370 #3 Rebar used in the 6-inch panel

Sample	f_y (ksi)	f_u (ksi)	e_{max}^*	E (ksi)**
#3-1	73745	113067	0.078	29000
#3-2	74593	112795	0.203	29000
#3-3	73258	112544	0.141	29000
Avg	73865	112802	0.141	29000

Table A-2. Summary of ASTM A 370 #4 Rebar used in the 8-inch panel and cavity wall

Sample	f_y (ksi)	f_u (ksi)	e_{max}^*	E (ksi)**
#4-1	67163	106980	0.125	29000
#4-2	66782	105888	0.195	29000
#4-3	66466	105331	0.109	29000
Avg	66804	106066	0.143	29000

*based on MTS stroke

** assumed value

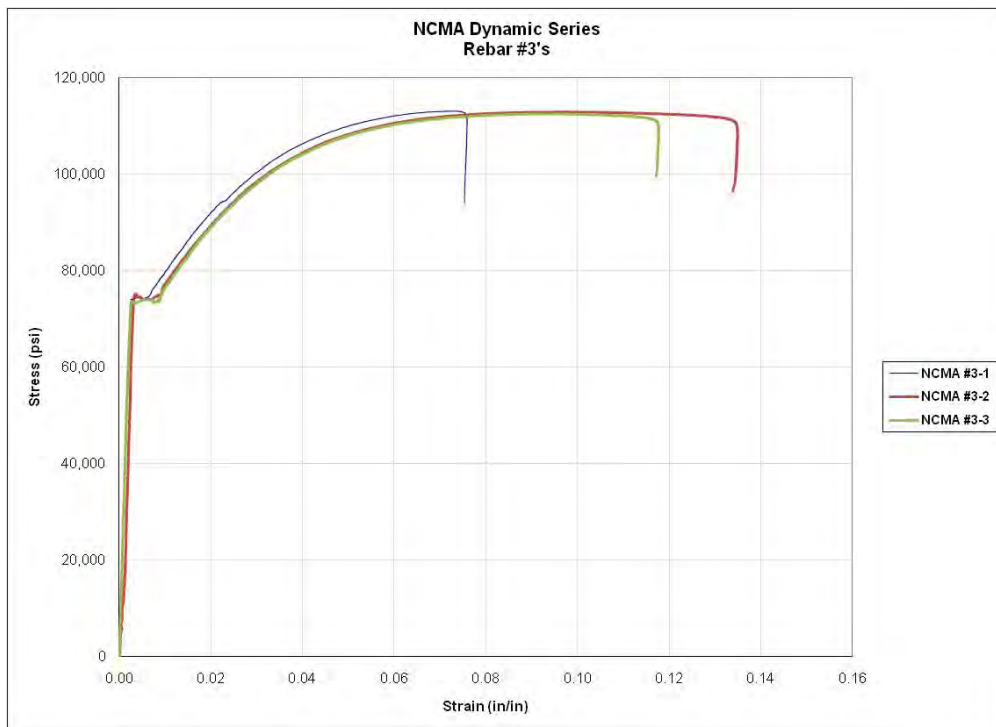
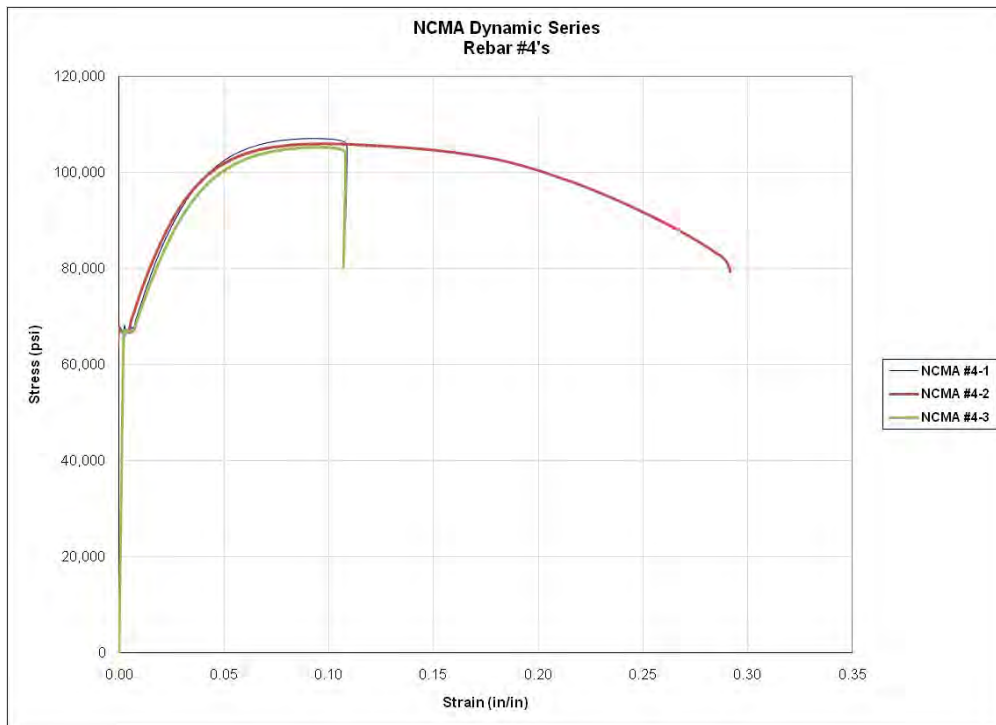


Figure A-1. Rebar Tension Test Results

Table A-3. ASTM C 1314-07 Grouted Concrete Prism Test Results

ID	Date Tested	Sample Size (in)	Corrected Gross Strength (psi)
Mark "6/24" - 1	11/24/2009	8x16x8	4590
Mark "6/24" - 2	11/24/2009	8x16x8	4140
Mark "6/24" - 3	11/24/2009	8x16x8	4170
		Avg	4300
Mark "6/25" - 1	11/24/2009	8x16x8	4260
Mark "6/25" - 2	11/24/2009	8x16x8	4100
Mark "6/25" - 3	11/24/2009	8x16x8	4010
Mark "6/25" - 4	11/24/2009	8x16x8	4120
		Avg	4123
Mark "6/26" -1	11/25/2009	6x16x8	3840
Mark "6/26" -2	11/25/2009	6x16x8	5420
Mark "6/26" -3	11/25/2009	6x16x8	5650
		Avg	4970
Mark "6/26" - 1	11/25/2009	8x16x8	4150
Mark "6/26" - 2	11/25/2009	8x16x9	4600
		Avg	4375
No Mark	11/25/2009	6x16x8	4770
No Mark	11/25/2009	6x16x8	4740
No Mark	11/25/2009	6x16x8	4810
		Avg	4773
		6" Average =	4872
		8" Average =	4266
		Total Average =	4508

Table A-4. ASTM C 1314-07 Hollow Concrete Prism Test Results

ID	Date Tested	Sample Size (in)	Corrected Gross Strength (psi)
Mark "6/10" - 1	12/1/2009	8x16x16	1110
Mark "6/10" - 2	12/1/2009	8x16x16	1340
Mark "6/10" - 3	12/1/2009	8x16x16	1160
		Avg	1203
Mark "6/24" - 1	11/24/2009	8x16x16	1520
Mark "6/24" - 2	11/24/2009	8x16x16	1480
Mark "6/24" - 3	11/24/2009	8x16x16	1380
		Avg	1460
Mark "6/30" -1	12/1/2009	6x16x16	2100
Mark "6/30" -2	12/1/2009	6x16x16	2070
Mark "6/30" -3	12/1/2009	6x16x16	2070
		Avg	2080
		6" Average =	2080
		8" Average =	1292
		Total Average =	1581

Table A-5. ASTM C 1314-07 Clay Brick Masonry Prism Test Results

ID	Date Tested	Sample Size (in)	Corrected Gross Strength (psi)
Mark "6/24" - 1	11/30/2009	4x13x8	4720
Mark "6/24" - 2	11/30/2009	4x13x8	4040
Mark "6/24" - 3	11/30/2009	4x13x8	4620
		Avg	4460

Table A-6. ASTM C 780 2-inch Mortar Cube Compressive Strength (C 109)

ID	Test Date	Cube Strength (psi)
"6/10 9:00 AM"	12/1/2009	2560
"6/10 12:00 AM"	12/1/2009	3800
"6/10 12:00 AM"	12/1/2009	3950
"6/10 2:00 PM"	12/1/2009	2450
"6/10 2:00 PM"	12/1/2009	2620
	Avg	3076
"6/24 3:00 PM"	11/24/2009	4260
"6/24 3:00 PM"	11/24/2009	3700
"6/24 12:00 PM"	11/24/2009	4460
"6/24 9:30 AM"	11/24/2009	3390
"6/24 9:30 AM"	11/24/2009	3130
	Avg	3788
"6/25 9:00 AM"	11/24/2009	2950
"6/25 9:00 AM"	11/24/2009	3110
"6/25 12:00 PM"	11/24/2009	2840
"6/25 3:00 PM"	11/24/2009	3360
"6/25 3:00 PM"	11/24/2009	3420
	Avg	3136
"6/26 9:00 AM"	11/25/2009	2240
"6/26 10:00 AM"	11/25/2009	2630
"6/26 10:00 AM"	11/25/2009	2320
"6/26 12:00 PM"	11/25/2009	2580
"6/26 12:00 PM"	11/25/2009	2240
	Avg	2402
"6/29 11:00 AM"	11/25/2009	3050
"6/29 11:00 AM"	11/25/2009	2930
"6/29 12:00 PM"	11/25/2009	4540
	Avg	3507
"6/30 3:00 PM"	12/1/2009	3230
"6/30 3:00 PM"	12/1/2009	3230
	Avg	3230
	Total Avg	3190

Table A-7. ASTM C1019-09 Sampling and Testing Grout / ASTM C476; Grouted Concrete Prisms Test Results

ID	Sample Size (in)	Compressive Strength (psi)
#1 Mark "Pour #1"	3x7	6580
#2 Mark "Pour #2"	3x7	7740
	Avg	7160
Mark "6/25" - 1	3x7	8020
Mark "6/25" - 2	3x7	8170
	Avg	8095
Mark "6" Wall, 6/29" - 1	3x7	7000
Mark "6" Wall, 6/29" - 2	3x7	7220
Mark "6" Wall, 6/29" - 3		6920
	Avg	7047
No Mark	3x7	8100
No Mark	3x7	7490
	Avg	7795
	Total Average =	7524

Appendix B: Construction Photos

LIST OF FIGURES

Figure	Page
B-1. Horizontal reinforcement tie	93
B-2. Veneer tie	92
B-3. Rebar spacer	93
B-4. Tie	93
B-5. Horizontal reinforcement	94
B-6. Base channels with welded dowels	94
B-7. Base channels with welded dowels	95
B-8. Base of the welded dowel	95
B-9. Bottom bond beam	96
B-10. Bottom bond beam	96
B-11. Bottom bond beam top view	97
B-12. Bottom bond beam grouted	97
B-13. Bottom bond beam rebar in position	98
B-14. End bed joint	98
B-15. Rebar positioned at end cell	99
B-16. Construction progressing	99
B-17. Construction progressing	100
B-18. Top view of dowel rebar positioned	100
B-19. 8-inch CMU panels almost complete	101
B-20. First embed positioned	101
B-21. Bottom view cavity wall base and channel	102
B-22. Construction wide view	102
B-23. Embed close-up	103
B-24. Embed close-up	103
B-25. Embed close-up	104
B-26. Two embeds positioned	104
B-27. Top bond beam complete	105
B-28. 8-inch CMU panel complete	105
B-29. Three 8-inch CMU panels complete	106
B-30. 8-inch CMU panel complete	106
B-31. 8-inch CMU panel complete	107
B-32. Rebar splice	107
B-33. Setting top bond beam	108
B-34. Positioning wind stability bracing	108
B-35. Insulation foam positioned for the cavity wall construction	109
B-36. Beginning of cavity wall veneer construction	109
B-37. Close-up of veneer tie	110
B-38. Side view of veneer tie	110
B-39. Side view of veneer tie	111
B-40. Cavity wall panel construction	111
B-41. Cavity wall panel construction	112

B-42.	Cavity wall panel construction.....	112
B-43.	Cavity wall panel construction.....	113
B-44.	Cavity wall panel construction complete.....	113
B-45.	Wall panel construction complete.....	114
B-46.	Wall panel construction complete.....	114
B-47.	Test panels complete with wind bracing.....	115
B-48.	Test panels complete with wind bracing.....	115
B-49.	Test panels being positioned for testing.....	116
B-50.	Test panels being positioned for testing.....	116
B-51.	Test panels being positioned for testing.....	117
B-52.	Test panels being positioned for testing.....	117
B-53.	Test panels being positioned for testing.....	118
B-54.	Test panels being positioned for testing.....	119
B-55.	Base of cavity wall being positioned for testing.....	120
B-56.	Test panels being positioned for testing.....	120
B-57.	Removing the stability frame.....	121
B-58.	Removing the stability frame.....	121
B-59.	Test panels being positioned for testing.....	122
B-60.	Test panels being positioned for testing.....	122
B-61.	Test panels being positioned for testing.....	123
B-62.	Test panels ready for testing	124
B-63.	Test panels ready for testing	125
B-64.	Test panels ready for testing	125

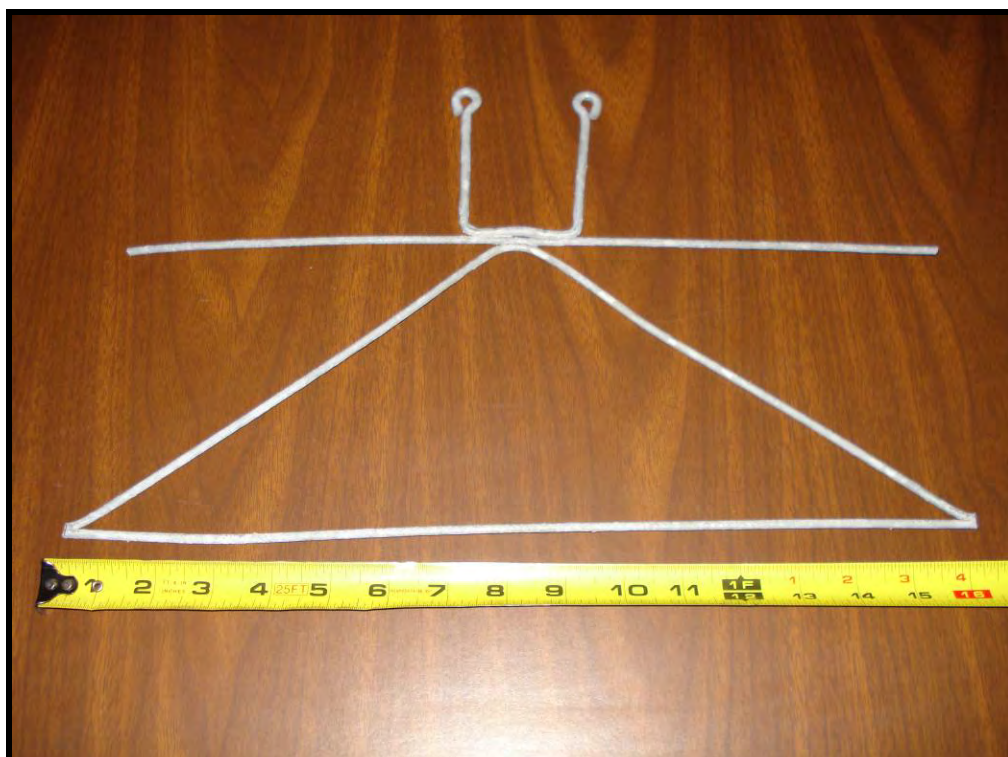


Figure B- 1. Horizontal reinforcement tie



Figure B-2. Veneer tie

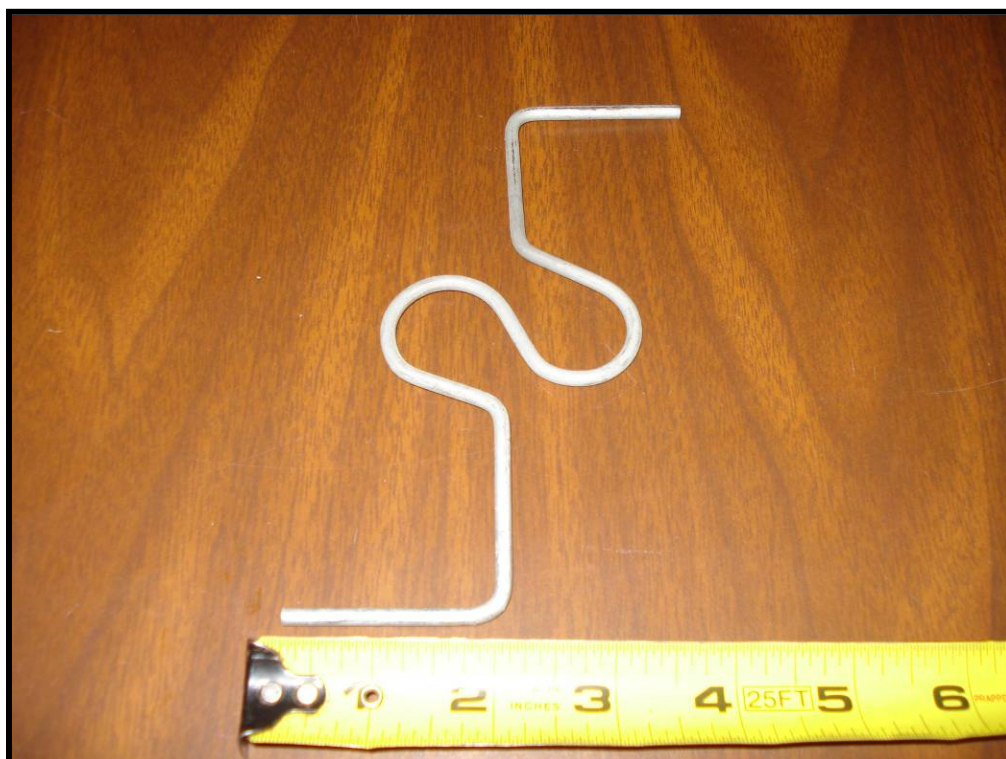


Figure B-3. Rebar spacer

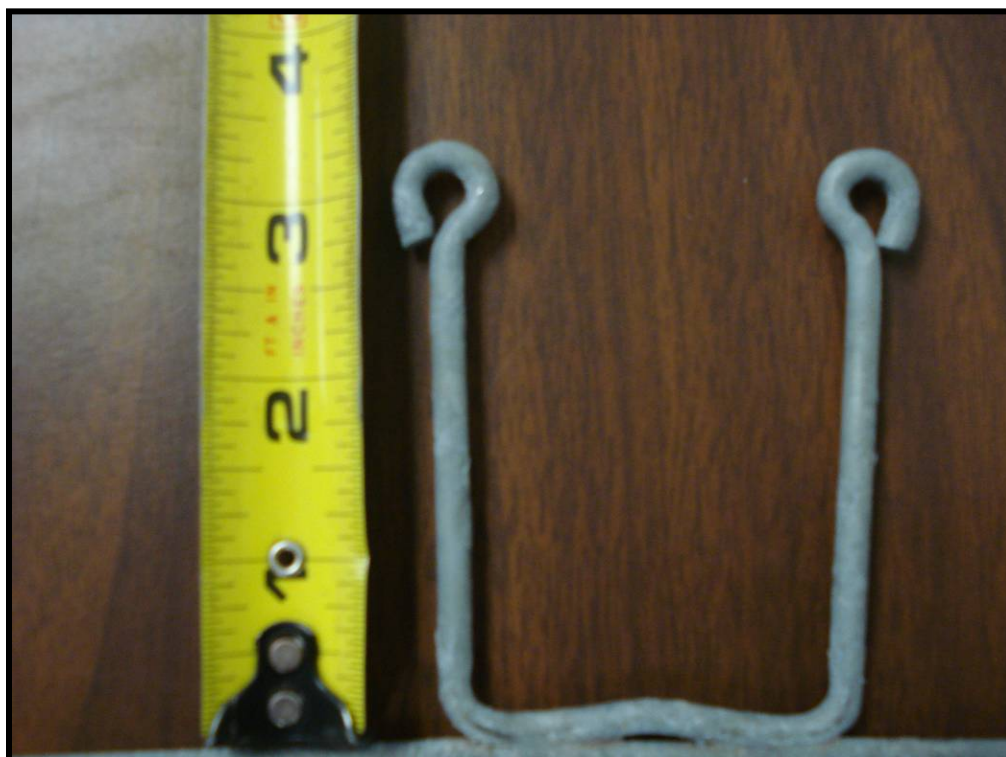


Figure B-4. Tie

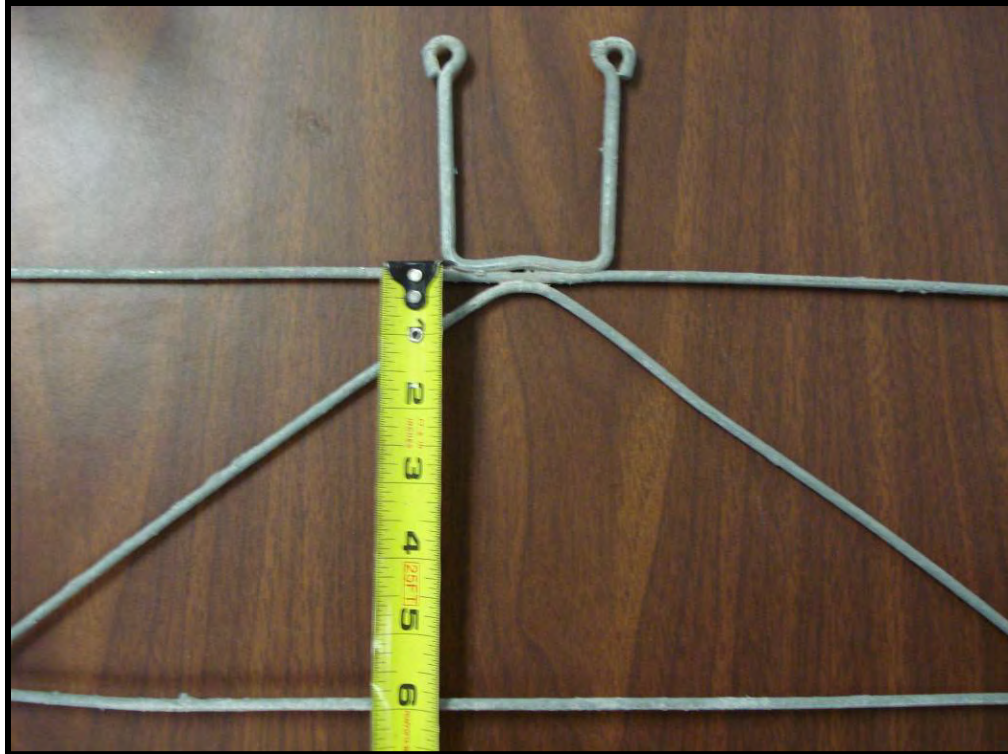


Figure B-5. Horizontal reinforcement



Figure B-6. Base channels with welded dowels



Figure B-7. Base channels with welded dowels



Figure B-8. Base of the welded dowel



Figure B-9. Bottom bond beam



Figure B-10. Bottom bond beam



Figure B-11. Bottom bond beam top view



Figure B-12. Bottom bond beam grouted



Figure B-13. Bottom bond beam rebar in position



Figure B-14. End bed joint



Figure B-15. Rebar positioned at end cell



Figure B-16. Construction progressing



Figure B-17. Construction progressing



Figure B-18. Top view of dowel rebar positioned



Figure B-19. 8-inch CMU panels almost complete



Figure B-20. First embed positioned



Figure B-21. Bottom view cavity wall base and channel



Figure B-22. Construction wide view



Figure B-23. Embed close-up



Figure B-24. Embed close-up



Figure B-25. Embed close-up



Figure B-26. Two embeds positioned



Figure B-27. Top bond beam complete

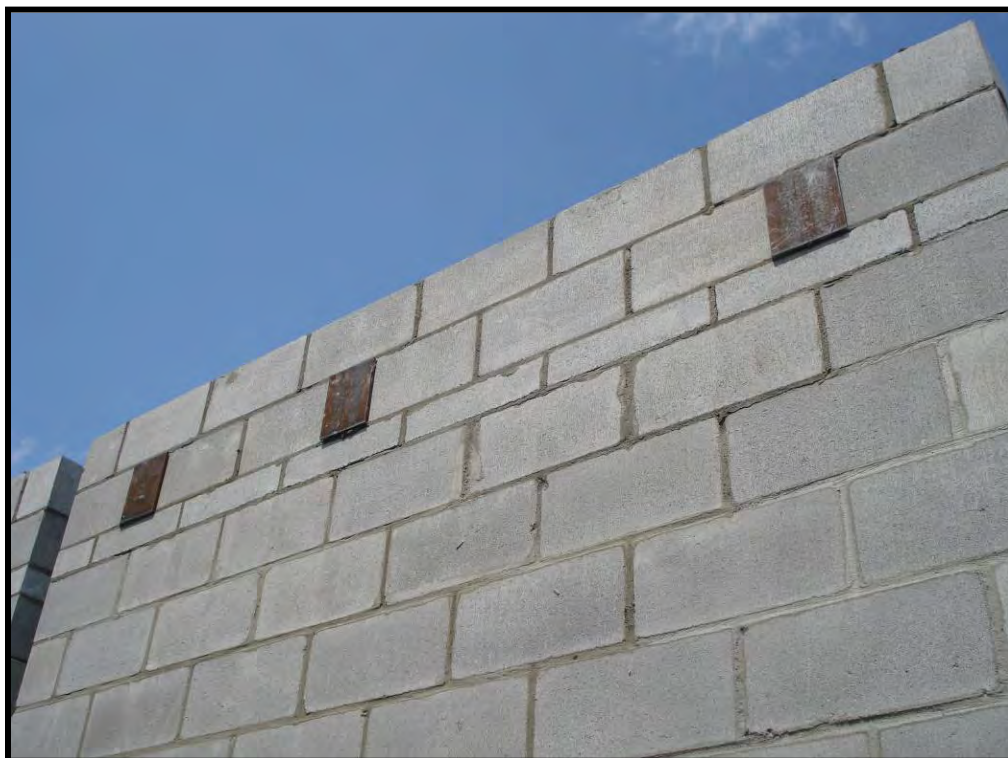


Figure B-28. 8-inch CMU panel complete



Figure B-29. Three 8-inch CMU panels complete



Figure B-30. 8-inch CMU panel complete



Figure B-31. 8-inch CMU panel complete



Figure B-32. Rebar splice



Figure B-33. Setting top bond beam



Figure B-34. Positioning wind stability bracing



Figure B-35. Insulation foam positioned for the cavity wall construction



Figure B-36. Beginning of cavity wall veneer construction



Figure B-37. Close-up of veneer tie



Figure B-38. Side view of veneer tie



Figure B-39. Side view of veneer tie



Figure B-40. Cavity wall panel construction



Figure B-41. Cavity wall panel construction



Figure B-42. Cavity wall panel construction



Figure B-43. Cavity wall panel construction



Figure B-44. Cavity wall panel construction complete



Figure B-45. Wall panel construction complete



Figure B-46. Wall panel construction complete



Figure B-47. Test panels complete with wind bracing



Figure B-48. Test panels complete with wind bracing



Figure B-49. Test panels being positioned for testing



Figure B-50. Test panels being positioned for testing



Figure B-51. Test panels being positioned for testing



Figure B-52. Test panels being positioned for testing



Figure B-53. Test panels being positioned for testing



Figure B-54. Test panels being positioned for testing



Figure B-55. Base of cavity wall being positioned for testing



Figure B-56. Test panels being positioned for testing



Figure B-57. Removing the stability frame



Figure B-58. Removing the stability frame



Figure B-59. Test panels being positioned for testing



Figure B-60. Test panels being positioned for testing



Figure B-61. Test panels being positioned for testing



Figure B-62. Test panels ready for testing



Figure B-63. Test panels ready for testing



Figure B-64. Test panels ready for testing

Appendix C: Test Results Photos

LIST OF FIGURES

Figure	Page
C-1. Experiment 1 full front view.....	129
C-2. Experiment 1 full front view.....	129
C-3. Experiment 1 full front view.....	129
C-4. Experiment 1 side left front view.....	130
C-5. Experiment 1 side right front view	131
C-6. Experiment 1 6-inch CMU panel front view	132
C-7. Experiment 1 6-inch CMU panel full interior view.....	133
C-8. Experiment 1 6-inch CMU panel close-up interior view.....	134
C-9. Experiment 1 8-inch CMU panel front view	135
C-10. Experiment 1 8-inch panel left side view	136
C-11. Experiment 1 8-inch CMU panel full interior view.....	137
C-12. Experiment 1 8-inch CMU panel close-up interior view.....	138
C-13. Experiment 1 8-inch CMU panel partial interior view	139
C-14. Experiment 1 8-inch CMU panel close-up interior view.....	139
C-15. Experiment 1 cavity wall front view.....	140
C-16. Experiment 1 cavity wall top	141
C-17. Experiment 1 cavity wall panel full interior view	142
C-18. Experiment 1 cavity wall panel close-up interior view	143
C-19. Experiment 2 full front view.....	143
C-20. Experiment 2 full front view.....	144
C-21. Experiment 2 6-inch panel front view	145
C-22. Experiment 2 6-inch panel front view	146
C-23. Experiment 2 6-inch CMU panel left side exterior close-up view	147
C-24. Experiment 2 6-inch panel front view	148
C-25. Experiment 2 6-inch panel front view	149
C-26. Experiment 2 6-inch panel full interior view	150
C-27. Experiment 2 6-inch CMU panel interior close-up view.....	151
C-28. Experiment 2 8-inch panel front view	152
C-29. Experiment 2 8-inch CMU panel exterior close-up view	153
C-30. Experiment 2 8-inch CMU panel exterior close-up view	153
C-31. Experiment 2 8-inch panel full interior view	154
C-32. Experiment 2 8-inch panel full interior view.....	155
C-33. Experiment 2 8-inch panel full interior view	156
C-34. Experiment 2 8-inch CMU panel interior close-up view.....	156
C-35. Experiment 2 cavity wall panel front view	157
C-36. Experiment 2 exterior view.....	158
C-37. Experiment 2 cavity wall panel exterior view	159

C-38.	Experiment 2 cavity wall panel exterior view	160
C-39.	Experiment 2 cavity wall panel veneer failure	161
C-40.	Experiment 2 cavity wall panel full interior view	162
C-41.	Experiment 2 cavity wall bottom interior view	163
C-42.	Experiment 3 full exterior view	163
C-43.	Experiment 3 full exterior left side view	164
C-44.	Experiment 3 6-inch CMU panel exterior view.....	165
C-45.	Experiment 3 6-inch CMU panel close-up breaching exterior view	166
C-46.	Experiment 3 6-inch CMU panel close-up breaching exterior view	167
C-47.	Experiment 3 6-inch CMU panel close-up reinforced cells not grouted properly.....	168
C-48.	Experiment 3 6-inch CMU panel full interior view.....	169
C-49.	Experiment 3 6-inch CMU panel breaching interior view.....	170
C-50.	Experiment 3 8-inch CMU panel full exterior view	171
C-51.	Experiment 3 8-inch CMU panel breaching exterior view, improperly grouted reinforced cells.....	172
C-52.	Experiment 3 8-inch CMU panel close-up exterior view	173
C-53.	Experiment 3 8-inch CMU panel right exterior view	174
C-54.	Experiment 3 8-inch CMU panel full interior view.....	175
C-55.	Experiment 3 8-inch CMU panel full interior view.....	176
C-56.	Experiment 3 8-inch CMU panel breaching interior view, improperly grouted reinforced cells.....	177
C-57.	Experiment 3 8-inch CMU panel breaching interior view, improperly grouted reinforced cells.....	178
C-58.	Experiment 3 8-inch CMU panel breaching interior close-up view	179
C-59.	Experiment 3 cavity wall panel full exterior view.....	180
C-60.	Experiment 3 cavity wall panel lower exterior view	181
C-61.	Experiment 3 cavity wall panel veneer tie close-up	182
C-62.	Experiment 3 cavity wall panel veneer side view close-up	183
C-63.	Experiment 3 cavity wall panel right side exterior view	184
C-64.	Experiment 3 cavity wall panel veneer close-up	185
C-65.	Experiment 3 cavity wall panel full interior view	186
C-66.	Experiment 3 cavity wall panel interior close-up view	187
C-67.	Experiment 3 cavity wall panel interior view	188
C-68.	Experiment 3 cavity wall panel interior view	189



Figure C-1. Experiment 1 full front view



Figure C-2. Experiment 1 full front view



Figure C-3. Experiment 1 full front view



Figure C-4. Experiment 1 side left front view



Figure C-5. Experiment 1 side right front view



Figure C-6. Experiment 1 6-inch CMU panel front view

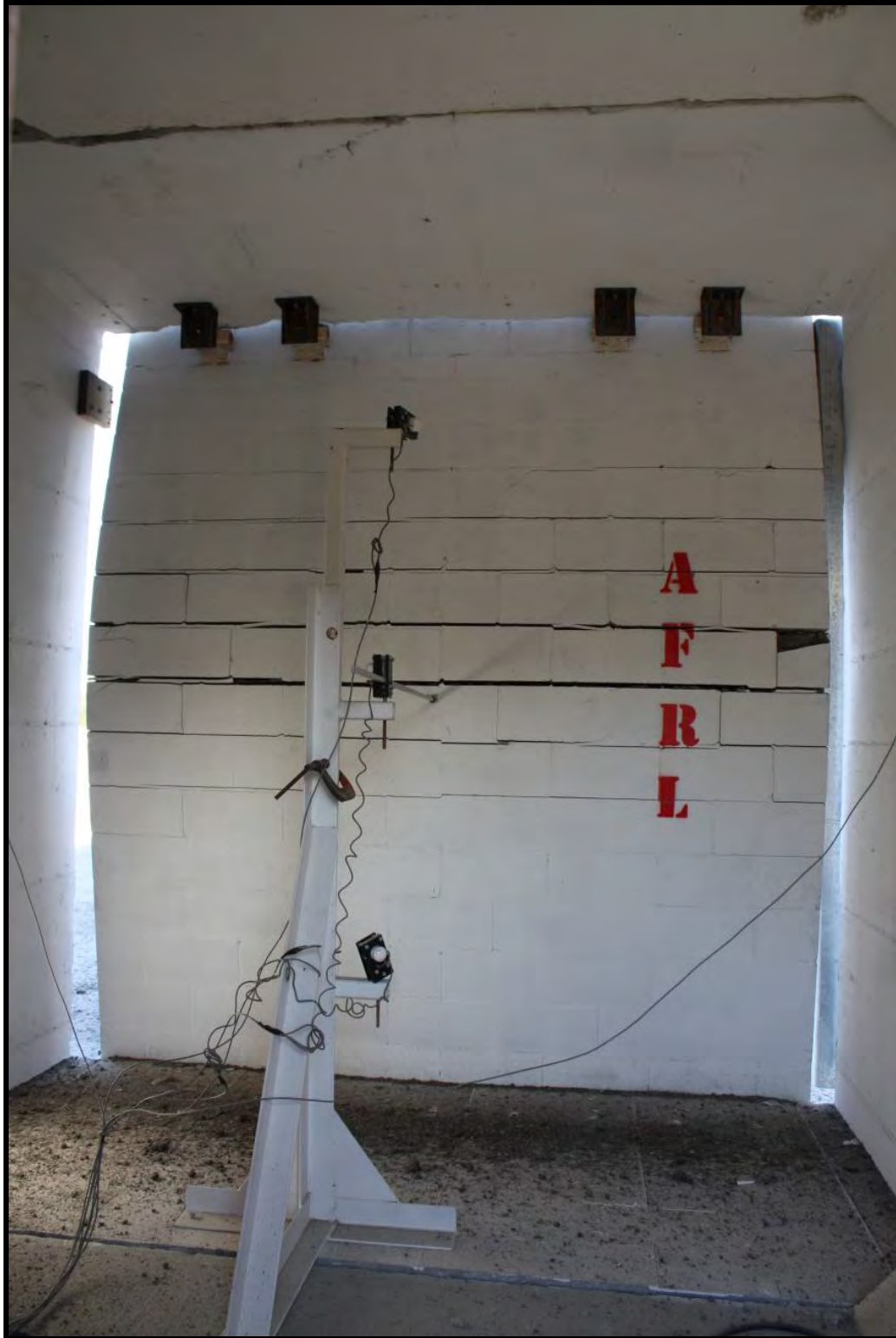


Figure C-7. Experiment 1 6-inch CMU panel full interior view

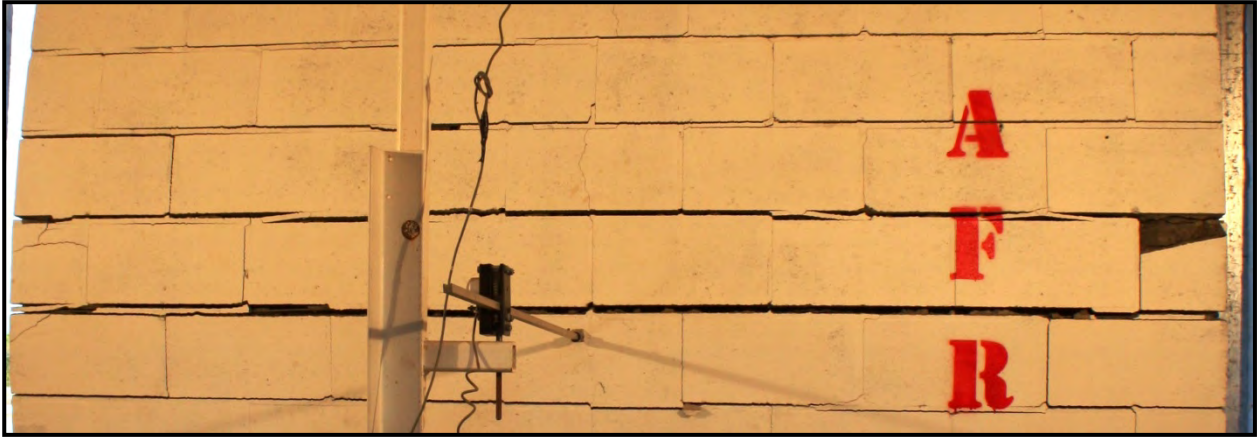


Figure C-8. Experiment 1 6-inch CMU panel close-up interior view



Figure C-9. Experiment 1 8-inch CMU panel front view



Figure C-10. Experiment 1 8-inch panel left side view



Figure C-11. Experiment 1 8-inch CMU panel full interior view



Figure C-12. Experiment 1 8-inch CMU panel close-up interior view



Figure C-13. Experiment 1 8-inch CMU panel partial interior view



Figure C-14. Experiment 1 8-inch CMU panel close-up interior view



Figure C-15. Experiment 1 cavity wall front view



Figure C-16. Experiment 1 cavity wall top



Figure C-17. Experiment 1 cavity wall panel full interior view



Figure C-18. Experiment 1 cavity wall panel close-up interior view



Figure C-19. Experiment 2 full front view



Figure C-20. Experiment 2 full front view



Figure C-21. Experiment 2 6-inch panel front view



Figure C-22. Experiment 2 6-inch panel front view



Figure C-23. Experiment 2 6-inch CMU panel left side exterior close-up view



Figure C-24. Experiment 2 6-inch panel front view



Figure C-25. Experiment 2 6-inch panel front view

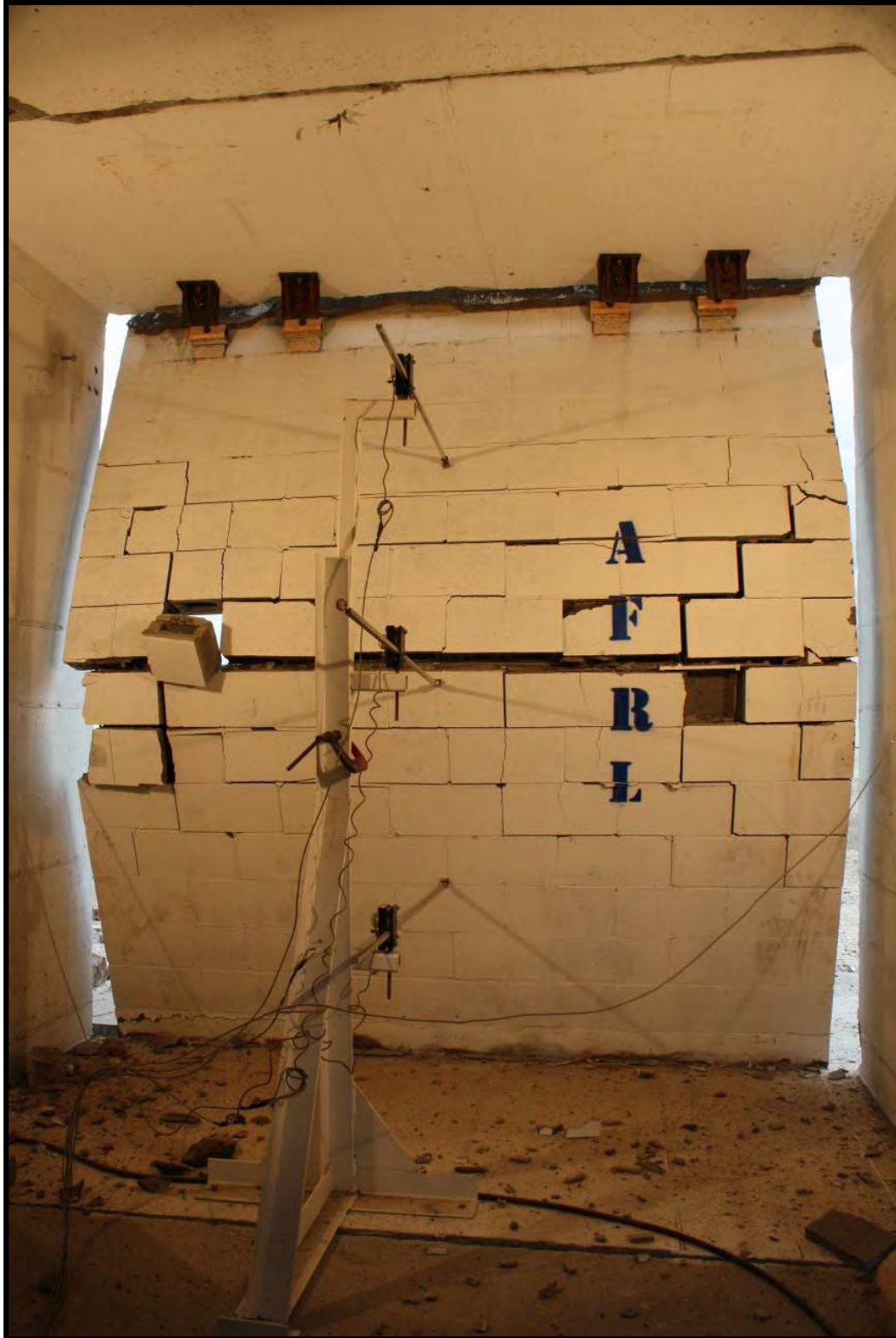


Figure C-26. Experiment 2 6-inch panel full interior view



Figure C-27. Experiment 2 6-inch CMU panel interior close-up view



Figure C-28. Experiment 2 8-inch panel front view



Figure C-29. Experiment 2 8-inch CMU panel exterior close-up view



Figure C-30. Experiment 2 8-inch CMU panel exterior close-up view



Figure C-31. Experiment 2 8-inch panel full interior view



Figure C-32. Experiment 2 8-inch panel full interior view



Figure C-33. Experiment 2 8-inch panel full interior view



Figure C-34. Experiment 2 8-inch CMU panel interior close-up view



Figure C-35. Experiment 2 cavity wall panel front view



Figure C-36. Experiment 2 exterior view



Figure C-37. Experiment 2 cavity wall panel exterior view



Figure C-38. Experiment 2 cavity wall panel exterior view



Figure C-39. Experiment 2 cavity wall panel veneer failure



Figure C-40. Experiment 2 cavity wall panel full interior view



Figure C-41. Experiment 2 cavity wall bottom interior view



Figure C-42. Experiment 3 full exterior view



Figure C-43. Experiment 3 full exterior left side view



Figure C-44. Experiment 3 6-inch CMU panel exterior view



Figure C-45. Experiment 3 6-inch CMU panel close-up breaching exterior view



Figure C-46. Experiment 3 6-inch CMU panel close-up breaching exterior view



Figure C-47. Experiment 3 6-inch CMU panel close-up reinforced cells not grouted properly



Figure C-48. Experiment 3 6-inch CMU panel full interior view



Figure C-49. Experiment 3 6-inch CMU panel breaching interior view



Figure C-50. Experiment 3 8-inch CMU panel full exterior view



Figure C-51. Experiment 3 8-inch CMU panel breaching exterior view, improperly grouted reinforced cells



Figure C-52. Experiment 3 8-inch CMU panel close-up exterior view



Figure C-53. Experiment 3 8-inch CMU panel right exterior view



Figure C-54. Experiment 3 8-inch CMU panel full interior view



Figure C-55. Experiment 3 8-inch CMU panel full interior view



Figure C-56. Experiment 3 8-inch CMU panel breaching interior view, improperly grouted reinforced cells



Figure C-57. Experiment 3 8-inch CMU panel breaching interior view, improperly grouted reinforced cells



Figure C-58. Experiment 3 8-inch CMU panel breaching interior close-up view



Figure C-59. Experiment 3 cavity wall panel full exterior view



Figure C-60. Experiment 3 cavity wall panel lower exterior view



Figure C-61. Experiment 3 cavity wall panel veneer tie close-up



Figure C-62. Experiment 3 cavity wall panel veneer side view close-up



Figure C-63. Experiment 3 cavity wall panel right side exterior view



Figure C-64. Experiment 3 cavity wall panel veneer close-up



Figure C-65. Experiment 3 cavity wall panel full interior view



Figure C-66. Experiment 3 cavity wall panel interior close-up view



Figure C-67. Experiment 3 cavity wall panel interior view



Figure C-68. Experiment 3 cavity wall panel interior view

LIST OF SYMBOLS, ABBREVIATIONS AND ACRONYMS

ACI	American Concrete Institute
A/E	architech/engineer
AFCESA	Air Force Civil Engineering Support Agency
AFRL	Air Force Research Laboratory
ASCE	American Society of Civil Engineers
ASTM	American Society for Testing and Materials
ATFP	Anti-Terrorism and Force Protection
CFA	Concrete Foundations Association
CMU	concrete masonry unit
CRADA	Cooperative Research and Development Agreement
DoD	Department of Defense
ERDC	Engineer Research and Development Center
GSA	General Service Administration
IBC	International Building Code
ICFA	Insulating Concrete Form Association
MILCON	Military Construction
msec	millisecond
MSJCC	Masonry Standards Joint Committee Code
NCMA	National Concrete Masonry Association
NRMCA	National Ready Mixed Concrete Association
PDC	Protective Design Center
PCA	Portland Cement Association
PCI	Precast/prestressed Concrete Institute
psi	pounds per square inch
R&D	Research And Development
SBEDS	SDOF Blast Effects Design Worksheet
SDOF	single-degree-of-freedom
TCA	Tilt-Up Concrete Association
TMS	The Masonry Society
UFC	Unified Facilities Criteria
USACE	US Army Corp of Engineers
VBIED	Vehicle Borne Improvised Explosive Device
WAC	wall analysis code